Centre for Radiological Protection and Dosimetry

Progress Report 199

Quotations from articles
in this report should referred to
as "personal communication".

TNO Centre for Radiological Protection and Dosimetry

Progress Report 1995

Editors: H.B. Kal and P.A.J. Bentvelzen

Typing: Hetty Jense

Graphical design and lay-out: Hans van Helden

Printed by Haeghepoorte, The Hague

P.O. Box 9034
6800 ES Arnhem
The Netherlands
Telephone: +31.26.356.30.55
Telefax: +31.26.445.07.87
E-mail: juliushw@csd.tno.nl

P.O. Box 5815
2280 HV Rijswijk
The Netherlands
Telephone: +31.15.284.27.54
Telefax: +31.15.284.39.98

TNO Centre for Radiological Protection and Dosimetry

H.W. Julius, *director*	Arnhem
J.J. Broerse, *advisor*	Rijswijk

Staff members:

A. van Aersen-Groot Hulze	Arnhem
R.W. Bartstra	Rijswijk
P.A.J. Bentvelzen	Rijswijk
L. van den Berg	Arnhem
H. Bruger	Arnhem
F.A.I. Busscher	Arnhem
J.W.E. van Dijk	Arnhem
W. van Dijk	Arnhem
H.H. Goedoen	Rijswijk
Th.G.L. Heymans	Arnhem
W.P. Hiestand	Arnhem
J.Th.M. Jansen	Rijswijk
H.M. Jense	Rijswijk
P. de Jong	Arnhem
H.B. Kal	Rijswijk
V.C. Lossau	Arnhem
J.C. Moor	Arnhem
J.W. Noomen	Rijswijk
J.H. Reumer	Arnhem
A. van Rotterdam	Rijswijk
F.W. Schultz	Rijswijk
A. Teunissen	Arnhem
C.W. Verhoef	Arnhem
D. de Vries-Kolder	Arnhem
N.J.P. de Wit	Rijswijk
J. Zoetelief	Rijswijk

Fifty years of radiation research at TNO

Almost immediately after Wilhelm Conrad Röntgen's discovery of X-rays, a century ago, this promising new tool found application in science and industry. Medical diagnostic radiology became widely spread within a few years and radiation therapy -for both benign and malignant afflictions- quickly developed as well. However, the dark backside of the medal was also soon discovered: the new radiation appeared to affect tissues, leading not only to acute effects, such as severe skin burns, but also to long term effects such as induction of malignant tumours. The notion of the risks associated with exposure to ionizing radiation was long kept within the scientific community but became public soon after World War II and is a popular subject for the media since, still often associated with the A-bombs on Hiroshima and Nagasaki, which forced the war to an end.

As early as 1946, the Netherlands Organization for Applied Scientific Research (TNO), started radiation research which was done at the Radiological Service (RD-TNO) in Arnhem. Although initially focused on Ultra Violet radiation, the work soon concentrated on ionizing radiation with the purpose of investigating and improving the radiation protection of the workforce and contributing to the amelioration of the quality of medical applications of radiation, especially radiotherapy. RD-TNO contributed significantly to the development of the first Royal Decree on Radiation Safety which became effective in 1957. Several years earlier the TNO Individual Monitoring Service became operational, at that time based on an entirely new type of photographic film dosemeter, developed by Dr. Louis van Stekelenburg, one of the pioneers in the field of radiological protection in the Netherlands. Van Stekelenburg has been the initiator of a large range of activities, among which were: calibration of radiotherapy sources, measuring of internal radioactive contamination by whole-body counting, and the development of new methods in nuclear medicine. The RD-TNO developed into an institute which combined research and development, public services and consultancy on applied radiological protection, covering occupational hygiene, environmental research and medical applications of ionizing radiation, and gained good reputation both nationally and internationally.

As of 1949 fundamental research was carried out on the biological effects of radiation in the Medical Biological Laboratory TNO, then a part of the TNO Defence Organization. Since the civil applications, among others in medicine, became more and more important, the TNO Organization of Health Research decided in 1956 to found the Radiobiological Institute TNO (RBI-TNO) to be branched off from the Medical Biological Laboratory. In 1960 Dr. Dirk van Bekkum became the director of the RBI-TNO, which was then moved to a separate, new building in Rijswijk.

Research on biophysical aspects of radiation induced damage led to extensive studies on dosimetry of various types of radiation, including fast neutrons. With regard to the possible application of fast neutrons to cancer therapy, the RBI-TNO organized a neutron dosimetry intercomparison and drafted a protocol for neutron dosimetry, which together with an American protocol resulted in a joint protocol of the International Commission on Radiation Units (ICRU-45). The RBI-TNO likewise contributed to the ICRU-report 48 on Phantoms and Computational Models in Therapy, Diagnosis and Protection, which concerned photons. The RBI-TNO has also contributed to the International Commission on Radiological Protection, which makes recommendations to protect workers as well as the general population against radiation-induced adverse health effects.

With regard to radiotherapy of malignant tumours, research at the RBI-TNO concerned the effectiveness of different types of radiation, influence of dose fractionation and dose rate, chemotherapeutic drugs, hyperthermia and combinations of treatment modalities on several types of experimental tumours in relation to the deleterious effect on normal tissues. The linear quadratic equation for the interpretation of dose-effect relationships and the concept of extrapolated tolerance dose as developed on the basis of studies on normal tissues have found wide application in clinical practice.

Another major line of research at the RBI-TNO concerned the therapy of the bone marrow syndrome, induced by relatively high doses of radiation, for example resulting from accidents in nuclear power stations like in Chernobyl. Van Bekkum was among the first who demonstrated that grafting of live intact bone marrow cells could cure this syndrome in experimental animals. This finding revived the concept of the pluripotent haemopoietic stem cell. The RBI-TNO was the first to purify the murine blood forming stem cell.

Bone marrow transplantation (BMT) initially developed for treating victims of radiation accidents has been successfully applied to the treatment of various diseases. The RBI-TNO contributed significantly to the successful cure by means of BMT of a child with the hereditary Severe Combined Immuno Deficiency Syndrome in the Netherlands in 1968. The RBI-TNO has played a major role in other clinical applications of BMT, such as in the treatment of leukaemias and lymphomas and metastatic solid tumours.

A third major line of research of the RBI-TNO was on the late effects (mainly tumour development) of ionizing radiation in rodents and rhesus monkeys. An extensive investigation was carried out on mammary tumour induction in rats by various types of radiation, in which genetical and endocrinological factors were taken into account, as well as the influence of dose fractionation. These studies were undertaken in view of the possible carcinogenic risks of mammography for mass screening on breast cancer.

During the late eighties and early nineties considerable economical and social changes became apparent in many countries. As a consequence TNO, following a general trend and adapting to shrinking support by the government, developed towards a more pragmatical and market-oriented organization. This process, partly necessary for the generation of alternative financial assets, required significant modification of its scientific research programme and conversion of the organizational structure. Evidently, this did not leave radiation research within TNO unaffected. The Radiological Service and the Department of Experimental Dosimetry of the Radiobiological Institute, which had operated separately for 36 years, decided in 1992 to merge, taking advance of the synergy resulting from the combination of fundamental and applied research, services and consultancy. In the new entity, named "TNO Centre for Radiological Protection and Dosimetry" (TNO-CSD) is now concentrated all radiation research performed in TNO. It includes, however, only a small fraction of the original biomedical research, which is partly continued in other institutes, partly discontinued.

The mission of the TNO-CSD is: to contribute, in the widest possible sense, to the limitation of exposure of man to ionizing radiation as it appears in the workplace, the natural and living environment and in the medical applications of radiation.

This mission is actualized by scientific (contract-) research, technical development, provision of services and consultancy. Thanks to an efficient network of contacts TNO-CSD successfully cooperates with the Dutch government, the European Commission and various institutes and organizations, both nationally and internationally.

TNO has a long and impressive history of fundamental and applied radiation research. This progress report shows that TNO-CSD is built on a firm basis, strong enough to prolong its excellent reputation in the field of radiological protection and dosimetry.

H.W. Julius

Contents

II. SERVICES

I. Research and Development

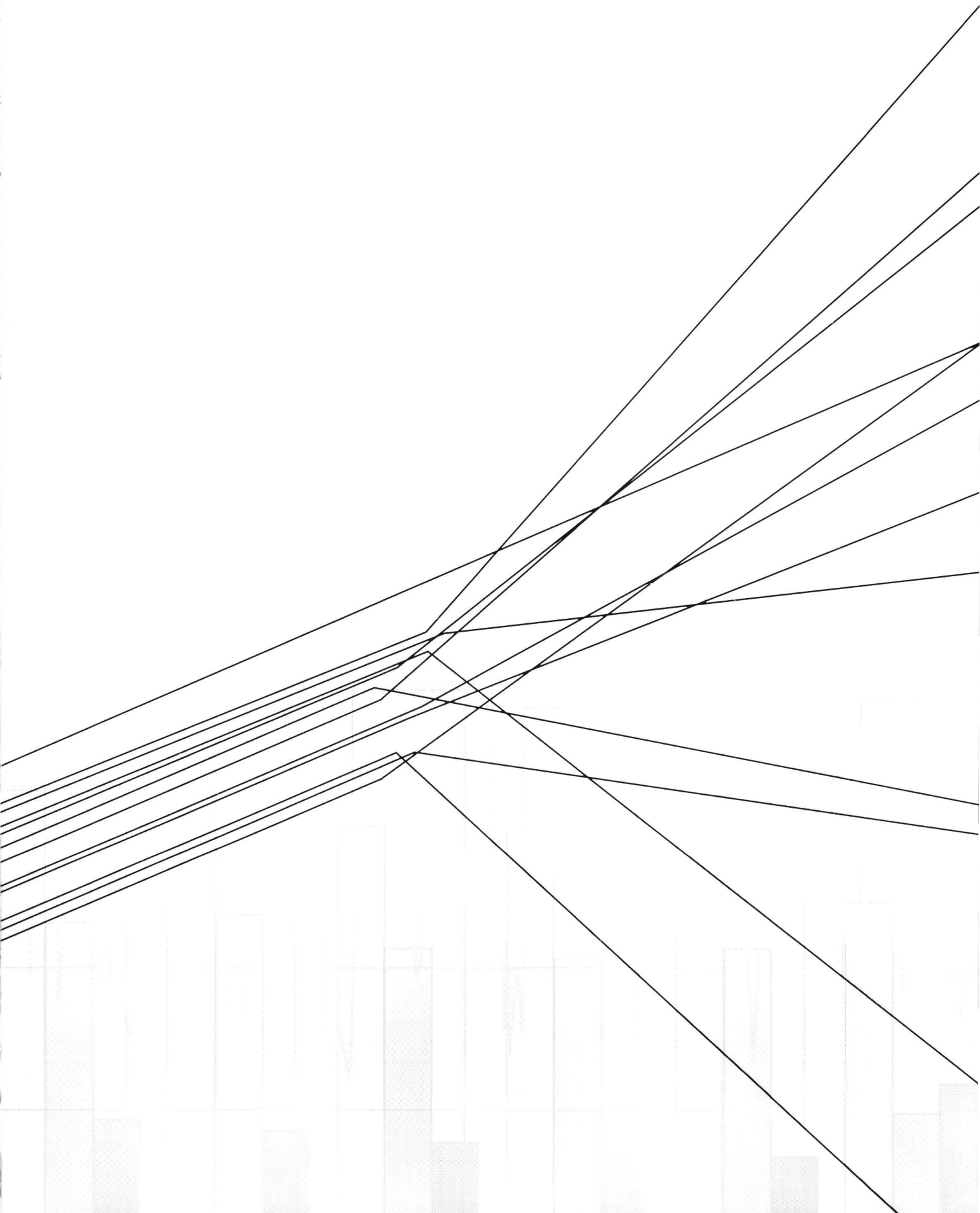

1. Individual monitoring

Core business of the TNO Centre for Radiological Protection and Dosimetry (TNO-CSD) is the individual monitoring of radiation workers. Approximately 85 per cent of the radiation workers in The Netherlands is covered by the TNO Individual Monitoring Service. In addition TNO-CSD runs the National Dose Registration and Information System (NDRIS), containing the occupational dose data of all radiation workers in The Netherlands. In the following contributions the principles of individual monitoring are discussed (1.1), and some interesting results obtained with NDRIS are presented (1.2 and 1.3).

1.1. Practice and principles of individual monitoring

H.W. Julius, F.A.I. Busscher, J.W.E. van Dijk, J.Th.M. Jansen and C.W. Verhoef

TNO's Individual Monitoring Service in a nutshell

TNO-CSD runs an approved Individual Monitoring Service (IMS) since the early fifties. To-day it serves more than 27,000 radiation workers, covering some 85 per cent of the country's needs. The dose record keeping system which, since 1972, includes the Central Dose Registration (CDR) for the Dutch nuclear power industry, formed the basis of the National Dose Registration and Information System (NDRIS) which is operated by TNO on behalf of the Dutch Ministry of Social Affairs and Employment since 1989 (1).

Individual monitoring at TNO is entirely based on thermoluminescence dosimetry (TLD). A fully automated TLD system, developed by TNO, was introduced in 1983. The dosimetrical characteristics of this personal dosimetry system easily comply with the performance requirements as proposed by the European Communities (2). Thanks to the reliable hot nitrogen gas readout technique, the reproducibility of the system under laboratory conditions is high (SD < 5 μSv). Combination of excellent stability of the readout equipment and individual calibration of all detectors, guarantees more than satisfactory overall precision and accuracy of the dosimetry system under real life conditions (3). An on-going blind test programme (i.e. bi-weekly, four-weekly and quarterly subscriptions assigned to a dummy customer) was started as early as 1987 for quality control purposes (4). The dosemeters included in this programme are exposed to a given set of doses ranging from below building background level to 12 mSv. The results from the exposures to 2.00 mSv of the bi-weekly subscription are plotted in Figure 1, which shows that the measured averaged annual dose relative to the delivered dose is very close to 1.00 and that the relative standard deviation is approximately 5 per cent.

For formal reasons as well as for the purpose of retrieving detailed technical information in case of rogue readings, all instrument parameters, calibration data and measuring results -including the glow curves of all evaluated TL detectors (close to a million per year)- are continuously logged. In order to further improve the performance of the TL dosimetry system, at both the low and the high end of the dose range, a method for glow curve treatment and analysis has been developed (5) and is presently being implemented in routine measurements.

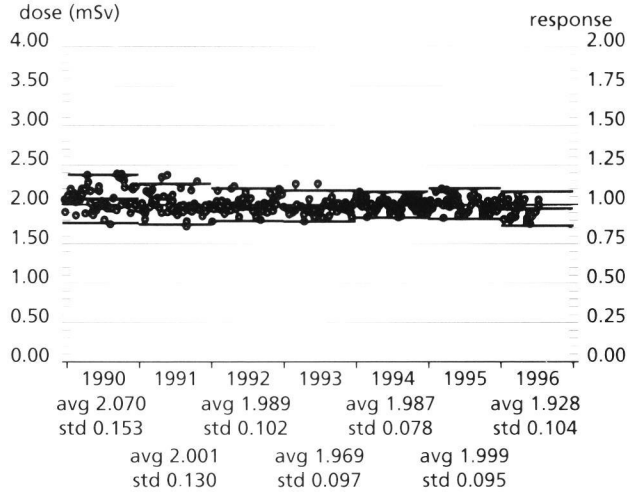

Figure 1. Quality Control test results at the 2.00 mSv level over the years 1990 to 1996

The principles: Quantities

The TNO dosemeter (Fig. 2), which accommodates regular LiF:Mg,Ti TLD-100 and very thin TLD-700 detectors, is designed to measure the personal dose equivalent quantities, $H_p(0.07)$ and $H_p(10)$ respectively, as recommended by the International Commission on Radiation Units and Measurements (ICRU) (6, 7, 8). These quantities have come a long way and are now widely accepted. Nevertheless, they still deserve discussion, even reconsideration. The following will explain why.

The system of dose limits of the International Commission on Radiological Protection (ICRP) (8) is based on the concept of effective dose, E, which is the sum of the weighted doses in all tissues and organs of the body as given by the expression

$$E = \sum_T w_T \cdot H_T$$

where H_T is the equivalent dose in tissue or organ T and w_T is the weighting factor for tissue T. The equivalent dose in tissue T is given by

$$H_T = \sum_R w_R \cdot D_{T,R}$$

where w_R is the radiation weighting factor and $D_{T,R}$ is the absorbed dose averaged over the tissue or organ T due to radiation R. Values for w_T and w_R are given in ICRP Report 60 (9).

The purpose of the primary quantity, E, is to provide a measure of detriment from stochastic effects for non-uniform irradiation of the body. Although it was recognized that the risk associated with a given exposure would vary -by up to a factor of about 10- with the age and sex of the individual exposed, only one set of (population averaged) values for w_T has been recommended by ICRP as being appropriate for the protection of any worker. In principle, E is the quantity that should be determined in radiation protection dosimetry. However, E is difficult to assess and impossible to measure directly. For measurement of external radiation ICRU therefore introduced the operational quantity "personal dose equivalent", $H_p(d)$, which is

defined as the dose equivalent in soft tissue at an appropriate depth, d, below a specified point on the body (usually taken to be the point at which the dosemeter is worn). For strongly penetrating radiation the appropriate depth is 10 mm and $H_p(d)$ is denoted as $H_p(10)$. It has been shown that, for uniform irradiation of the body, $H_p(10)$ can be considered a satisfactory representative of effective dose, overestimating this protection quantity by only some 20 per cent for photon radiation of 50 keV and greater. For lower photon energies, however, the overestimate is significant and may be as high as a factor of 5 at 15 keV (10, 11).

The concept of operational quantities was meant to provide a metrologically sound quantity which would facilitate setting and interpreting dosimetric criteria for the purpose of designing and type testing of personal dosemeters, intended to measure $H_p(10)$. However, $H_p(10)$ is not as metrologically sound as it seems. This may become clear from its definition which implies that the actual value of $H_p(10)$ depends not only on the "specified point on the body" where the dosemeter is worn but also on the individual's size and shape (influencing, by scattering and attenuation, the dose equivalent at 10 mm depth). The latter suggests that $H_p(10)$, like the protection quantity effective dose, is to be considered an individual oriented quantity. This raises the question whether a personal dosemeter should be designed so as to be sensitive to the physical characteristics of (i.e. backscatter radiation from) the body in order to correctly measure the individual's $H_p(10)$. This concept, which is advocated by several experts, would imply significant constraints on the technical design of dosemeters which would include a detector in front of an open window at its back side. It is worth noting that, generally, both $H_p(10)$ and the radiation field at the surface of the body –and hence the response of the dosemeter– will increase with increased size of the individual due to increased backscatter. However, the equivalent dose to organs and consequently the individual's effective dose are expected to decrease owing to greater attenuation of the radiation within the body. Obviously, a dosemeter which would correctly measure $H_p(10)$ by sensing backscatter radiation from the wearers body, would do just the opposite of what is intended. Clearly, the answer to the question raised above is: No.

Two more aspects are worth mentioning (10, 11):

1. The tissue weighting factor, w_T, for the female breast equals 0.05, which can neither be reflected in $H_p(10)$ for the male nor in the reading of a dosemeter (assuming that the latter is not different for female and male workers).
2. Effective dose, E, cannot be assessed for a given individual. Even if it were possible to obtain the equivalent doses in the organs of the individual concerned, calculation of E would require the use of tissue weighting factors as given by ICRP. These factors, however, are population values averaged over sex and age and are therefore not related to the individual in question.

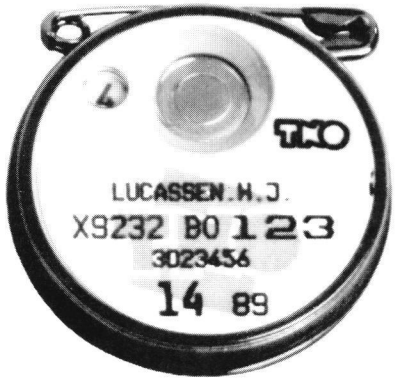

Figure 2. The TNO TL-dosemeter for photon and beta radiation.

Both considerations seem to underline that there is no point in spending a great deal of effort to design personal dosemeters capable of responding to or measuring radiation backscattered from the wearers body in order to measure an "individual specific $H_p(10)$". This does not imply that $H_p(10)$ would not be a useful operational quantity. For practical application it would, however, be better if its definition were based on physical or mathematical rather than on individual related concepts, e.g. the dose equivalent in a specific phantom.

The principles: Phantoms

For the purpose of designing and type testing of a dosemeter, its response as a function of radiation energy and angle of incidence, $R_{E,\phi}$, is to be compared to a reference value. According to ICRU, this may be $H_p(10)$ in a 30 cm x 30 cm x 15 cm slab phantom made of ICRU tissue equivalent material. Hence ideally $R_{E,\phi}$ should be equal to $H_p(10)_{phantom}$. The latter can be calculated from air kerma measurements in free air by multiplying K_a by $C(E,\phi)$, the conversion coefficient for energy E and angle of incidence ϕ, hence $H_p(10)_{phantom} = C(E,\phi)\, K_a$.

Because ICRU tissue material cannot be fabricated, ICRU suggests that for practical laboratory experiments PMMA may be used as a cheap and easily available substitute. This material, however, suffers from dosimetric complications resulting from significant differences in absorption and backscatter as compared to tissue (10, 11). For dosemeters that are sensitive to backscatter this easily provides difficulties when it comes to interpretation of type testing results in terms of performance criteria (which are a crucial part of the official approval of a dosimetry system for individual monitoring). Clearly, dosemeters designed to and capable of correctly measure $H_p(10)$ in the ICRU slab phantom may, when type tested on a PMMA slab, show a relative response as a function of photon energy and angle of radiation incidence quite different from $H_p(10)_{phantom}$ and as a result may not comply with the officially required performance criteria and hence not be approved. For this reason ISO recently adopted a 30 cm x 30 cm x 15 cm water filled thin walled PMMA

phantom the backscatter properties of which are less then 3 per cent different from those of the ICRU tissue slab.

The principles: Operational quantity revisited?

As mentioned earlier, for low photon energies the operational quantity $H_p(10)$ severely overestimates the protection quantity E. Interestingly enough many, if not all, practical dosemeters (especially those based on TLD) significantly underestimate $H_p(10)$ in this energy region (12) thus compensating for the overestimate of $H_p(10)$ and giving a better estimate of E! It has therefore been suggested (9,10) that dosemeters could be designed to have an air kerma response matching that of E, rather than of $H_p(10)$. This means that the relative response of a dosemeter as a function of energy and angle of incidence, $R_{E,\phi}$, would follow as closely as possible the relation: $R_{E,\phi} = C(E,\phi)\, K_a(10)$, where $C(E,\phi)$ is the coefficient which converts air kerma into the effective dose of a standard mathematical -anthropomorphic- phantom (e.g. ADAM or EVA). Type testing of dosemeters could be performed on the standard ISO phantom or, preferably even, on a water-filled thin walled PMMA elliptical cylinder phantom which, unlike the slab, would not suffer from inadvertent shadow effects at large angles of radiation incidence. The field quantity used to determine the response characteristics would be unchanged, i.e. air kerma for photons. Difficulties arising because of inappropriate wearing positions are no different from those currently for $H_p(10)$.

Postscript

From the point of view of technology in radiation (TL) dosimetry, dose record keeping, logistics and quality control TNO-CSD's Individual Monitoring Service complies with the highest possible standards. At the same time TNO, complying with its mission in applied scientific research, contributes to the development of concepts in radiation dosimetry and puts effort in bringing practice and principles in balance. ❑

1. JWE van Dijk, HW Julius. The national dose registration and information system, this Progress Report.
2. P Christensen, HW Julius, TO Marshall. Technical recommendations for monitoring individuals occupationally exposed to external radiation, European Commission Report EUR 14852 EN, 1994.
3. JWE van Dijk, HW Julius. Dose thresholds from statistical analysis of routine individual monitoring TLD data, this Progress Report.
4. JWE van Dijk, HW Julius. "Performance analysis of the TNO TLD individual monitoring service, Proc. 9th Solid State Dosim Con., Vienna, 1989, Radiat Prot Dos, 2nd, 34, 171-174, 1990.
5. JWE van Dijk, HW Julius. Glow curve analysis for constant temperature hot gas TLD readers, Proc 10th Solid State Dosim Conf, Washington, 1992. Radiat Prot Dosim 47, 479-482, 1993.
6. International Commission on Radiation Units and Measurements. Determination of dose equivalents resulting from external radiation sources. Bethesda Md: ICRU Report 39, 1985.
7. International Commission on Radiation Units and Measurements. Determination of dose equivalents from external radiation sources, Part 2. Bethesda Md: ICRU Report 43, 1988.
8. International Commission on Radiation Units and Measurements. Measurements of dose equivalents from external photon and electron radiations. Bethesda Md: ICRU Report 47, 1992.
9. International Commission on Radiological Protection. 1990 Recommendations of the International Commission on Radiological Protection. Oxford: Pergamon Press, ICRP Publication 60, 1991.
10. HW Julius, Some remaining problems in the practical application of the ICRU concepts of operational quantities in individual monitoring. Proc 11th Solid State Dosim Conf. Budapest, 1995. Radiat Prot Dosim (to be published).
11. HW Julius, Individual monitoring, some conceptual and practical aspects, Proc 9th IRPA Congress, Vienna, 1996.
12. HW Julius, TO Marshall, P Christensen, JWE van Dijk, Type testing of personal dosemeters for photon energy and angular response, Radiat Prot Dosim. 54, 273-277, 1994.

1.2. The national dose registration and information system

J.W.E. van Dijk and H.W. Julius

Centralized dose registration

The monitoring of radiation workers is performed by more than one Approved Dosimetry Service (ADS) in The Netherlands. From the point of view of radiation protection, there is a need to combine all dose data in order to prevent doses in excess of the annual dose limits from remaining unnoticed. This is of particular importance for employees of contractors who, for instance, work in the controlled areas of various nuclear power plants. This has been recognized by both national governments and the European Commission (EC). In 1988 the Dutch Ministry of Social Affairs and Employment decided to centralize all dose information in The Netherlands. The government committed TNO-CSD to extend its dose registration and information system (DRIS) of their Individual Monitoring Service (IMS), which covers about 85 per cent of the need for personnel monitoring in The Netherlands, to the National Dose Registration and Information System, NDRIS. The NDRIS now contains the dose information of all radiation workers in The Netherlands since January 1, 1989.

NDRIS conforms to both the "centralized national network" as referred to in the EURATOM Directive on outside workers (90/641/EURATOM) and the recommendations given in the "Technical recommendations for monitoring individuals occupationally exposed to external radiation" (EUR 14852).

Trends in occupational exposures

The Dutch National Dose Registration and Information System has now been in operation for over five years. A typical example of the statistical information that can be obtained from the system is shown in the Figures 1 and 2. In these figures the open bars show for each year the number of radiation workers in The Netherlands. The light gray, gray and black bars represent NR_E, i.e. the fraction of the workforce having received an annual dose in excess of E, with E equalling 0.05, 0.5 and 5 mSv, respectively.

A slight decrease in the fraction of workers who receive noticeable doses can be observed from 1989 to 1992 (Fig. 1). For very low doses this trend is less obvious for workers using mobile equipment in industrial radiography (Fig. 2). However, the number of workers exposed to more than 5 mSv per year was reduced. The slight increase in the fraction of workers receiving an annual dose in excess of 0.05 mSv in 1993 (Fig. 1) is due to improved dose assessments with the TNO-TLDosemeters for doses in the range from 0.00 to 0.02 mSv per issuing period.

Implications of the introduction of lower dose limits

The Figures 3 and 4 show the parameter NR_E plotted against the dose for 1989 and 1993. In Figure 3 the cumulative distribution is plotted for all radiation workers and in Figure 4 for workers in cardiological radiography. From a detailed analysis of these figures the increase in the number of workers who will receive a dose in excess of the annual limit can be estimated, in case the limits are reduced from 50 to 20 mSv. In The Netherlands this number will rise from approximately 10 every year to more than 50. For cardiologists an increase by a factor of seven will occur if no measures are taken. ❑

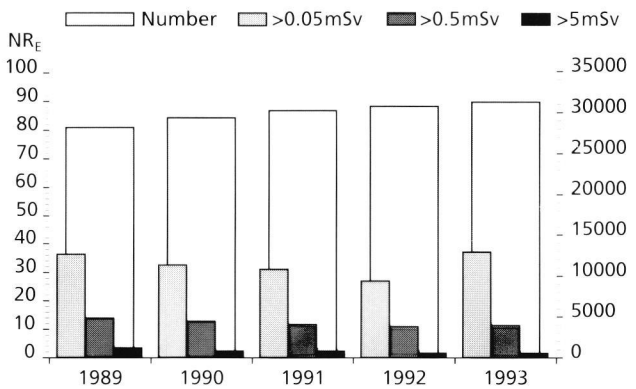

Figure 1. Dose distribution (left y-axis) and number of workers (right y-axis) for all radiation workers in the years 1989-1993.

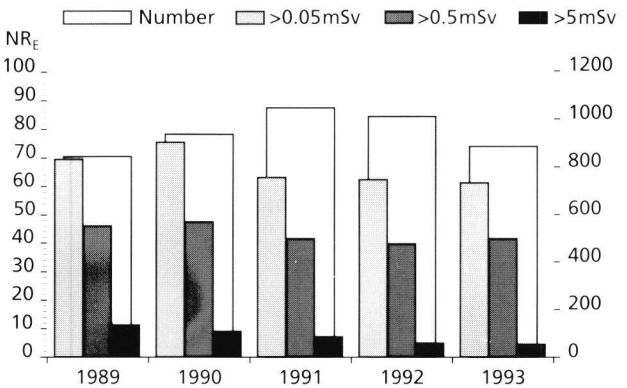

Figure 2. Dose distribution (left y-axis) and number of radiographers using mobile equipment (right y-axis) in the years 1989-1993.

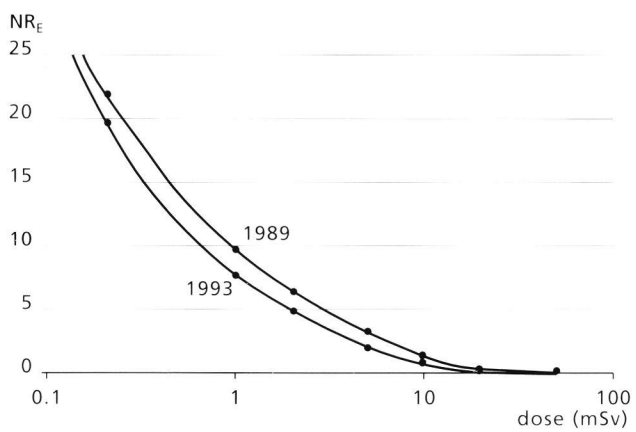

Figure 3. Cumulative distribution of the dose for all radiation workers in 1989 and 1993.

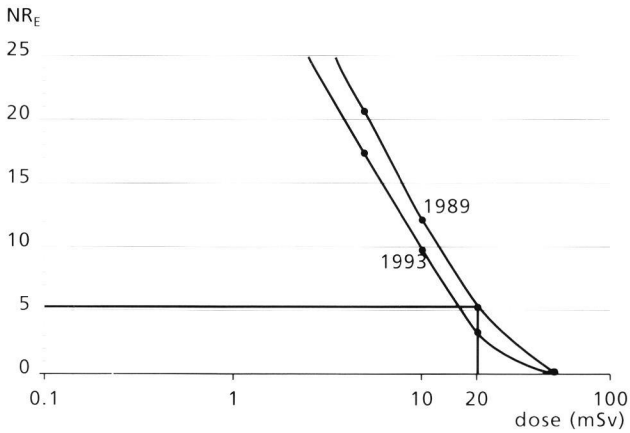

Figure 4. Cumulative distribution of the dose for cardiological radiography in 1989 and 1993.

1.3. Dose thresholds from statistical analysis of routine individual monitoring TLD data

J.W.E. van Dijk and H.W. Julius

Often customers of Individual Monitoring Services (IMS) use the reported dose data not only to verify compliance with legal dose limits, but also to assist in implementing the "As low as reasonably achievable" (ALARA) principle. Since the International Commission on Radiological Protection (ICRP) in Report 60 (1), recommended to lower the annual dose limit by - on average - a factor of 2.5, the ALARA goals tend to be reduced as well. In many situations, e.g. in diagnostic radiology, it is argued that, if procedures are strictly followed, the occupational dose need not be significantly above the level of the natural background. This implies that the doses which must be determined, often approach natural background levels and can easily be of the same order as the threshold of measurability of the dosimetry system. TNO-CSD supplies routine individual monitoring services complying with these needs by using TLD100 based dosemeters and a TNO developed TLD-reader system in which the detectors are heated by hot nitrogen gas of constant temperature.

At low dose levels the error in a dose assessment is not longer governed by the relative errors but rather by the absolute error in the reading of dosemeters exposed to natural background radiation only. The dose reported by an IMS is the occupationally received radiation dose, H_{occ}, which is the total dose, H_{read}, minus the contribution from natural radiation, H_{nat}. Obviously the uncertainty in the natural background dose rate may contribute significantly to the uncertainty in the reported dose. The uncertainty in the background dose is mainly caused by variations in the dose rate from place to place while in practice one national or regional average for the natural background dose is subtracted. In The Netherlands this dose is taken to be 2.16 μSv for every day elapsed since the readout of the dosemeter. The relative standard deviation in this rate, which was determined in a national survey, is about 15 per cent (2).

The errors in the reported occupational dose can be found by statistical analysis of the doses routinely measured for the customers of the IMS. This statistical analysis data is primarily based on the study of frequency distributions. For these calculations it is assumed that the majority of the workers monitored is not occupationally exposed to artificial radiation sources. This implies that the majority of the reported occupational doses may be taken to be 0.00 mSv or, in statistical terms, the modus of the frequency distribution will be 0.00 mSv (3,4).

The data points in Figure 1 represent the observed dose distribution of the biweekly subscriptions to the TNO-IMS for 1995. For a robust estimate of the modus and the standard deviation, the distribution is approximated by a Gauss-function using a non-linear least squares procedure. The parameters of the best fitting Gauss curve are shown in Figure 1. The modal dose appears to be -0.008 mSv and the standard deviation in an occupational dose of about 0.00 mSv is 0.011 mSv. This slightly negative value for the modal dose indicates that for the majority of our customers the contribution of the natural background might be slightly overestimated, although other phenomena may play a role as well.

The standard deviation in the occupational dose, s_{occ}, is

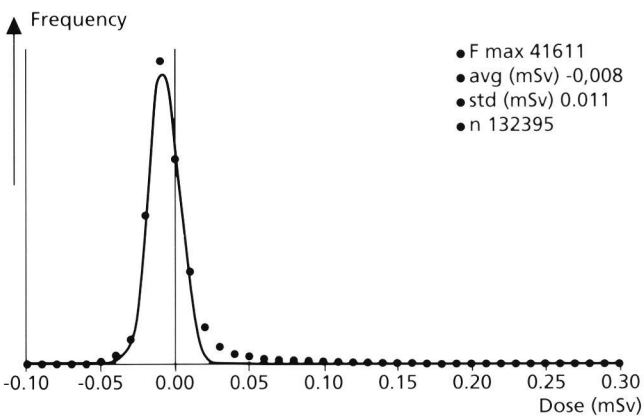

Figure 1. Frequency distribution for the biweekly subscriptions in 1995 for all customers. The solid line represents the best fitting Gauss-function, the parameters of which are shown in the figure. The measured dose is on the horizontal axis and the number of dosemeters in each class (width=0.01 mSv) on the vertical axis.

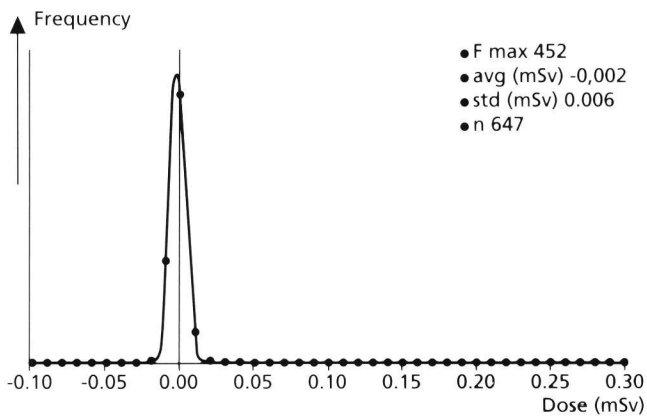

Figure 2. Frequency distribution for the bi-weekly issued spare dosemeters of a nuclear power plant. The solid line represents the best fitting Gauss-function, the parameters of which are shown. The measured dose is on the horizontal axis and the number of dosemeters in each class (width = 0.01 mSv) on the vertical axis.

the resultant of the standard error in the measurement of the total dose, s_{read}, and the standard error in the contribution from natural background radiation, s_{nat}. The uncertainty in the natural background dose can be found from the results of the national survey but also from frequency analysis of the IMS data of one large customer.

In Figure 2 the dose distribution of the unused dosemeters of a nuclear power station is shown. The standard deviation of this distribution is 0.0057 mSv. As these dosemeters were all stored at one place in the power plant, there will be no variation in the accumulated background dose and thus s_{nat} can be assumed to be almost zero. Consequently this standard deviation of 0.0057 mSv will approximate s_{read}. Using the additivity of the variances s^2_{read} and s^2_{nat}, the above mentioned error terms are estimated to be:

s_{occ}= 0.011 mSv
s_{read}= 0.0057 mSv
s_{nat}= 0.0094 mSv

For the occupational dose, H_{occ}, the following thresholds, as conventionally used (e.g. ANSI 13.11 appendix D (5)), can be calculated (6,7):

Critical level (the probability that a dose is reported as being greater than 0.00 mSv while it is not, is limited to 5%):

L_C=0.02 mSv

Detection limit (the probability that a dose is reported as being greater than 0.00 mSv while it is not and the probability that a dose is reported to be 0.00 mSv while it is greater, are both limited to 5%):

L_D=0.04 mSv

Determination limit (the dose which can be determined with a relative precision of 10% or better):

L_Q=0.11 mSv

Both the need for traceability of the reported doses to the original measurements and the requirements of the ISO-9001 certificate, lead us to record all doses measured in the IMS databases in the precision of the reader systems, which is of the order of 1 μSv (the glow curves are in fact stored). It should be emphasized that negative values for H_{occ} should be recorded as well because they are needed for the statistical analysis, which latter is indispensable for quality control.

As the standard deviation in a single measurement of H_{occ} is of the order of 0.01 mSv, we report the doses to our customers in multiples of 0.01 mSv starting at 0.01 mSv. All doses below 0.005 mSv are reported as "< 0.01 mSv" (in calculations of the annual sum they are taken to be 0.00 mSv). We do not use, as proposed by ICRP (1), a recording or reporting level of 1/10 of the fraction of the annual limit, corresponding to the issuing period used, which amounts to 0.08 mSv for biweekly subscriptions and an annual dose limit of 20 mSv. We prefer to explain to our customers the meaning of the dose data reported in terms of statistical uncertainties and confidence limits. ❑

1. International Commission on Radiological Protection. 1990 Recommendations of the International Commission on Radiological Protection. Oxford: Pergamon Press. ICRP Publication 60, 1990.
2. HW Julius, R van Dongen. Radiation doses to the population in The Netherlands, due to external natural sources, The Science of Total Environment 45, 449-458, 1985.
3. JWE van Dijk, HW Julius. Performance analysis of the TNO TLD individual monitoring service. Radiat Prot Dosim 1990 34, 171-174, 1994.
4. JWE van Dijk, HW Julius. Dose thresholds and quality assessment by statistical analysis of routine individual monitoring TLD data. Radiat Prot Dosim, in press.
5. ANSI, Personnel dosimetry performance - criteria for testing, Health Phys, SN13-11, 1993.
6. LA Currie. Limits of qualitative detection and quantitative determination. Anal Chem 40, 586-593, 1968.
7. P Christensen, RV Griffith. Required accuracy and dose thresholds in individual monitoring, Radiat Prot Dosim 54, 279-285, 1994.

2. Medical applications

Medical applications of ionizing radiation are causing by far the largest radiation burden to the population due to man-made sources. Among the medical applications, diagnostic radiology is contributing by about 16.5 per cent and nuclear medicine by about 1.4 per cent to the average annual radiation exposure per caput of the Dutch population which amounts about 2.7 mSv.

The general radiation protection principle of the International Commission on Radiological Protection (ICRP) postulates that all exposures "should be kept as low as reasonably achievable". In the case of medical applications, this implies that each procedure (treatment or diagnosis) is justified and optimized. For diagnostic radiology and nuclear medicine imaging optimization means that the radiation dose to the patients should be kept as low as possible, but still providing images compatible with the clinical requirements.

The majority of the studies carried out within TNO-CSD on medical applications of ionizing radiation concerns diagnostic radiology. The contributions to this chapter concern methods for assessment of effective dose in the patient due to diagnostic radiology (2.1 to 2.3); assessment of patient dose and image quality in practice (2.4); a risk-benefit analysis of breast cancer screening employing mammography (2.5); and a method for describing the time dependent distribution of radioactive substances inside the human body relevant for nuclear medicine (2.6).

2.1. Effective doses for different techniques used for PA chest radiography

F.W. Schultz, J. Geleijns[1] and J. Zoetelief

A survey of X-ray units, with which diagnostic chest examinations are routinely performed in the Leiden region, showed a considerable variety of exposure conditions and employed technique parameters. For instance, besides to conventional radiography the use of a mobile unit and application of lung-shaped filters could be distinguished, and different beam qualities (tube voltage, filters) and exposure geometries (focus-film distance, FFD, and focus-skin distance, FSD) were used. Concerning the radiation protection of the patient, it is important to obtain information about organ doses for the specific examinations to identify those procedures that yield the lowest values of effective dose (E), i.e., the lowest risk of fatal cancer induction.

The Monte Carlo Neutron and Photon radiation transport code (MCNP-3B) was used to calculate organ doses, normalised to air-kerma free-in-air at the point where the beam's central axis would enter the patient. Skin dose per unit of air kerma at the point of exit was also evaluated. Exposure conditions were varied to correspond with those for postero-anterior (PA) chest radiography as met in the survey. FFD and FSD were varied while the screen size was kept constant. Photon spectra were chosen that by approximation cover the total range of observed X-ray beam qualities, expressed in first and second half value layer (HVL). Standard adult male and female patients were simulated with the mathematical phantoms ADAM and EVA, respectively.

Taking tissue weighting factors from the ICRP-60 report (1), for each case the effective dose, normalised to air kerma, was calculated from the organ doses resulting from the MC simulations. Gonads were taken as testes for ADAM, and as ovaries for EVA. Thymus was taken as a reasonable substitute organ for the oesophagus, the latter risk organ not yet being modelled in the phantoms. For ADAM, muscle dose replaces breast dose.

The position of the beam along the longitudinal axis of the phantom is important. In one case a shift of 5 cm resulted in a 22 per cent relative difference in normalised E, because important organs (partly) moved into or out of the primary beam. In general the normalized E increases with increasing HVL, with relative differences of 127 to 148 per cent between maximum and minimum values. FSD dependence, with maximum differences up to 26 per

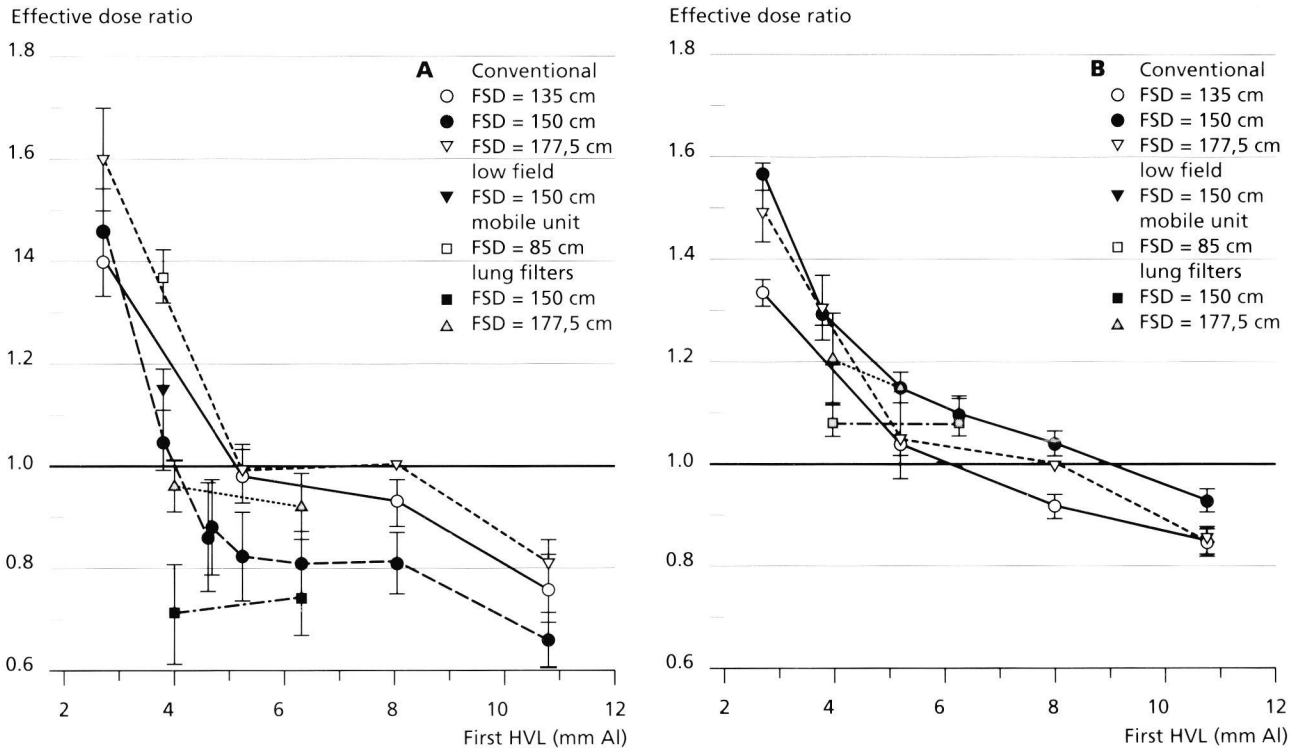

Figure 1. Effective dose corresponding to 4 μGy skin exit dose, normalised to median exposure conditions observed in the survey of X-ray units (HVL= 8 mm Al, FSD= 177.7 cm), for A: ADAM and B: EVA.

cent, is different for male and female; for EVA FSD=135 cm yielded the lowest E, for ADAM this happened at FSD=150 cm (highest E for EVA). For similar exposures the normalised E for EVA is always 1.1 to 1.5 times higher than for ADAM.

To evaluate E in absolute terms, it is assumed that a constant exit skin dose yields a constant image quality in all cases. Making the exit skin dose in all cases equal to 4 μGy, a typical value observed in the survey, it was found that the corresponding value of E for the different exposures ranges from 7 to 17 mSv. Thus, proper choice of technique parameters allows a 2.5-fold dose reduction for ADAM, 1.8-fold for EVA (Fig. 1). For similar exposure conditions, E for EVA may differ up to +28 per cent and -20 per cent from its value for ADAM. Varying FSD only, differences in E may reach 34 per cent. Lowest doses were found for ADAM at medium FSD, for EVA at small FSD. Best beam quality for radiation protection is offered by large-HVL beams or, for ADAM, small-HVL beams plus lung filters (the contours of which, in projection, fully shield the lungs). ❑

1. International Commission on Radiological Protection. 1990 Recommendations of the International Commission on Radiological Protection. Oxford: Pergamon Press. ICRP report 60, 1991.

[1]) Department of Clinical Oncology, State Univerity of Leiden, The Netherlands

2.2. Calculation of air kerma to average glandular tissue dose conversion factors for mammography

J. Zoetelief and J.Th.M. Jansen

Among the quantities used for dose specification in mammography the average absorbed dose in glandular tissue is most appropriate for risk assessments. Generally, average absorbed dose in glandular tissue is derived from measurement of air kerma free-in-air combined with conversion factors obtained from radiation transport calculations in mathematical breast models.

Air kerma to glandular tissue dose conversion factors are published by various authors (1-5) as a function of half value layer (HVL) for breast phantoms. Calculations by different authors differ in radiation transport codes, photon interaction data, photon spectra, composition and thickness of superficial layer (representing skin and subcutaneous adipose tissue) and presence of compression plate are not performed with the tissue compositions recommended by the ICRU (6). Protocols for dosimetry in mammography in different European countries (UK, The Netherlands, Sweden) make use of results of different authors. It is therefore of interest to study the influence of the parameters indicated on air kerma to glandular tissue dose conversion factors, g-values, calculated using the Monte Carlo Neutron and Photon radiation transport code, MCNP (7).

At fixed HVL, the spectral influence on g-values is small between data of Birch and Marshall (8) and Panzer et al. (9): the maximum difference is 4.5 per cent, but in general less than 2 per cent. The g-values derived with data from Fewell and Shuping (10) and Doi and Chan (11) are approximately 7 per cent smaller, Figure 1.

The use of a compression plate results in a 4.5 ± 1.5 per cent smaller g-value for the same HVL, which is in agreement with calculations of Carlsson and Dance (5).

The use of MCPLIB (12) cross-sections results in 10 per cent higher g-values compared to the use of XCOM data (13). This indicates a need for further investigations on the actual cross-sections used in the other studies.

The influence of the backscatter material (composition and thickness) on the g-value is marginal (less than 1 per cent). The influence on the exit dose is, however, greater but needs more accurate simulations.

The different superficial layers used result in differences in g-values of 9.5 per cent (ICRU composition (6), 2 cm breast thickness), 3.4 per cent (ICRU, 8 cm), 19 per cent (Hammerstein (14), 2 cm) and 11 per cent (Hammerstein, 8 cm), Table 1.

The g-values decrease when the breast thickness is

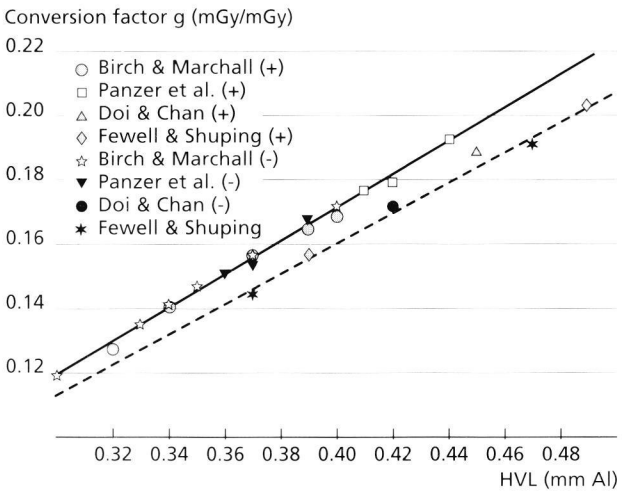

Figure 1. Conversion factor g as a function of HVL employing photon spectra from various authors in presence and absence of a 3 mm thick PMMA compression plate. The values refer to a 5.5 cm thick breast phantom (superficial layer: 0.5 cm adipose tissue) and ICRU (6) tissue compositions.

changed from 2 cm to 8 cm by factors of 4.0 (HVL: 0.37 mm Al) and 3.8 (HVL: 0.42 mm Al), Table 2. This is in agreement with calculations of Dance (3). The variations in g-values with breast thickness found in the present study are larger than those reported by Wu et al. (4) and Stanton et al. (1).

The g-values employing Hammerstein (14) tissue compositions compared to those employing ICRU (6) tissue compositions are 14 per cent and 11 per cent higher for 2 and 8 cm breast thickness, respectively. ❑

A full paper on this subject has appeared under the same title in Radiation Protection Dosimetry 57, 397-400, 1995.

1. L Stanton, T Villafana, JL Day, DA Lightfoot. Dosage evaluation in mammography. Radiology 150, 577-584, 1984.
2. M Rosenstein, LW Andersen, GG Warner. Handbook of glandular tissue doses in mammography. HHS Publication FDA 85-8239. Center for Devices and Radiological Health, Rockville, Maryland, USA, 1985.
3. DR Dance. Monte Carlo calculation of conversion factors for the estimation of mean glandular breast dose. Phys Med Biol 35, 1211-1219, 1990
4. X Wu, GT Barnes, DM Tucker. Spectral dependence of glandular tissue dose in screen-film mammography. Radiology 179, 143-148, 1991.
5. GA Carlsson, DR Dance. Breast absorbed doses in mammography: evaluation of experimental and theoretical approaches. Radiat Prot Dosim 43, 197-200, 1992.
6. International Commission on Radiation Units and Measurements. Tissue substitutes in radiation dosimetry and measurement. Bethesda, Md: ICRU Report 44, 1989.
7. J Briesmeister. MCNP- A general Monte Carlo Code for neutron and photon transport. LA-7396-M, Rev 2, 1986.
8. R Birch, M Marshall. Program to calculate photon spectra; spectra were kindly provided by Dr. DR Dance, 1992, pers. comm.
9. W Panzer, G Drexler, L Widenmann, L Platz. Spectra and exposure values in mammography. GSF-Bericht S 518, Munich: Gesellschaft für Strahlen- und Umweltforschung, 1978.
10. TR Fewell, RE Shuping. Handbook of mammographic X-ray spectra. HEW Publication FDA-79-8071, Rockville, Md, 1979.
11. K Doi, H-P Chan. Evaluation of absorbed dose in mammography: Monte Carlo simulation studies. Radiology 135, 199-208, 1980.
12. MCPLIB, Cross-section data of the MCNP code based on refs. 10 and 11.
13. MJ Berger, JH Hubbell. XCOM: photon cross-sections on a personal computer, version 1.2. Gaithersburg, Md: National Bureau of Standards, 1987.
14. GR Hammerstein, DW Miller, DR White, et al. Absorbed radiation dose in mammography. Radiology 130, 485-491, 1979.

Table 1. Influence of thickness and composition of superficial layer on g (mGy/mGy) for different thicknesses of reference breasts (central region 50 per cent adipose and 50 per cent glandular tissue or BR-12) employing ICRU-44 tissue compositions and (μ_{en}/ρ)-values, a 3-mm thick PMMA compression plate, FFD of 60 cm and spectrum of Birch and Marshall 25 kV (HVL: 0.34 mm Al)

	g (mGy/mGy)					
	0.4 cm		0.5 cm		0.5 cm	
breast	glandular tissue		adipose tissue		BR-12	
thn. (cm)	ICRU	Ham.	ICRU	Ham.	ICRU	Ham.
2.0	0.348	0.369	0.381	0.438	0.341	0.392
4.0	0.187	0.195	0.199	0.224	0.178	0.205
5.5	-	-	0.141	-	-	-
6.0	0.122	0.127	0.128	0.143	0.114	0.131
8.0	0.089	0.092	0.092	0.102	0.082	0.094

Table 2. Influence of breast thickness on g (superficial layer: 0.5 cm adipose tissue, central region 50 per cent adipose and 50 per cent glandular tissue) employing different (ICRU-44 vs Hammerstein et al.) tissue compositions and (μ_{en}/ρ)-values, a 3-mm thick PMMA compression plate, FFD of 60 cm and spectrum of Birch and Marshall 28 kV (HVL: 0.37 mm Al) and Panzer et al. 28 kV (HVL: 0.42 mm Al)

	g (mGy/mGy)			
breast	Birch, 28 kV		Panzer, 28 kV	
thn. (cm)	ICRU	Ham.	ICRU	Ham.
2.0	0.410	0.468	0.448	0.512
4.0	0.220	0.247	0.251	0.280
5.0	0.174	0.194	0.200	0.222
5.5	0.157	0.175	0.180	0.200
6.0	0.142	0.158	0.164	0.182
8.0	0.103	0.114	0.119	0.132

2.3. Calculation of computed tomography dose index to effective dose conversion factors based on measurement of the dose profile along the fan shaped beam

J.Th.M. Jansen, J. Geleijns[1], D. Zweers[1], F.W. Schultz and J. Zoetelief

The number of computed tomography (CT) examinations is increasing in The Netherlands as well as in other countries; relatively high effective doses are involved. It is important to quantify the effective dose from CT examinations. Effective doses in patients depend on the presence of a beam shaping filter. In most types of CT scanner a beam shaping filter is applied to increase attenuation of the radiation at the edges of the beam compared with its centre, to compensate for the roughly cylindrical shape of a patient, thus yielding more uniform signals from the detectors in the image plane. Differences in construction between beam shaping filters in CT scanners are large, both in geometry and elemental composition.

The variation in computed tomography dose index

(CTDI) (1) derived by measurements free-in-air with a pencil type ionization chamber to effective dose (2) conversion factors between different types of CT scanner is large (i.e., a factor of about 2 due to differences in beam shaping filters). Consequently, scanner specific conversion factors have to be applied. For some types of scanner, however, detailed information on the construction of beam shaping filters is not provided by the manufacturers. It is of interest to investigate the use of measured dose profiles for the calculation of conversion factors with the Monte Carlo neutron and photon radiation transport code (MCNP) (5). Organ and effective dose conversion factors were calculated, based upon measured dose profiles, two appropriate photon spectra (3) selected on the basis of measured half value layers, and gender specific adult phantoms ADAM and EVA (4). To validate the method, a comparison is made between results for measured and calculated beam profiles for a Philips Tomoscan 350. The results in terms of effective dose per slice per unit of CTDI are compared with published data. The relative difference in conversion factors per slice averaged over all slices used for the calculations is 13 ± 4 per cent between the two spectra; 10.2 ± 0.2 per cent between measured and calculated beam profiles and 50 ± 191 per cent between the phantoms of different gender (see Figure 1 for the ADAM and Figure 2 for the EVA phantom). The relative difference between the averaged results for the ADAM and EVA phantoms and published results for a hermaphrodite phantom (6) is on average equal to or less than 15 ± 13 per cent, depending on the spectrum and beam profile used, although larger differences can occur for specific slices (see Fig. 3). It is concluded that CTDI to effective dose conversion factors can be derived on the basis of measured beam profiles. ❑

A full paper on this subject has appeared onder the same title in the British Journal of Radiology 69, 33-41, 1996.

1. TB Shope, RM Gagne, GC Johnson. A method for describing the doses delivered by transmission X-ray computed tomography. Medical Physics, 8, 488-495, 1981.
2. International Commission on Radiological Protection, 1990 Recommendations of the International Commission on Radiological Protection, Oxford: Pergamon Press. ICRP Publication 60, 1991.
3. WW Seelentag, W Panzer, G Drexler, et al. A catalogue of spectra for the calibration of dosemeters. Munich: Gesellschaft für Strahlen- und Umweltforschung, GSF-Bericht S 560, 1979.
4. R Kramer, M Zankl, G Williams, G Drexler. The calculation of dose from external photon exposures using reference human phantoms and Monte Carlo methods. Part 1: The male (Adam) and female (Eva) adult mathematical phantoms. Munich: Gesellschaft für Strahlen- und Umweltforschung, GSF-Bericht S-885, 1986.
5. J Briesmeister. MCNP- A general Monte Carlo code for Neutron and photon transport, version 3A, LA-7396-M, Rev. 2, Los Alamos NM: Los Alamos National Laboratory, 1986.
6. DG Jones, PC Shrimpton. Normalised organ doses for X-ray computed tomography calculated using Monte Carlo techniques. NRPB-SR250, Chilton: National Radiological Protection Board, 1993.

[1]) Department of Clinical Oncology, State University of Leiden, The Netherlands

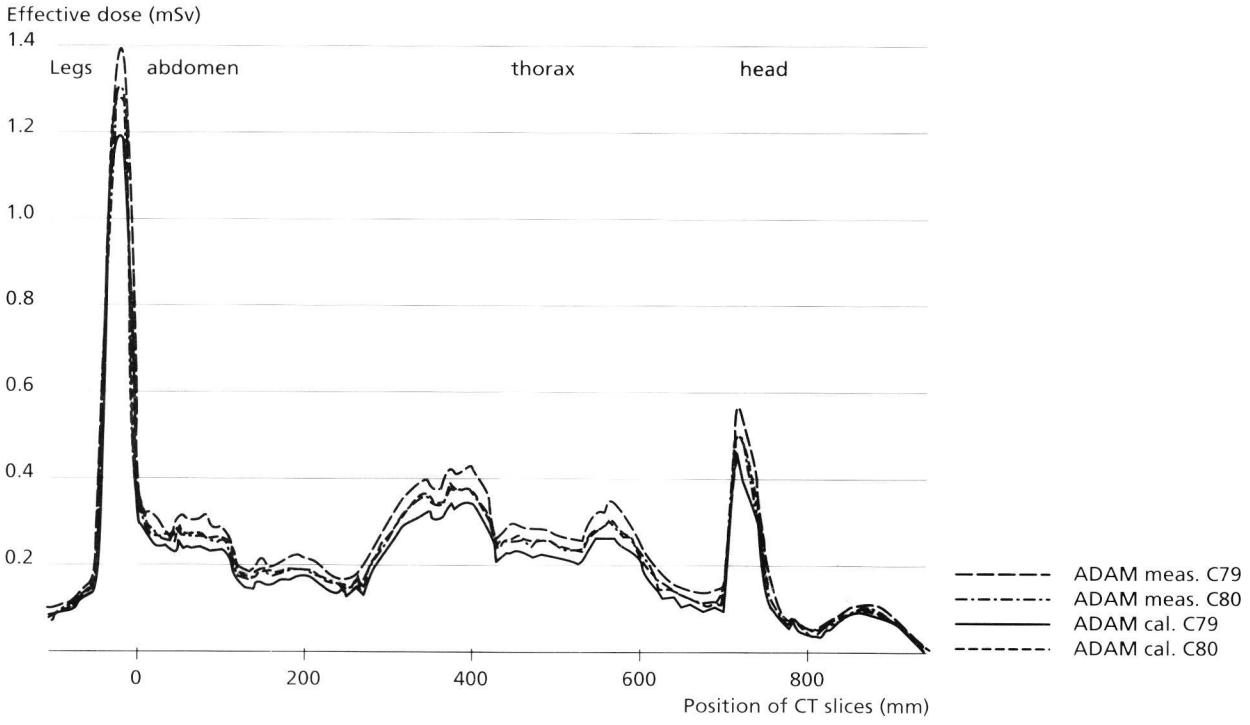

Figure 1. Calculated effective dose as a function of the position of the CT slices for the ADAM phantom. The calculations were performed for a Philips Tomoscan 350 CT scanner, a slice thickness of 5 mm and a CTDI expressed in air of 100 mGy, employing the measured (meas.) or calculated (cal.) beam profile along the fan and using spectra of Seelentag et al. (3), coded C79 and C80.

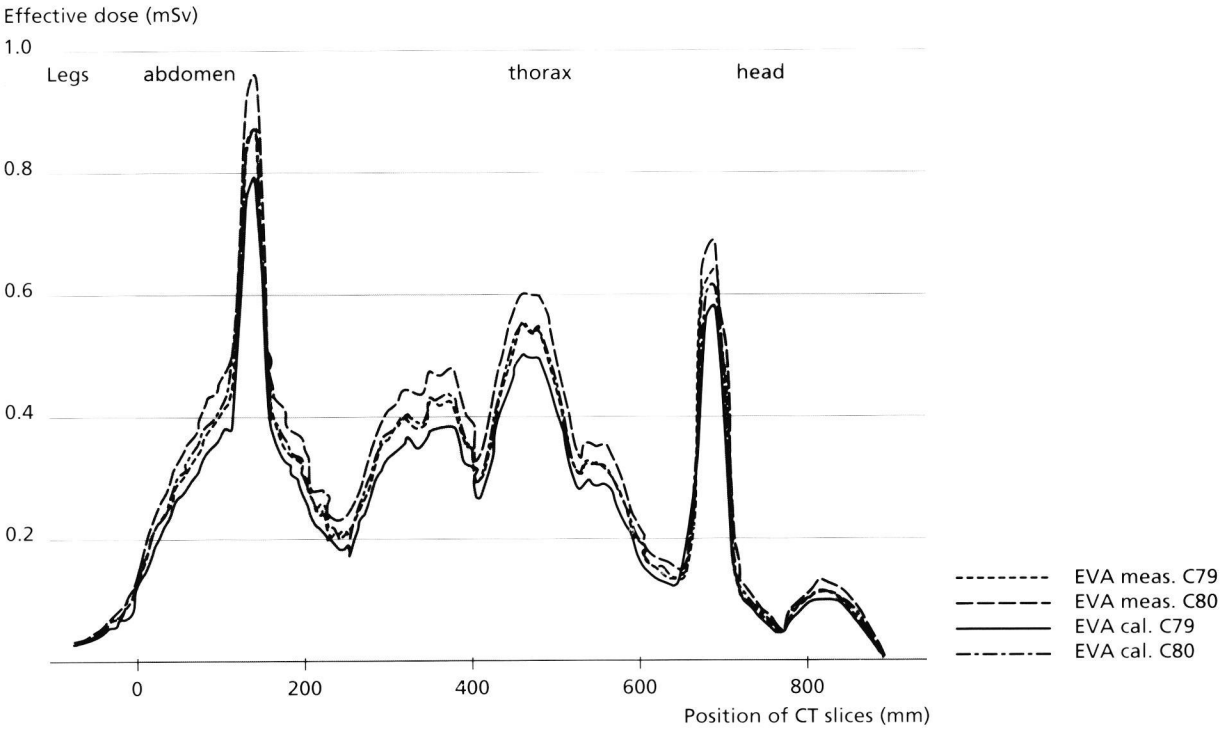

Figure 2. Calculated effective dose as a function of the position of the CT slices for the EVA phantom. The calculations were performed for a Philips Tomoscan 350 CT scanner, a slice thickness of 5 mm and a CTDI expressed in air of 100 mGy, employing the measured (meas.) or calculated (cal.) beam profile along the fan and using spectra of Seelentag et al. (3), coded C79 and C80.

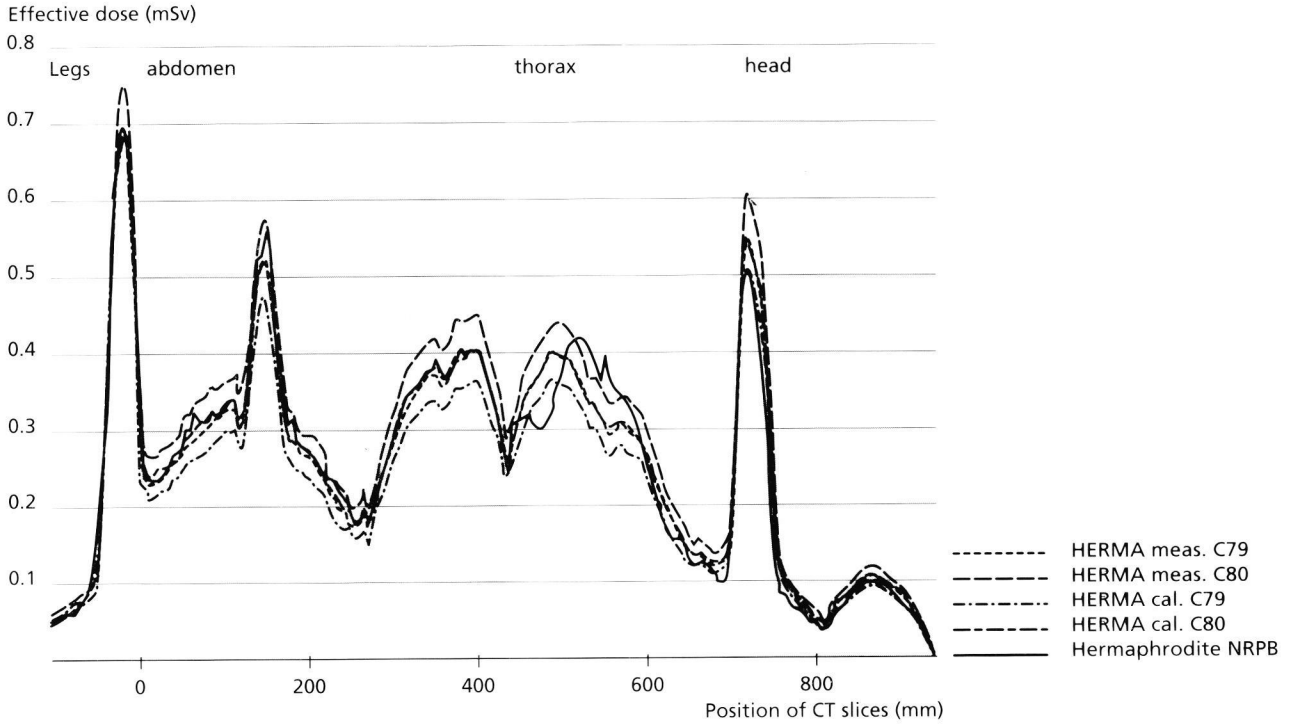

Figure 3. Calculated effective dose as a function of the position of the CT slices is shown for the mimicked hermaphrodite phantom (average of ADAM and a scaled EVA) and the hermaphrodite phantom used by Jones and Shrimpton (NRPB) [6]. The calculations were performed for a Philips Tomoscan 350 CT scanner, a slice thickness of 5 mm and a CTDI expressed in air of 100 mGy. For the mimicked hermaphrodite phantom, measured (meas.) or calculated (cal.) dose profiles along the fan shaped beam and spectra of Seelentag et al. (3), coded C79 and C80, were employed.

2.4. Patient dose and image quality for computed tomography in several Dutch hospitals

J. Geleijns[1], J.J. Broerse, J. Zoetelief, D. Zweers[1] and J.G. van Unnik[2]

Studies carried out in different countries have shown a relatively high radiation burden to the patient due to computed tomography (CT) examinations and revealed important variations in absorbed dose. Shrimpton et al. (1) concluded that for the population of the United Kingdom the major contribution to the collective dose from diagnostic X rays is due to CT examinations, owing to the relatively high doses incurred and the increasing frequency. In other countries CT examinations might also contribute significantly to the collective dose.

In the past decade, dose reduction has received attention but there is still a potential for optimization of CT techniques. This implies that the procedures to be followed must yield images of a good diagnostic quality at the lowest compatible radiation dose to the patient. Recent information on patient dose due to CT is lacking in The Netherlands. Therefore, a survey of routine CT examinations at a limited number of CT scanners in different hospitals was made. The manufacturer, type and number of scanners included in the study are given in Table 1.

During the survey attention was focused on absorbed dose and image quality met in daily practice at the participating hospitals. The methods employed for the survey of CT scanners had to be practical and to be performed within less than two hours. The Computed Tomography Dose Index (CTDI) (2) was measured free-in-air with a pencil type ionization chamber. These measurements yield dose values related to a single CT scan of one slice whilst radiation exposure of patients due to a complete CT examination preferably should be expressed in terms of organ and tissue doses or effective dose. Organ and effective doses were derived from CTDI by application of published organ dose conversion factors (1, 3). The survey also comprised the assessment of parameters related to image quality, i.e. detail resolution and noise (standard deviation of Hounsfield-Units, HU (4)) associated with the CT scanners and protocols at the different locations.

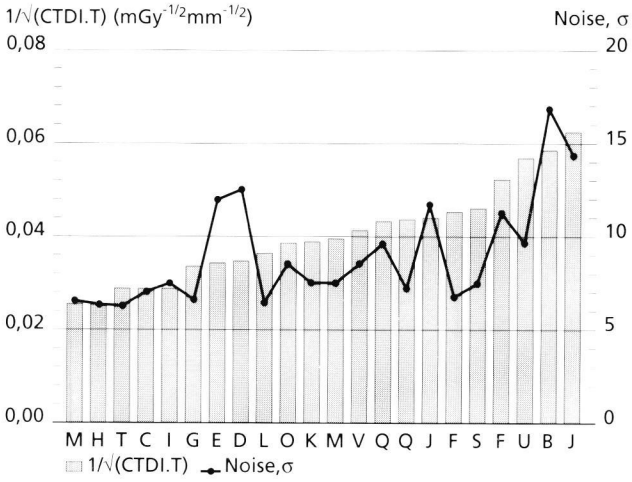

Figure 1. CT abdomen examinations: Parameters 1/√(CTDI.T) and noise (σ) in the centre of an image of a 30 cm cylindrical water phantom

CTDI values for different CT examinations showed variations by about a factor of 5 to 6. For head examinations some high CTDI values, e.g., in excess of 200 mGy, were measured. The radiation burden to the patient due to CT expressed as effective dose varied from 0.7 mSv to 21 mSv (Table 2). Especially for CT body scans effective doses are high compared to, for example, conventional radiography.

For a specific examination such as a CT scan of the head, chest or abdomen, effective dose varied by a factor of 2 to 3. Variations in CTDI values are larger than variations in effective dose. This indicates that CTDI free-in-air

Table 1. Manufacturer, type and number of CT scanners included in the survey

GE PACE	2
GE Sytec 3000	1
Philips Tomoscan 350	3
Philips Tomoscan LX	3
Siemens Somatom Plus	1
Siemens Somatom Plus S	1
Toshiba TCT 600 HQ	2
Toshiba TCT 900 S	1

Table 2. Effective doses calculated for some scanners from CTDI values and organ dose conversion factors

	dose (mSv)		
Scanner	CT Head	CT Chest	CT Abdomen
A	1.5	11	15
B	1.3	13	16
C	1.5	9.2	12
D	0.7	--	9.8
F	2.2	11	21
H	0.9	11	13
I	1.2	6	7.1
J	0.8	10	13
M	0.8	9.5	11
N	0.8	--	--

is not the most suitable parameter for estimations of the radiation risks and it illustrates the importance of the use of CT scanner specific organ dose conversion factors.

In the survey of CT scanners no clear correlation was found between effective dose and image quality quantified as noise (Fig. 1) or high contrast resolution. This might be due to differences in the characteristics of the CT scanners such as the sensitivity of the detector elements or due to differences in the selected radiation quality or image reconstruction algorithms. Variations in noise and high contrast resolution were modest for the different locations. Noise levels were for example at the different locations for CT head 3.4 ± 0.9 H.U., for CT chest 12.1 ± 3.8 H.U. and for CT abdomen 9.2 ± 3.4 H.U. ❑

A full paper on this subject appeared under the same title in Radiation Protection Dosimetry 57, 129-133, 1995.

1. PC Shrimpton, DH Jones MC Hillier, et al. Survey of CT practice in the UK. Part 2: Dosimetric aspects. NRPB-R249, ISBN 0 85951 342 4, 1991.
2. TB Shope, RM Gagne, GC Johnson. A method for describing the doses delivered by transmission X-ray computed tomography. Med Phys 8, 488-495, 1981.
3. M Zankl, W Panzer, G Drexler. The calculation of dose from external photon exposures using reference human phantoms and Monte Carlo methods. Part VI: Organ doses from computed tomographic examinations. GSF-Bericht 30/91, Munich: Gesellschaft für Strahlen- und Umweltforschung, 1991
4. EC McCullough, JT Payne, HL Baker, et al. Performance evaluation and quality assurance of computed tomography scanners, with illustrations from the EMI, ACTA and Delta scanners. Radiology, 120, 173-188, 1976.

[1]) Department of Clinical Oncology, State University of Leiden, The Netherlands
[2]) Onze Lieve Vrouwe Hospital, Amsterdam, The Netherlands

2.5. A model for risk-benefit analysis of breast cancer screening

J. Th. M. Jansen and J. Zoetelief

Breast cancer screening programmes employing mammography are being implemented in various European countries. Different screening protocols are used in demonstration projects and nationwide programmes. To evaluate and improve screening protocols, a computer model for the evaluation of breast cancer screening programme has been developed. The availability of such a model can be of great importance for obtaining a better insight into the influence of various parameters.

The Monte Carlo computer model is based on random selection from distributions of relevant parameters including tumour onset, tumour growth rate, lifetime expectancy, tumour detection size at screening and at spontaneous observation. The radiation risk is calculated for various screening protocols employing multiplicative and additive risk models with risk factors derived from a Canadian study (1) and corrected to mammographic radiation quality (2) combined with lifetime expectancy, number of females screened and an absorbed dose per screening session of 2 mGy. The benefit is calculated on the basis of the reduction in tumour size at detection due to screening compared with spontaneous observation and the survival as a function of tumour diameter based on data of Tabár et al. (3).

Data from the Swedish two-county study are used to validate the model in terms of prevalence (4), interval tumour rates (4) and interval tumour diameter distributions (5). Except for the spontaneous tumour diameter dis-

Table 1. Comparison of the distribution of spontaneous tumour diameters obtained with the simulation of the Swedish two-county study (MBS) with observations of Duffy et al. (5), Coebergh et al. (6) and Buttlar and Templeton (7). Distribution of size of spontaneous tumours given as percentages in various diameter (d) classes

	tumours (%)			tumours (%)	
d(cm)	MBS	Duffy	d(cm)	Coebergh	Buttlar
d<1.0	2.5	7.1 ± 1.1			
1.0 ≤ d < 1.5	8.6	15.4 ± 1.6	d≤2	26	34
1.5 ≤ d < 2.0	13.1	19.7 ± 1.8			
2.0 ≤ d < 3.0	27.1	29.0 ± 2.2			
3.0 ≤ d < 5.0	31.8	20.0 ± 1.8	2<d≤5	44	53
5.0 ≤ d	16.9	8.8 ± 1.2	5<d	30[1]	13

[1] Greater than 5.0 cm plus growing through the skin

Table 2. Comparison of the size distribution of screened and interval tumours obtained with the simulation of the Swedish two-county study (MBS) with the actual observations published by Duffy et al. (5).
Distribution of size of two types of tumours given as percentages in various diameter (d) classes

	screened tumours (%)		interval tumours (%)	
d(cm)	MBS	Duffy	MBS	Duffy
< 1.0	27.2	27.2 ± 2.7	6.6	8.1 ± 1.8
1.0 ≤ d < 1.5	29.2	26.4 ± 2.7	18.0	21.0 ± 2.9
1.5 ≤ d < 2.0	19.5	24.0 ± 2.5	20.6	17.3 ± 2.6
2.0 ≤ d < 3.0	16.7	16.5 ± 2.1	28.9	31.5 ± 3.6
3.0 ≤ d < 5.0	6.4	4.8 ± 1.1	20.1	15.3 ± 2.6
5.0 ≤ d	1.0	1.1 ± 0.5	5.8	6.8 ± 1.7

tribution (Table 1), the model can describe well the results of the Swedish two-county study (e.g., Table 2). Specific information is presented on the distributions of relevant parameters.

Table 3. Simulation of annual screening for a stable Swedish population. Given are absolute numbers of breast tumours per year, when one million women are followed throughout their lives

Age group (year)	Spont. tum.	Screen. tum.	Interv. tum.	Excess tum.	Tum. fatal ind.[1]	Net effect screening tumours[2]
20-24	10	6	5	0	56	-54
25-29	58	34	30	0	18	-8
30-34	208	141	91	0	17	25
35-39	472	355	176	0	7	101
40-44	791	636	264	2	6	186
45-49	1143	1159	313	9	6	352
50-54	1469	1576	232	29	5	502
55-59	1752	1850	251	62	4	581
60-64	1995	2084	268	131	3	625
65-69	2123	2218	270	251	2	615
70-74	2095	2200	254	428	1	534
75-79	1916	2021	226	601	1	407
80-84	1525	1623	173	676	0	254
85-89	995	1078	111	584	0	122
90-94	469	525	52	348	0	39
95-99	122	149	12	120	0	5

[1] Radiation induced fatal tumours, multiplicative risk model with average risk factors

Simulation of screening of a stable Swedish female population (see Table 3) indicates, e.g., that a starting age for screening of 40 years seems optimal. Screening at ages in excess of 80 years results in detection of a high number of tumours that would not cause mortality due to a limited lifetime expectancy. ❑

Full papers on this subject have appeared in: The British Journal of Radiology 68, 141-149 (1995) and Radiation Protection Dosimetry 57, 217-220 (1995)

1. AB Miller, GR Howe, GJ Sherman, et al. Mortality from breast cancer after irradiation during fluoroscopic examinations in patients being treated for tuberculosis. New Eng J Med, 321, 1285-1289, 1989.
2. DJ Brenner, HI Amols. Enhanced risk from low-energy screen-film mammography X rays. Brit J Radiol, 62, 910-914, 1989.
3. L Tabár, G Fagerberg, NE Day, et al. Breast cancer treatment and natural history: new insights from results of screening. The Lancet, 339, 412-414, 1992.
4. NE Day, Screening for breast cancer. Brit Med Bull, 47, 400-415, 1991.
5. SW Duffy, L Tabar, G Fagerberg, et al. Breast screening, prognostic factors and survival - results from the Swedish two county study. Brit J Cancer, 64, 1133-1138, 1991.
6. JWW Coebergh, MA Crommelin, HM Kluck, et al. Borstkanker in zuidoost Noord-Brabant en in Noord-Limburg; beloop van incidentie en vervroeging van de diagnose in een nietgescreende vrouwelijke bevolking, 1975-1986. Ned Tijdschr Geneesk, 134, 760-765, 1990.
7. CA Buttlar, AC Templeton. The size of breast masses at presentation; the impact of prior medical training. Cancer, 51, 1750-1753, 1983.

2.6. An algorithm for solving compartmental models describing the stochastic behaviour of radioactive compounds in the body

A. van Rotterdam

For the evaluation of the effective dose due to of injected, ingested or inhaled radioactive compounds in the body, metabolic models for the retention, deposition, clearance and transport of substances need to be used. These models are, in general, linear compartmental models. Their behaviour can be described by a set of linear first order differential equations. If the parameters of the compartmental model are known, the activities (and the cumulated activities as a function of time) can be readily analytically expressed as a convolution integral of the input (driving function) and the impulse response function. In the case of a model with several compartments, this integral takes the form of a negative exponential matrix function.

A numerical evaluation, however, may cause serious problems in the case that the number of compartments is large (order of magnitude 10 to 100) and the residence times are widely different (stiff system). For instance, the "classical" method of Runge-Kutta (1) is not well suited for the problem mentioned above, because the method requires an inordinate number of steps to achieve stability in a stiff system. Also other methods proposed such as the method of numerical transform inversion (2) and the approximation of the exponential of the parameter matrix (3) are inappropriate because these methods can only be advantageously used in finding solutions in a limited number of time samples for a system excited instantaneously.

Apparently, a part of the problems in numerically evaluating the differential equations lies in the fact that the real solutions are infinitesimally exact and continuous in time. Consequently, numerical solutions can only be

approximations of the exact ones. The question rises whether the approximation of continuous functions is the most useful approach and whether a set of continuous differential equations is the most appropriate description of physical and biological processes, which inevitably have a certain indeterminacy both in time and amplitude.

It will therefore be convenient to refrain from the redundant continuous description and to reformulate the physical and biological problem in the form of difference equations which should not be considered as approximations of the differential equations but as a sufficient description for the problem under study (4, 5). This is done by *a priori* defining a measure of uncertainty in time Δt and assuming that quantities within this interval are not of interest to the observer. The advantage of such a formulation is that the solutions can always be computed directly from the difference equations themselves, even when no analytical solutions are known (4).

For the biokinetic models used in internal dosimetry, some further considerations about the system as well as about the input and output signals can be made. Radioactive decay is a stochastic process. The transport properties of the various organs are only known with finite precision. Also, the amounts of radioactivity taken and transported through the compartments are of a quantal character and can therefore be conceived as a sum of elementary amounts of activity (EAA's).

In conclusion: a realistic compartmental model for the behaviour of radioactive compounds in the body should be a stochastic model which should be based on the following: the biokinetics are sufficiently described at discrete instances of time; the residence times of EAA's in the different compartments are negatively exponentially distributed; the transfer of an EAA from one compartment to all the others is also randomly distributed with probabilities equal to the transfer fractions as given in the deterministic compartmental model.

The behaviour of one EAA through the various compartments of an n-dimensional stochastic compartmental model can be described as follows:

$$(1)\quad y(i;k) = (1-d(i))y(i;k-1) + \Sigma t(i,m)d(m)y(m;k-1) + \delta(i,j)d(k,l)$$

for i:1..n and k≥0. In this expression the product of the two Kronecker delta's ($\delta(i,j)=1$ for i=j and zero otherwise) represents the intake of one EAA in compartment j at time instance l, i.e. at some time within interval $(l\Delta,(l+1)\Delta)$. y(i;k) is the stochastic response function of compartment i (stochastic variables underscored and compartment number and instance variable separated by a semicolon) describing the existence or absence of the EAA in that compartment at instance k. The model is characterized by the random, binary, decay function d(i) and the transit functions t(i,m). The decay variables describe the probability of the exit of the EAA from the various compartments, P(d(i)=1)=d(i), whereas the transit functions t(i,m) denote the possible transfer of the EAA from compartment m to i with probabilities P(t(i,m)=1)=t(i,m).

The expectancies (denoted by angle brackets) of the sum of the stochastic binary responses caused by the consecutive intake of N EAA's in the same compartment in the same instance obey:

$$(2)\quad N\langle y(i;k)\rangle = (1-d(i))N\langle y(i;k-1)\rangle + \Sigma t(i,m)d(m)N\langle y(m;k-1)\rangle + N\delta(i,j)\delta(k,l)$$

for i:1..n, because it can be assumed that the system parameters fluctuate independently from each other and from the inputs.

Equation (2) is of the same form as that describing the responses in a deterministic compartmental model with system parameters d(i) and t(i,m). Hence, it can be concluded that the correspondence principle holds. This means that in the limit of an infinite number of realizations, the averaged responses of a stochastic model approach the deterministic responses of an averaged stochastic model.

The movement of an EAA through the different compartments, in stable systems resulting in an eventual departure from the system, is called a random walk. It is a realization of a stochastic process and can, according to equation (1), be described as follows: The appearance or disappearance of an EAA at compartment i at instance k is called event (i;k). An intake is supposed to occur in compartment one at instance one. In other words, event (1;1) occurs and y (1;1) becomes one. Then, at consecutive instances of time, samples are drawn from the distribution of d(1) until the sample becomes one. When this is the case at instance k event (1;k) causes y(1;k) to be reset to zero because the EAA leaves the compartment. Also at that instance a sample is drawn from an (n-1)-valued distribution with probability t(m;1) that the EAA is transferred to the m'th compartment. Event(m;k) takes place and y(m;k) becomes one because the EAA enters compartment m. Samples are then drawn from the distribution of d(m) to determine the residence time in compartment m.

The random walk can end in a compartment for which the transfer probabilities do not sum up to one and hence, the sample can denote the transfer to outside the model. This is, for instance, the case in models without recycling in which the EAA, once it resides in the last compartment, is bound to leave the system sooner or later. In any case, the decay of radioactive nuclides into stable daughters will cause the random walks in models for internal dosimetry to be of finite duration.

Figure 1 shows the structure diagram of the procedure 'RandomBlockWalks' which can be used to evaluate the responses in stochastic compartmental models with a dimensionality 'dim' (dim≤maxdim) over a fixed interval of time of 'nsp' time samples (instances of time). For time sample counts larger than 'nsp' the procedure has to be incorporated in a repeat loop and called recursively. The

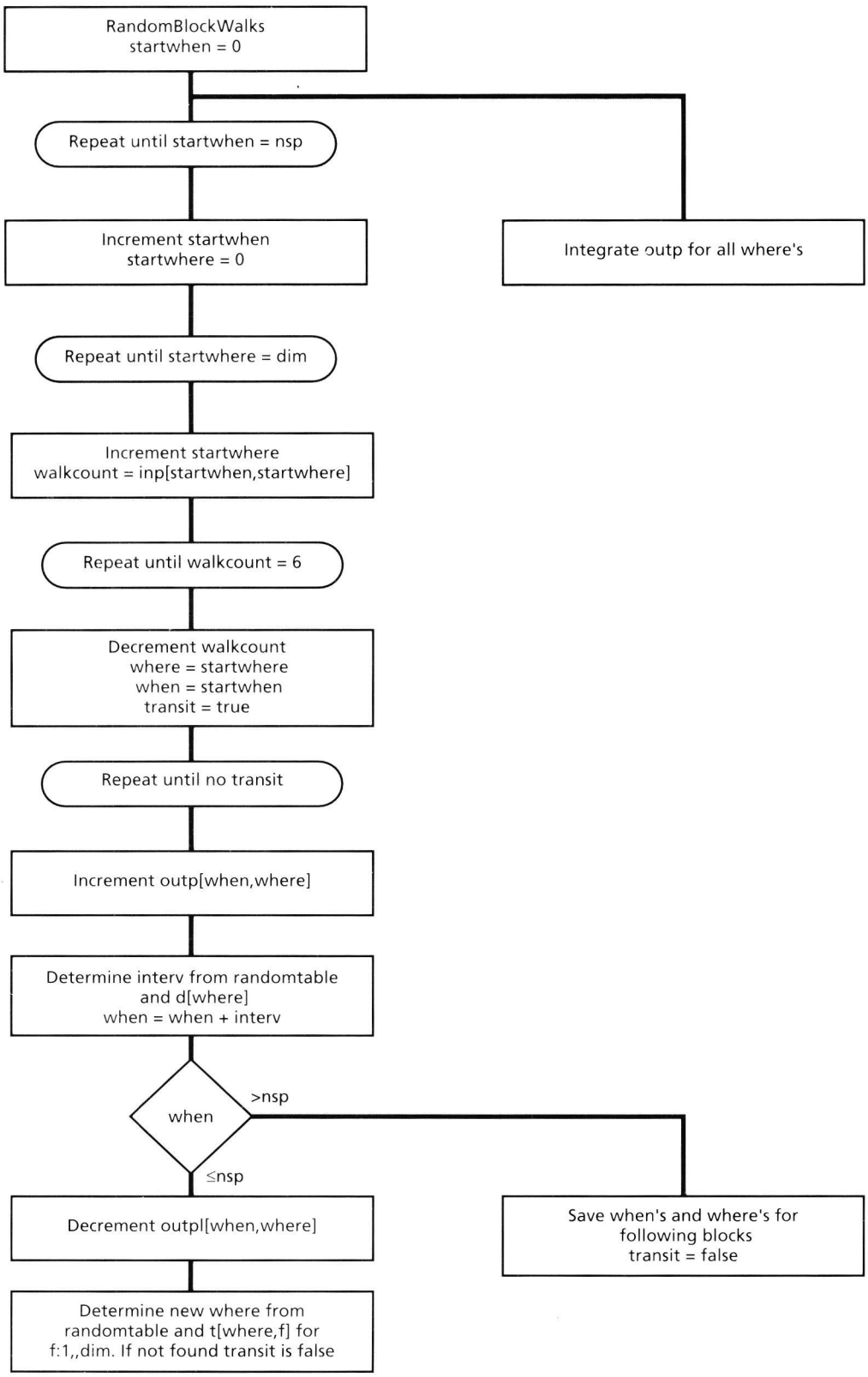

Figure 1. Structure diagram of procedure 'RandomBlockWalks'. The procedure evaluates the blocks of instructions from top to bottom and from left to right. Conditional statements are represented by diamonds, repetative statements by rounded boxes. For reasons of simplicity only the main instructions are shown.

procedure is called with the following variable parameters: intake and response data 'inp' and 'outp' of type array[1..nsp,1..maxdim] of integer; integer scaled decay parameters 'd' of type array[1..maxdim] of integer; transit parameters 't' of type array[1..maxdim,1..maxdim] of integer and integer random numbers, homogeneously distributed over the integer number range (-32768, 32767) and contained in 'randomtable' of type array[1..tablecount] of integer.

As can be seen from Figure 1, in the first two repeat loops 'inp' is scanned for all 'nsp' time samples and 'dim' compartments on the existence of EAA's. In case EAA's are detected, the number of them is stored in the variable 'walkcount' and the walks are evaluated one by one in the third repeat loop. In the fourth repeat loop the individual events in one walk are evaluated with the help of 'randomtable', the decay parameters and the transition matrix. First, the appearance of the EAA at instance 'when' and compartment 'where', i.e. event(when,where), is stored in the output block by incrementing 'outp[when,where]' by one. Next, the residence time 'interv' is evaluated by sampling random numbers from 'randomtable' and comparing them with the decay parameter 'd[where]' for the compartment onder study.

In case the decay out of the compartment takes place within the range '1..nsp' the output at decay time is decremented by one. The transition to a new compartment is then determined by comparing a random sample with the transition parameters for the old compartment. If no transition can be found, the walk is ended. Otherwise a new event in the walk will be computed.

In case the decay occurs after time sample 'nsp' the event is temporarily stored and has to be used in the next call of the procedure. Finally, because only events have been stored in 'outp', the responses have to be obtained by integrating the 'outp' block.

Derivation of the distribution of intervals between decay instances

A binary sequence consisting of events with a time independent, fixed, probability of occurrence d can also be conceived as an interval sequence, denoting the number of time samples between two consecutive events. Assume, an event occurs at a certain time instance. Then the probability of an event at the next time instance is d. Hence P(interv=1)=d. Intervals of duration two are formed by the existence of an event at a certain time instance, the absence of an event at the nex time instant with a probability (1-d) and the occurrence of an event thereafter with probability d. Consequently P(interv=2)=d(1-d). This is readily generalized to $P(interv=k+1)=d(1-d)^k$. A first order deterministic compartment with decay parameter $\lambda=\ln(2)/T1/2$, with T1/2 denoting the halflife time, and instanteneously excited is characterized by the following difference equation:
$y(k)=(1-\lambda\Delta t)\, y(k-1)+\underline{\delta}(k,1)$ in which Δt is the sampling interval. The solution of this equation can be readily found to be $y(k+1)=(1-\lambda\Delta t)^k$, which, in the limit of Δt approaching zero and $k\Delta t=t$, will approach $y(t)=\exp(-\lambda t)$.

It can therefore be concluded that the response of a stochastic compartment with decay probability $d=\lambda\Delta t$ behaves, on average, in a negative exponential way and an EAA has a negative exponential distributed residence time. ❑

1. WH Press, BP Flannery, SA Teukolski, WT Vetterling. Numerical Recipes. Cambridge: Cambridge University Press, 1987.
2. BA Luxon. Solution of large compartmental models using numerical transform inversion. Bull Math Biol 49, 395-402, 1987.
3. A Birchall, AC James. A microcomputer algorithm for solving first-order compartmental models involving recycling. Health Phys 56, 857-868, 1987.
4. A Ralston. Discrete mathematics: The new mathematics of science. Am Scientist 74, 611-618, 1986.
5. A van Rotterdam. Electric and magnetic fields of the brain computed by way of discrete systems analytical approach: Theory and validation. Biol Cybern 57, 301-311, 1987.

3. Environmental protection

Radon is a chemically inert, naturally occurring radioactive gas. The radon concentration in Dutch dwellings ranges from 10 to 140 $Bq \cdot m^{-3}$ with a mean value of about 30 $Bq \cdot m^{-3}$. The main risk to humans is the induction of lung cancer. TNO has reliable measurement techniques for measuring radon concentrations in air as well as in other matrices such as building materials, soil and drinking water. Also computer models have been developed for estimating radon concentrations inside houses and for determining the effect of counter-measures. A radon inhalation facility for animal experiments and a laboratory test dwelling for testing counter-measures are available.

In the following contributions the risk on lung tumour induction in rats will be described. A method has been developed to measure radon daughter concentrations that can be used in the future to evaluate counter-measures in dwellings. In the laboratory test dwelling at Arnhem experiments have been performed to determine the influence of crawl space ventilation on indoor radon concentrations. Radon concentration measurements were carried out in dwellings in the building project *Ecolonia* in the Dutch city Alphen aan den Rijn. A survey of recent epidemiological literaure on the association between radon and lung cancer and a model to predict hormesis in radon carcinogenesis will be discussed in the last two contributions.

3.1. Lung tumour induction in rats after radon exposure

R.W. Bartstra and P.A.J. Bentvelzen

In the past, exposure of Sprague Dawley rats to high concentrations of Rn-222 in the TNO radon inhalation facility have yielded markedly different results as compared to those obtained by other laboratories, e.g. COGEMA in Razes, France. Table 1 summarizes the results of the TNO study and the corresponding results as obtained by COGEMA, both with respect to malignant lung tumour induction and to lifespan-shortening. In the French laboratory control rats and rats exposed to doses up to 2000 Working Level Months (WLM) live 90 - 120 weeks in average. It can be concluded from Table 1 that in the TNO study, as compared to the COGEMA results, hardly any tumours appear at higher doses, whereas at the same time severe lifespan-shortening occurs. In view of this last phenomenon, the observed low incidence of tumours is not surprising, since the latency time for lung tumours in rats is over one year. The lifespan-shortening itself, however, could not readily be explained, as different causative factors could be envisaged, like genetic differences between the TNO and COGEMA Sprague Dawley rat lines or differences in exposure conditions.

In a cross experiment, Sprague Dawley rats from TNO have been exposed to 1000 WLM in the COGEMA inhalation facility in France, and taken back again to TNO after the exposures. In this experiment, no lifespan-shortening could be observed. Histopathological examination of lung lesions, which at present has nearly been completed, indicates a malignant lung tumour incidence of 30-40 per cent. These results are all in good agreement with the COGEMA results of Table 1, clearly indicating that genetic differences between the TNO and COGEMA rat lines cannot be an explanation for the discrepancy of Table 1 between the TNO and COGEMA results. Survival curves of this cross-experiment and the earlier 1600 WLM-experiment can be found in Figure 1.

Another aspect influencing the results could be the fact that TNO and COGEMA have very different exposure conditions in their inhalation facilities. In the TNO facility, air is continuously being refreshed and filtered in which process most naturally occurring aerosols are being removed from the air. As a result, a very high unattached fraction and a very low equilibrium factor exists in the TNO facility. In the COGEMA inhalation chamber, which is much larger than the TNO chamber, no additional air-handling is necessary, and the presence of natural aerosols results in a radon atmosphere with a relatively low unattached fraction and high equilibrium factor. Because of these physical differences, similar radon concentrations will lead to different lung doses, and for this reason TNO has chosen lung dosimetry, instead of radon (daughter) concentration, as a starting point in the assessment of cumulative radon exposure.

To examine the possible influence of exposure conditions, TNO has started during 1994 and 1995 a new series of experiments, in which rats have been exposed to 1600 WLM. For some groups, however, exposure conditions have been changed by supplying additional aerosols to the circulating air in the inhalation chamber, thus mimicking the exposure conditions of the COGEMA inhalation facility. All exposures have been completed by July 1995, and at present all animals are at least one year of age. Definite results on lung tumour incidences will not be available until 1997, but preliminary results so far on survival time clearly show that the presence or absence of aerosols has a dramatic effect on animal lifespan (see Fig. 2). Without aerosols, substantial lifespan-shortening in radon exposed rats can again be observed at 1600 WLM, as in the earlier experiments. The additional supply of aerosols, however, definitely increases the lifespan of exposed rats. So far, no statistical significant discrepancies between the aerosol

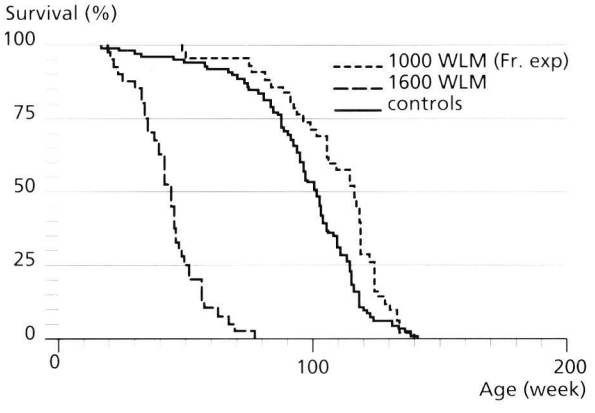

Figure 1. Data showing survival curves of rats after radon exposure of 1600 WLM in the Rijswijk radon inhalation facility, and 1000 WLM using the inhalation facility of COGEMA, France.

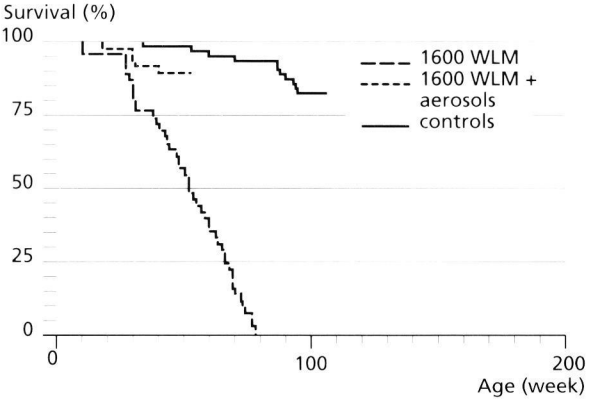

Figure 2. Survival of rats after radon exposure of 1600 WLM, with and without additional supply of aerosols.

group and controls can be observed (p=0.025), whereas the difference between the aerosol group and the non-aerosol group is highly significant (p=0.001). It can therefore be concluded that aerosols play an important role in the health effects of radon exposure.

Histopathological analysis of the dead rats revealed that they usually died from aspiration pneumonia. It is assumed that in the absence of aerosols the nose of the rat will be exposed to considerably higher doses due to deposition of unattached radon daughters. Histopathological examination of the nose revealed metaplastic changes of the nasal epithelium, presumably caused by the high doses of radon daughters. It is hypothesized that the disappearance of cilia from the metaplastic cell layers allows commensal micro-organisms such as Staphylococcus bacteria to invade the lungs and to cause fatal pneumonia. ❑

Table 1. Malignant lung tumour incidence and lifespan-shortening after exposure of rats to radon with different total doses, as obtained by TNO and by COGEMA, France

	Lung tumour incidence (%)		Median lifespan (week)	
Dose (WLM)	TNO	COGEMA	TNO	COGEMA
0	0	0	103	93
200	10	12	100	95
800	8	25	80	99
1600	0	40	45	90

3.2. Radon daughter measurements

R.W. Bartstra, P. de Jong and H.B. Kal

Enhanced indoor concentrations of radioactive radon gas and its daughter products are a potential threat to public health, and are therefore a major issue in environmental radiation protection. Mitigation of daughter concentrations of Rn-222 in homes and buildings may be realized by several air-cleaning techniques. Testing the efficacy of such techniques involves the assessment of radon daughter concentrations, and the change of those due to the applied technique. In the usual Dutch indoor environment, these concentrations are usually very low, and a practical test therefore involves the use of very sensitive methods for measuring radon daughters.

For this purpose, we have developed an experimental method for the assessment of low concentrations of radon daughter activity in air (1). It allows for the determination of both attached and unattached activity concentrations of the individual radon daughters Po-218, Pb-214 and Bi-214, and for the calculation of the attached and unattached potential alpha energy concentration (PAEC) as expressed in radon equilibrium-equivalent concentration (Rn-EEC).

The method involves collection of radon daughter activity on a filter by air sampling, and subsequent measurements of the filter activity using alpha spectroscopy and a two-count measuring regime, as has been described by Nazaroff et al. (2). Discrimination between attached and unattached activity is accomplished by mounting a gauze in front of the sample filter. The gauze will collect (part of) the unattached fraction. When the collecting efficiencies of gauze and filter are known for both the attached and unattached fractions, separate and simultaneous counting of gauze and filter activities will allow for the

Table 1. Theoretical detection limits for sampling times of 5, 10 and 20 minutes. These concentrations may be discriminated from 0 Bq•m^{-3} with 95 per cent certainty

sampling time (min)	radon daughter	concentration (Bq•m^{-3}) unattached	attached	total
5	Po-218	20	15	8
	Pb-214	5	4	2
	Bi-214	5	4	2
	Rn-EEC	2	1,5	0,8
10	Po-218	15	10	5
	Pb-214	3	2	1,5
	Bi-214	3	2	1,5
	Rn-EEC	1	0,8	0,5
20	Po-218	15	10	5
	Pb-214	2	1,5	1
	Bi-214	2	1,5	1
	Rn-EEC	0,8	0,5	0,3

Table 2. Theoretical values of the resolving power for sampling times of 5, 10 and 20 minutes at a radon concentration of 20 Bq/m^3 (see text). These values are concentration differences that can theoretically be detected with 95 per cent certainty

sampling time (min)	radon daughter	concentration (Bq•m^{-3}) unattached	attached	total
5	Po-218	20	20	15
	Pb-214	7	10	9
	Bi-214	7	10	9
	Rn-EEC	2	4	4
10	Po-218	15	15	12
	Pb-214	5	8	7
	Bi-214	5	8	7
	Rn-EEC	1,5	3	3
20	Po-218	15	15	12
	Pb-214	3	7	6
	Bi-214	3	7	6
	Rn-EEC	1	3	3

determination of attached and unattached fractions of the individual radon daughters.

The sensitivity of the method will depend on the sampling volume, and hence on the sampling time, which typically will be 5-20 minutes. For several sampling times, theoretical detection limits for radon daughter concentrations have been estimated, which can be found in Table 1. Also, the resolving power, which is the ability to assess concentration differences, has been theoretically estimated for a radon concentration of 20 Bq • m^{-3} with an equilibrium factor of 1.0 and an unattached fraction of 5 per cent for all daughters. Values for the resolving power can be found in Table 2.

One complete measurement, including air sampling for 10 minutes and counting of the samples, will approximately take one hour to perform. ❑

1. RW Bartstra, P de Jong, HB Kal. Ontwikkeling van een meetmethode voor de bepaling van activiteitsconcentraties van radondochters in lucht.
TNO rapport nr. RD-I/9601-364, 1996.
2. WW Nazaroff, AV Nero, KL Rezvan. Alpha spectroscopic techniques for field measurement of radon daughters. Second special symposium on natural radiation environment, Bombay. CONF 810153-1, KG Vohra et al. eds. New Delhi: Wiley Eastern Lim, pp 350-357, 1982.

3.3. Radon counter-measures

W. van Dijk and P. de Jong

A number of radon counter-measures were evaluated in a radon test facility. This facility consists of two enclosed spaces, simulating a living room with a crawl space beneath. The crawl space is 1 m high, the living room is 2.6 m high. Both spaces have dimensions of approximately 3.5 m x 2 m. The two spaces are separated by a concrete floor, 15 cm thick; the air-permeability of this floor can be fully regulated. In the crawl space, phosphogypsum blocks with a total source strength of about 800 Bq/h radon-222 have been installed. The house is equipped with a climate control unit, which can regulate the temperature and relative humidity. Temperature, relative humidity, radon concentrations, volume air flows, differential pressure across the concrete floor and other data are collected by an acquisition system and recorded.

The facility enables the effectiveness of diverse radon-reducing measures to be tested quickly, under precisely defined and strictly controlled conditions.

The following radon counter-measures were tested:
- Increased crawl-space ventilation.
- Use of polyurethane foam and sealant to seal openings in the concrete floor.
- Use of polyethylene film to reduce radon infiltration from the crawl space.

Three options were examined:
- Film applied to the under-surface of the ground floor.
- Film applied to the under-surface of the ground floor with additional ventilation provided (creating a so-called pressure lock floor).
- Film spread over the ground beneath the crawl space.

The results of these tests were as follows:
- The more permeable the floor, the more efficient increased ventilation was observed. It was also found that ventilation was more effective at lower ventilation rates than at higher rates (Fig. 1).
- The use of polyurethane foams and sealants proved to be effective for sealing seams, cracks and conduits. All the materials tested reduced the passage of air through the floor to levels well within the requirements of the building regulations.
- Depending on the permeability of the concrete floor prior to application of the film, the effectiveness of film on the under-surface of the floor varied between 20 per cent at 1 BRL and 85 per cent at 6 BRL (BRL, building regulations level, is the permeability of the floor of $2 \cdot 10^{-5}$ $m^3/(m^2 \cdot s)$ at a pressure difference of 1 Pa).

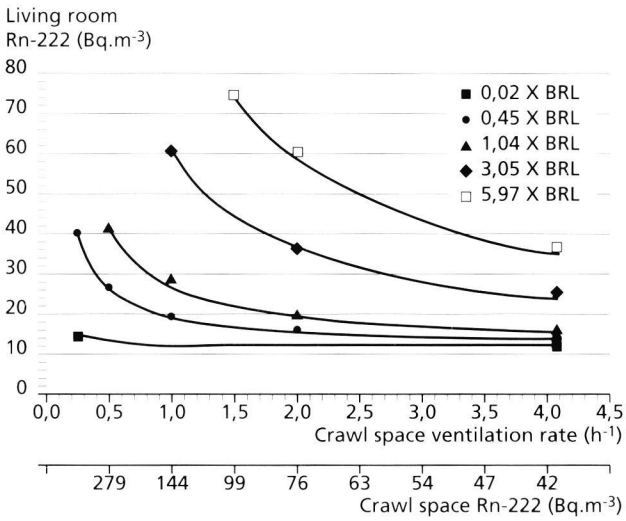

Figure 1. The influence of the crawl space ventilation rate on radon-222 concentration in the living room at different ground floor permeabilities and in the crawl space for a Ra source of 800 Bq/h. BRL, building regulation level = permeability of a floor of $2 \cdot 10^{-5}$ $m^3/(m^2 \cdot s)$ at a pressure difference of 1 Pa.

The pressure lock floor was highly effective: the radon concentrations in the living room were the same as those in the air supply. For the film spread across the ground of the crawl space a differential pressure of about 2 Pa across the film was assumed. This figure was considered to be realistic for buildings in The Netherlands. On this basis, the effectiveness of the technique, which was not influenced by the permeability of the concrete floor, proved to be 25 per cent.

It should be noted that these results were obtained under controlled conditions in the laboratory house. In practice, the effectiveness of a given measure may vary. ❑

3.4. Radon measurements in dwellings in the building project Ecolonia

P. de Jong and W. van Dijk

Ecolonia is a residential area in the Dutch community Alphen aan den Rijn (Alphen-on-Rhine), where 101 homes are built according to nine different designs. The objective of this demonstration project was to show that, with the present-day knowledge, it is possible to construct houses in a more environment-minded fashion than before. It is presumed that this project would stimulate the construction of houses in The Netherlands in a way which is compatible with environmental protection and energy conservation. Nine architects worked out the three main lines of the Dutch National Environmental Policy Plan: reduction of energy consumption, integral chain control and advancement of quality.

In the evaluation phase of this building project, a research programme was performed in which a number of parameters were verified in relation to the design. Among these parameters were air-tightness, temperature distribution, relative humidity, comfort, noise transmission and concentrations of volatile organic compounds. TNO-CSD was involved in tracing the radiation burden to the occupants of dwellings in this project, subdivided into (a) the internal radiation dose due to inhalation of radon progeny and (b) the external dose rate due to gamma-ray emitting nuclides in building materials and soil.

Both components were examined separately in three houses of each design in the crawl space, the living room and a first floor bed room. The radon concentration was determined for one year using radon track etch detectors, whereas the radiation field in the dwellings was determined by thermoluminescence dosimetry. The main conclusions that could be drawn from the results are:

- The radiation dose to the inhabitants of *Ecolonia* as a result of inhalation of radon daughters is 15 per cent lower than the average value found in the Dutch national survey performed in 1984.
- Rather large differences in radon concentrations were observed between the different designs: the radon concentration averaged per design in the living room ranges from 10 - 60 Bq • m^{-3}; in the bedrooms from 10 - 30 Bq • m^{-3}.
- The lowest radon concentration in both living room and bedroom is found in houses built according to a timber frame building system with timber floorings and inner walls made of flue gas desulphurization gypsum byproduct.
- In one design, a relative high radon concentration was found in the crawl space. However, this did not result in higher indoor radon levels: 15 Bq • m^{-3} in average in the living room. Obviously, this design is characterized by an air-tight ground floor. The high crawl space concentrations appeared to be caused by stopped gratings in all three dwellings.
- Radon concentrations in the crawl space are normally elevated with respect to living rooms.
- The average effective external dose rate in the living rooms is 0.48 mSv/a (relative standard deviation 10%), which is almost the same as the average value in the open air (0.50 mSv/a).
- The contribution of the applied building materials to the effective external dose rate in the living room is estimated at 0.27 mSv/a (range 0.17 - 0.33 mSv/a). This value is about 25 per cent lower than the Dutch national average value. ❑

3.5. Survey of epidemiological literature since 1990 on the association between radon and lung cancer

P.A.J. Bentvelzen, A. van Rotterdam and R.W. Bartstra

Radioactive radon (Rn-222) is an inert gas that can percolate through the earth's crust and accumulate in underground mines and residential dwellings. Rn-222 in dwellings is the dominant source of exposure to ionizing radiation in most countries. The average radon concentration in houses varies from 20 Bq • m^{-3} in the United Kingdom, to 30 in The Netherlands, to 40 in the USA and to 100 in Sweden.

It has been convincingly demonstrated that the high concentrations of Rn-222 in mines (at least 2 kBq • m^{-3}) are associated with elevated risks of lung cancer. A recent combined analysis of eleven cohorts of miners from all over the world indicated a dose-effect (lung cancer risk) relationship which was not significantly deviant from linearity (1). On the basis of linear extrapolation of the miners data to low Rn-222 concentrations in dwellings it was estimated that in the United States approximately 10 per cent of all lung cancer deaths would be due to indoor radon (1). The same would hold true for The Netherlands (2).

In order to establish the lung cancer risk in relation to indoor radon case-control studies have been carried out in which radon concentrations are determined for a prolonged period in as many houses as possible of lung cancer patients and age- and sex-matched controls. Before 1990 several case-control studies can be regarded as being inadequate because only a few residences were taken into consideration, radon concentrations were determined for a short period and the strong confounding factor smoking was not dealt with in a statistically appropriate way (3).

From 1990 onward, six case control studies have been published, which may be regarded as having been carried out in an acceptable way. The results of the six studies are as follows:

- *Women in the American State New Jersey.* A weak but statistically significant positive association ($p = 0.04$) was found from 37 Bq • m^{-3} onward (3).
- *Women in Shenyang, capital of the Chinese province Laoning.* A negative but statistically not significant association was found (4).
- *Women in the Swedish county Stockholm.* A weak but statistically significant positive association was found from 76 Bq • m^{-3} onward (5).
- *Men and women all over Sweden.* In the concentration interval 140-400 Bq • m^{-3} a significantly increased relative risk (RR) of 1.3 was found. In the category > 400 Bq • m^{-3} an RR of 1.8 was obtained (6).
- *Nonsmoking white women in the American state Missouri.* No statistically significant association was found (7).
- *Men and women in the Canadian town Winnipeg.* No association was found between the degree of exposure to Rn-222 and lung cancer risk (8).

A combined analysis of these six studies will not provide an indication of an elevated RR for radon concentrations lower than 150 Bq • m^{-3}. However, this does not contradict the hypothesis of linear extrapolation.

Another epidemiological approach is the ecological study in which average radon concentrations in houses in different geographical areas are related to lung cancer mortality data of these regions.

In many of such ecological studies no actual measurements of radon concentrations in houses have been performed, but only information was provided on surrogate markers such as the radium concentration in the drinking water or the nature of the soil in a given area. The confounding factor smoking and mobility are often not dealt with. Such ecological studies are regarded as being uninformative (9).

Recently, Cohen (10) concluded a survey of radon concentrations in 1729 American counties comprising 90 per cent of the US population (10). This included more than 400,000 measurements. The comparison of mean radon concentrations with lung cancer mortality per county resulted in a strong negative association over a range from 20 to 240 Bq • m^{-3}. In order to exclude mobility as a confounding factor he excluded counties in Florida, Arizona and California and furthermore assumed that for the remaining part of the USA people in average have lived 70 per cent of their lifetime in the county they die in. Correction for smoking was based on information about tobacco consumption (available per state, not per county) taking into account the rate of urbanization of a given county. The correction affected the negative association, but this remained statistically significantly negative. A great number of socio-economic variables did not influence the negative relationship between radon concentrations and lung cancer mortality.

This study raises serious doubts about the applicability of the linear extrapolation - no threshold hypothesis, to residential radon in the concentration range 20-140 Bq • m^{-3}. ❑

1. JH Lubin, JD Boice Jr, C. Edling, et al. Lung cancer in radon-exposed miners and estimation of risk from indoor exposure. J Nat Cancer Inst 87, 817-827, 1995.
2. LH Vaas, HB Kal, P de Jong, W Slooff (ed.). Integrated Criteria Document Radon. Nat Inst Public Health Environm Prot. Bilthoven, The Netherlands, 1993, Report 7104401021.
3. JB Schoenberg, JB Klotz, HB Wilcox, et al. Case-control

study of residential radon and lung cancer among New Jersey women. Cancer Res 50, 6520-6524, 1990.
4. WJ Blot, Z-Y Xu, JD Boice Jr, et al. Indoor radon and lung cancer in China. J Nat Cancer Inst 82, 1025-1030, 1990.
5. G Pershagen, Z-H Lian, Z Hrubec, et al. Residential radon exposure and lung cancer in Swedish women. Health Physics 63, 179-186, 1992.
6. G Pershagen, G Akerblom, O Axelson, et al. Residential radon exposure and lung cancer in Sweden. New Engl J Med 330, 159-167, 1994.
7. MCR Alavanja, RC Brownson, JH Lubin, et al. Residential radon exposure and lung cancer among non-smoking women. J Nat Cancer Inst 86, 1829-1837, 1994.
8. EG Létourneau, D Krewski, NW Cho, et al. A case-control study of residential radon and lung cancer in Winnipeg, Manitoba. Am J Epidemiol 140, 310-322, 1994.
9. CA Stidley and JM Samet. A review of ecologic studies of lung cancer and indoor radon. Health Physics 65, 234-251, 1993.
10. BL Cohen. Test of the linear-no threshold theory of radiation carcinogenesis for inhaled radon decay products. Health Physics 68, 157-174, 1995.

3.6. Prediction of hormesis in radon carcinogenesis

R.W. Bartstra

Risk assessment in radon carcinogenesis is extremely difficult in the low dose region of environmental exposure. Therefore, risk factors for indoor radon traditionally have been based on data from highly exposed underground miners, employing the concept of linear extrapolation in order to obtain risk estimates in the low dose region. This concept, however, is becoming a matter of scientific controversy. Moreover, epidemiological data have recently become available that show a *negative* correlation between radon exposure and lung cancer risk for radon concentration to 200 $Bq \cdot m^{-3}$, thus suggesting the possibility of hormesis for indoor radon exposure (1).

The idea of radiation hormesis has not been generally accepted; an important reason for this being the fact that a solid scientific explanation for the effect has not yet been given. Therefore, we have investigated whether a negative correlation between low level radon exposure and lung cancer risk can be explained from a theoretical point of view.

We have constructed a biologically based mathematical model of lung cancer induction, describing the kinetics of cell transformation events leading to cancer (Fig. 1). Normal pulmonary stem cells may undergo spontaneous or radon induced mutations -with frequencies of $\mu_0(a^{-1})$ or ρ_0 (a^{-1} per $Bq \cdot m^{-3}$ radon)-, respectively, resulting in a transition of a cell to the second (or third) compartment of the model. The third compartment is assumed to describe a biological phenomenon known as hyperplasia. Hyperplastic cells are often considered to be pre-malignant: they do proliferate but only at a slow rate and without exhibiting the specific characterics of truly malignant cells, such as infiltration. Hyperplastic cells may or may not develop into a malignancy. This process is described in our model by the transition from the third to the fourth compartment (with probability μ_H (a^{-1}) for spontaneous transitions and $\rho_H(a^{-1}$ per $Bq \cdot m^{-3})$ for radon induced transitions). Malignantly transformed cells are assumed to always give rise to lung cancer, the time lag of which is neglected in the model calculations. Proliferation of hyperplastic cells is incorporated into the model by assuming that those cells will divide and multiply spontaneously with growth rate $H(a^{-1})$, giving rise to an exponentially expanding clone of hyperplastic cells. On the other hand, this exponential expansion is tempered by the possi-

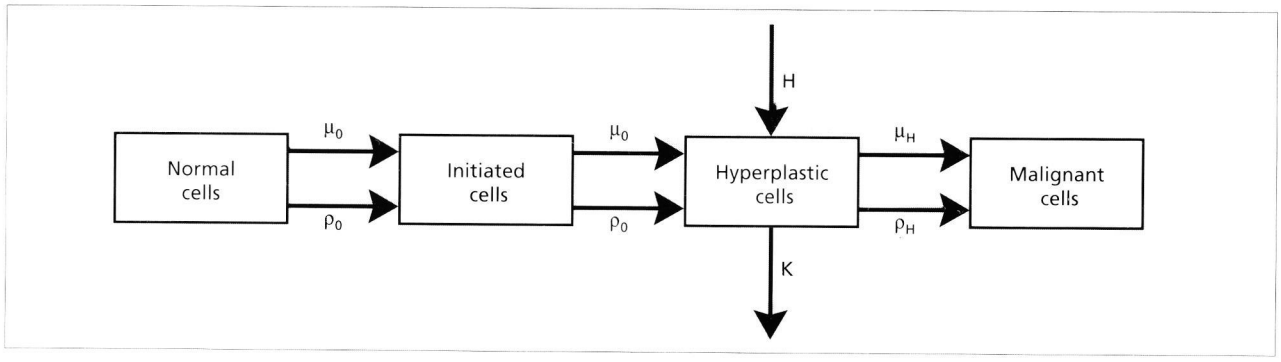

Figure 1. Three-compartment model of lung cancer induction by radon exposure. Essential to the model is the stage of hyperplastic cells, exhibiting constant clonal expansion with rate H (a-1), and from which cells may be removed by cell kill from a-particle hits with rate K (a^{-1} per $Bq \cdot m^{-3}$). The rates μ and ρ are the spontaneous, respectively radon-induced, mutation frequencies ultimately leading to malignantly transformed cells. It is assumed that, once malignantly transformed, a cell will inevitably develop into a malignant lung tumour.

bility of radon-induced cell loss with probability K(a^{-1} per $Bq \cdot m^{-3}$), due to the high probability of cell (reproductive) death after an α-particle hit. Cell losses in the other compartments are either assumed to be compensated by homeostasis (normal cells and second compartment), or merely affect the lag time (which is neglected) between the appearance of a malignant cell in the fourth compartment and the moment the resulting tumour will be detected.

The parameters of the model have been fitted to three sets of data: age-specific incidence of lung tumours among men in the UK (Fig. 2); relative risk of lung cancer in radon exposed miners (Lubin data; Fig. 3); and relative risk of male lung cancer in US counties in relation to average radon levels in these counties (Cohen data; Fig. 4). The fit of Figure 2, in which a radon level of 0 $Bq \cdot m^{-3}$ for reasons of simplicity has been assumed, provides numerical values for the parameters μ_0, μ_H and H. The fits of Figures 3 and 4 provide numerical values for ρ_0, ρ_H and K. All numerical values obtained seem to be reasonable, or to agree with values that are more or less known from literature. The quality of the fit is quite good for Figures 2 and 3. In Figure 4 the hormetic data only seem to be simulated by the model in a qualitative way, but the goodness of the fit may improve considerably, when instead of simulating exposure to one single (average) radon level, a *distribution* of radon levels is simulated corresponding to that same average value. Such distributions are much more realistic in describing the true exposure of a population in a

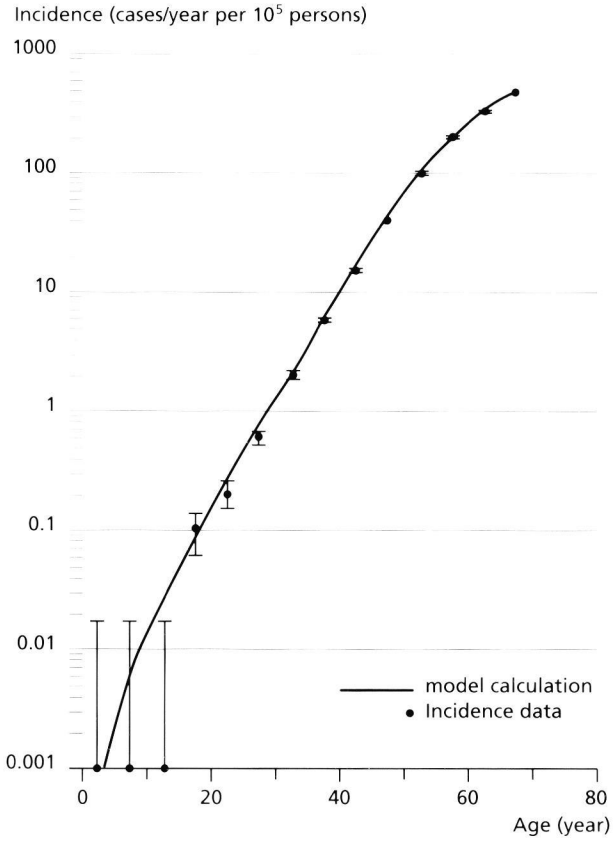

Figure 2. Model calculations, fitted to age-specific lung tumour incidence among UK males (2).

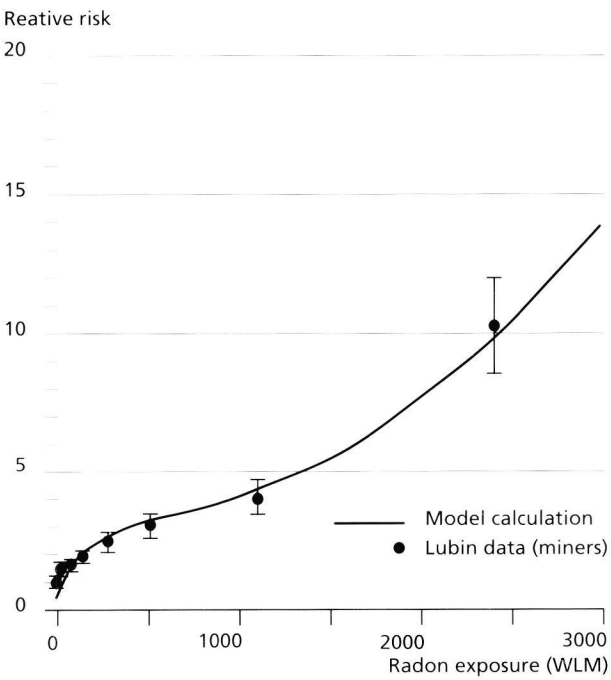

Figure 3. Model calculations, fitted to relative risks among radon exposed miners (2).

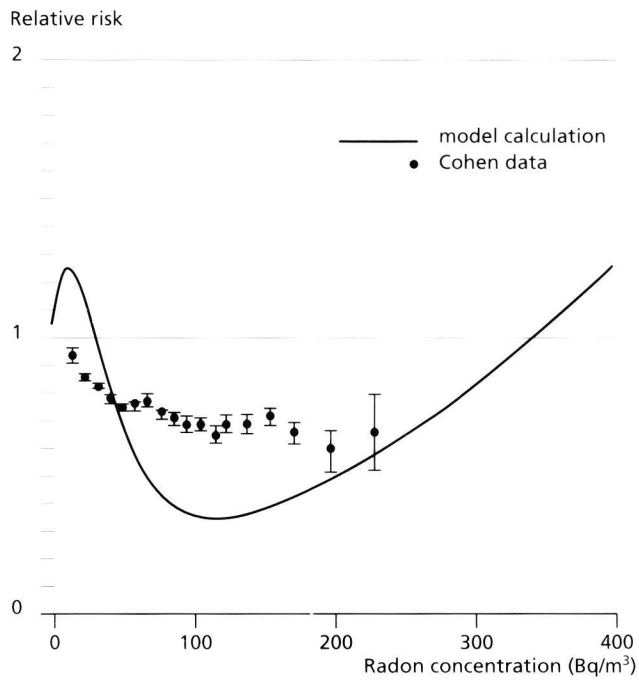

Figure 4. Model calculations, fitted to relative risk of male populations of US counties in relation to the average radon concentration in these counties (1). The fitted curve will become less pronounced (and thus the agreement with the data will improve) when a distribution of radon levels is simulated.

county with a certain average radon concentration.

It may be concluded that hormetic effects can indeed be described by a biologically based theoretical model, and that such a model at the same time may describe correctly the effects that have been found at much higher radon doses. Therefore, there seem to be no reason to reject a negative correlation between radon exposure and lung cancer risk on a theoretical basis only. ❑

1. BL Cohen. Test of the linear-no threshold theory fo radiation carcinogenesis for inhaled radon decay products. Health Physics 68, 157-174, 1995.
2. Office of Population Censuses and Surveys. Mortality statistics: Area: 1980, 1981, 1982, 1983. Series DH5 no 7. London: HMSO, 1985.
3. JH Lubin, JD Boice Jr, C Edling, et al. Lung cancer in radon-exposed miners and estimation of risk from indoor exposure. J Nat Cancer Inst 87, 817-827, 1995.

4. Radiation dosimetry research

The development and improvement of dosimetric methods is a general task of TNO-CSD. Adequate dosimetry is required for studies in all fields of radiological protection, i.e., protection of workers, patients, the general public and the environment.

The first contribution (4.1) refers to the use of ionization chambers in diagnostic radiology. Section 4.2 on neutron W-values is a spin-off of work carried out in the past on neutron dosimetry with ionization chambers. In section 4.3 a study is presented on conversion factors which can be used to derive organ and effective doses from fluence measurements in the case of exposure to electrons. The field of application concerns the protection of both the worker and members of the general public.

4.1. General ion recombination in air-filled ionization chambers

J. Geleijns[1], J.J. Broerse and J. Zoetelief

Ionimetric methods, which are based on collection of the charge produced by ionizing radiation in the air-filled cavity, are often applied for dose measurements in diagnostic radiology. Incomplete charge collection can occur due to recombination of positive and negative charge carriers, i.e. ions and electrons. Collection efficiency (f) depends on the geometry and dimensions of the ionization chamber, the collecting potential, exposure time, and exposure conditions. Wagner (1) reported on the relative dose rate dependence of a large number of diagnostic dosimeters. He concluded that recombination losses can be significant under diagnostic radiology conditions. At dose rates of 190 mGy/s, that may occur during some examinations, these losses amounted up to 25 per cent and more. Wagner normalized the dose rate dependence of each ionization chamber to unity at a dose rate of 17.5 mGy/s. A disadvantage of this method is that it yields therefore only relative recombination losses. Another disadvantage is that Wagner did not make a distinction between pulsed and continuous radiation although both exposure conditions require different theoretical models.

In this study general recombination was investigated for a number of ionization chambers of different dimensions (Table 1) at various irradiation conditions. Simple methods were proposed for estimating recombination losses of ionimetric dosimeters exposed to pulsed or continuous radiation.

The ion transit time is defined as the maximum time that ions need, after production, to reach the collecting electrode. For small ionization chambers, such as the 0.6 cm^3 Farmer type and the 15 cm^3 Keithley ionization chamber, ion transit time will be much shorter than the pulse duration under conditions relevant for diagnostic radiology (continuous radiation). For larger ionization chambers, such as the NE 35 cm^3 ionization chamber and the 600 cm^3 Keithley scatter chamber, the ion transit time can be of the same order of magnitude as the pulse duration, or even longer (pulsed radiation). Figures 1 and 2 show graphs of the inverse of the collection efficiency as a function of absorbed dose rate (continuous radiation model) or absorbed dose (pulsed radiation model). In all graphs experimentally determined values of 1/f that are assessed from measurements at various collecting potentials are shown. Measurements of 1/f that were derived from measurements at constant collecting potentials while exposing the ionization chamber to several dose rates (Fig. 1) or doses (Fig. 2) are also shown. Finally are drawn in the figures the theoretical graphs of 1/f versus dose rate or versus dose.

For the NE 35 cm^3 ionization chamber ion loss, due to general recombination, varies from 1 to 20 per cent at 1 m from the focus under diagnostic conditions. At shorter distances to the focus and for a larger tube current, considerably more recombination will occur. For the smaller Keithley 15 cm^3 parallel plate and the NE 0.6 cm^3 ionization chamber, recombination losses are negligible under diagnostic circumstances. Scattered radiation is often measured with large ionization chambers, such as the

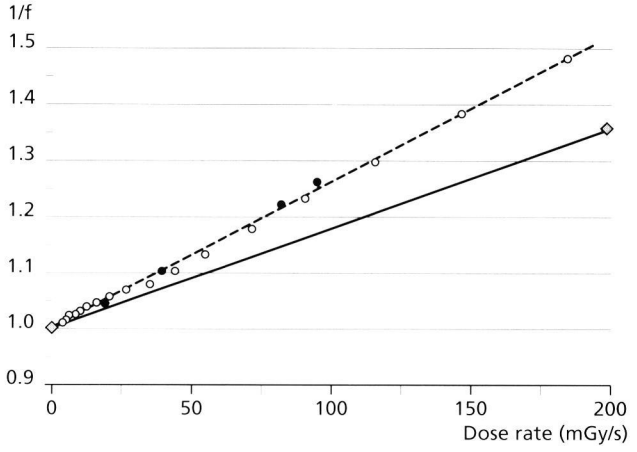

Figure 1. Recombination in the 35 cm^2 ionization chambers exposed to continuous radiation. Experimental values determined from measurements at different collecting potentials (•) and determined from measurements at different dose rates (o). Fit of experimental data (dotted line) and the theoretical estimation of recombination (solid line).

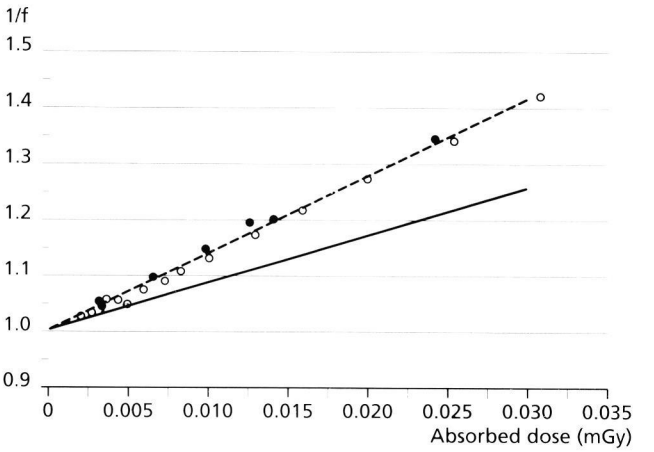

Figure 2. Recombination in the 600 cm^2 ionization chambers exposed to pulsed radiation. Experimental values determined from measurements at different collecting potentials (•) and determined from measurements at different dose rates (o). Fit of experimental data (dotted line) and the theoretical estimation of recombination (solid line).

Keithley 600 cm^3 ionization chamber. For this ionization chamber, recombination losses become considerable (i.e. in excess of 30%) for continuous radiation when the dose rate of scattered radiation exceeds 0.05 mGy/s. At short exposure times, recombination is described by the pulsed radiation model, and recombination losses become considerable at doses of 0.02 mGy.

In this study, two methods were applied to estimate ion recombination. The first one was based on measurements at different collecting potentials, the second one on measurements at different dose rates or different doses. With both methods it was possible to estimate ion recombination but the second method (varying dose rates or doses) has as an advantage that it can also be used for dosemeters which do not offer the option of varying the collecting potential of the ionization chamber as is the case for most dosemeters used at diagnostic departments. Calculation of recombination losses from theoretical models did not yield similar results as obtained by measurements. Reasons for these deviations may be differences between actual and nominal dimensions and volumes of the ionization chambers, errors in the shape and deviations of the shape of the ionization chambers from the supposed perfect cylindrical or parallel plate geometry. Corrections for recombination losses should therefore be based on experimental verification rather then on theoretical models. ❑

[1]) Department of Clinical Oncology, State University of Leiden, The Netherlands

1. LK Wagner. Energy and rate dependence of diagnostic x-ray exposure meters, Medical Physics, 15, 749-753, 1988.

Table 1. Some characteristics of the ionization chambers used for the measurement of recombination

Manufacturer and model	sensitive volume (cm^3)	Inner radius of outer electrode (cm)	Outer radius of inner electrode (cm)	Effective electrode distance (cm)	Calibration factor (mGy/nC)	Collecting potential[2] (V)
NE type 2571	0.69	0.315	0.05	0.298	42.4	-250
Keithley model 96035	15	1)	1)	0.65	2.12	-300
NE type 2530/1	35	1.405	0.15	1.48	0.831	-250
Keithley model 96050	600	5.56	0.238	6.97	0.0517	-300

[1] The electrode spacing of this parallel plate ionization chamber is 0.65 cm
[2] Collecting potential as advised by the manufacturer

4.2. Neutron W values in methane-based tissue-equivalent gas up to 60 MeV

G.C. Taylor[1], J.Th.M. Jansen, J. Zoetelief and H. Schuhmacher[2]

Since ionisation chambers and proportional counters, frequently used for (neutron) dosimetry, register events in terms of ion pair production rather than recording energy deposition directly, accurate dosimetry requires knowledge of the quantity that relates the two. This quantity is known as the W value, or the mean energy required to produce an ion pair.

The determination of reliable neutron W values for a dosimetrically important medium such as methane-based tissue-equivalent gas relies on knowledge of the W values of the charged particles produced by the neutron interactions in that medium. Following the recent evaluation of proton W values in methane-based tissue equivalent gas by Siebert et al. (1), it was thought appropriate to perform a similar re-evaluation for other significant secondary charged particles, namely ^4He, ^{12}C, ^{14}N or ^{16}O. This would allow the calculation of neutron W values with a completely revised data set. The re-evaluation shows evidence of a "bump" in the ^4He W value curve at approximately 200 keV.amu^{-1} (atomic mass unit) similar to that reported for protons, but not for ^{12}C, ^{14}N or ^{16}O ions. It also highlights the almost complete absence of experimental data above 60 keV.amu^{-1} for heavy recoils. All experimental ion W value data were fitted using the same basic function proposed by Siebert et al. (1), which takes the form:

$$W_i(E') = \frac{A}{[\ln(E'+B)]^D} + C\left(\frac{E'E_b}{E'^2+E_b^2}\right) + W_\infty$$

where $W_i(E')$ represents the W value of particle species i, E' the energy of the particle per atomic mass unit, E_b the energy of the "bump", W_∞ the W value for infinitely energetic particles and A, B, C and D represent fitting parameters. The parameters for protons and the new evaluated ions are shown in Table 1 together with the relative standard deviation deduced from the least square fitting procedure between the experimental data and the fitted

curves. Determination of neutron W values has shown a small increase below about 1 MeV, and a small decrease above about 8 MeV, when compared to the values reported by Siebert et al. (1) (Fig. 1). The deviation from neutron W values of Goodman and Coyne (2) is larger than from neutron W values of Siebert et al. (1), indicating that the change in W value for neutrons due to the new proton data accounts for the largest difference. Furthermore, neutron W values have been calculated for energies up to 60 MeV for the first time. ❑

A full paper on this subject appeared under the same title in Radiation Protection Dosimetry, 61, 285-290, 1995.

1. BRL Siebert, JE Grindborg, B Großwendt, H Schuhmacher. New analytic representation of W values for protons in methane-based tissue-equivalent gas. Radiat Prot Dosim 52, 123-127, 1994.
2. LJ Goodman, JJ Coyne. W_n and neutron kerma for methane-based tissue-equivalent gas. Radiat Res 82, 13-26, 1980.

[1]) National Physical Laboratory, Teddington, United Kingdom
[2]) Physikalisch-Technische Bundesanstalt, Braunschweig, Germany

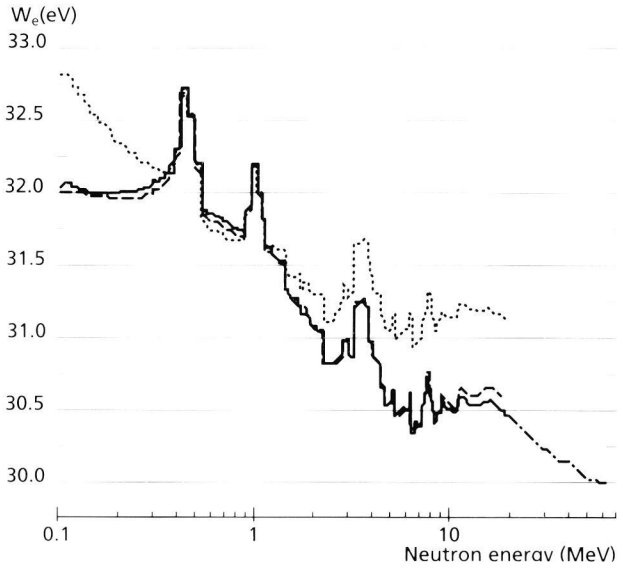

Figure 1. Comparison of different neutron W value evaluations as a function of neutron energy for an infinite cavity of methane-based tissue-equivalent gas. Siebert et al. (1) (- - -), Goodman and Coyne (2) (. . .), this work below a neutron energy of 20 MeV (——) and this work above a neutron energy of 20 MeV (-·-·-).

Table 1. Parameters for the new evaluation of W values in methane-based tissue-equivalent gas for ^{4}He, ^{12}C, ^{14}N and ^{16}O, together with the evaluation for protons from Siebert et al. (1). The relative uncertainty refers to the relative standard deviation of the experimental data from the fitted curves

Ion	A (eV)	B (keV.amu^{-1})	C (eV)	D	Eb (keV.amu^{-1})	W_∞ (eV)	Relative uncertainty (%)
^{1}H	16.56 ± 0.39	1.043 ± 0.037	2.007 ± 0.186	1.653 ± 0.054	400 (fixed)	29.1 ± 0.1	2.5
^{4}He	36.2 ± 0.3	1 (fixed)	4.1 ± 0.6	0.817 ± 0.010	201 ± 25	23 (fixed)	1.6
^{12}C	44.1 ± 0.6	1 (fixed)	-	0.799 ± 0.015	-	23 (fixed)	3
^{14}N	43.3 ± 0.4	1 (fixed)	-	0.715 ± 0.006	-	23 (fixed)	3
^{16}O	46.3 ± 0.5	1 (fixed)	-	0.737 ± 0.012	-	23 (fixed)	3

4.3. Organ and effective doses in the male phantom ADAM exposed in AP direction to broad unidirectional beams of mono-energetic electrons

F.W. Schultz and J. Zoetelief

For radiological protection purposes assessment of the risks of exposure to ionizing radiation is essential. Therefore, the International Commission on Radiological Protection (ICRP) had introduced the concept of effective dose equivalent (H_E) and associated risk factors (1). H_E should be monitored constantly for radiological workers lest the annual dose limit is exceeded. Owing to a re-evaluation of the risk organs, however, H_E has become obsolete. The quantity effective dose (E) was introduced instead (2). Both H_E and E can be calculated from the organ doses. Information on organ doses resulting from external irradiation with electrons of relatively low energies (<5 MeV) was not yet available and data should be generated.

Organ doses per unit of fluence were calculated through Monte Carlo simulation of radiation transport (MCNP code, version 4.2) for the mathematical phantom, ADAM, placed in vacuum and irradiated in antero-posterior (AP) direction with broad unidirectional electron beams. The electrons are monoenergetic in the energy range of 0.1 to 10 MeV. The ADAM phantom represents the reference male adult.

In general, organ doses increase with increasing electron energy. Three types of behaviour can be distin-

guished in Figure 1. Surface organs (skin, eyes) absorb a high dose at low electron energies. After a moderate increase with increasing energy a plateau level is reached. As can be expected for weakly penetrating radiation, other organs absorb a very low dose at low electron energies; below 1.5 MeV, doses in skin and eye lenses are at least a factor of 10 higher. Organs with a shallow location (testes, marrow) show a subsequent slow, rapid and slow dose increase pattern with increasing electron energy. For deeper organs (like stomach or lungs) the rapid increase is delayed. Eventually, all organs reach dose levels of about 10^{-10} Gy • cm^2 at the highest electron energies.

Using weighting factors from the ICRP-60 publication (2) effective dose per unit of fluence is calculated from the organ doses for each evaluated electron energy. This quantity increases with increasing electron energy from 8×10^{-14} to 2×10^{-10} Sv • cm^2 (Fig. 2). A correction for skin dose is applied to allow for the radiation insensitivity of the upper skin layer (by ignoring the dose absorbed in the first 70 μm) which results in significantly lower effective doses for electron energies below 0.6 MeV.

Corresponding effective dose equivalents are also calculated using weighting factors from ICRP Report 26 (1). At the high end of the energy range considered, the present values agree reasonably well with the results of a series of calculations performed with the MIRD-5 male phantom in the 5 to 46 MeV electron energy range, as published in ICRU Report 43 (3). The difference between effective dose and effective dose equivalent is relatively small for electron energies between 1.5 and 10 MeV. However, the difference increases rapidly when the electron energy decreases. Below 0.5 MeV, the effective dose equivalent is about a factor of 100 less than the effective dose. This is due to the fact that the skin, with its very dominant dose contribution in this energy range, is not considered a risk organ in the calculation of effective dose equivalent. Thus, in this low energy range annual dose limits are reached sooner if effective dose instead of effective dose equivalent is used as the parameter of risk assessment.

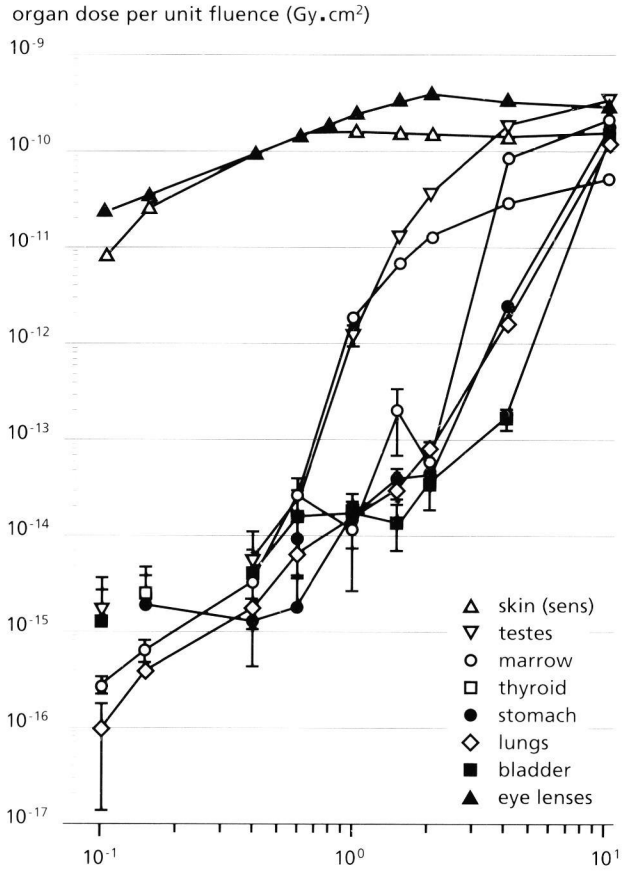

Figure 1. Organ dose per unit of fluence as a function of electron energy for various organs. Statistical uncertainty (1 standard deviation) is indicated by error bars.

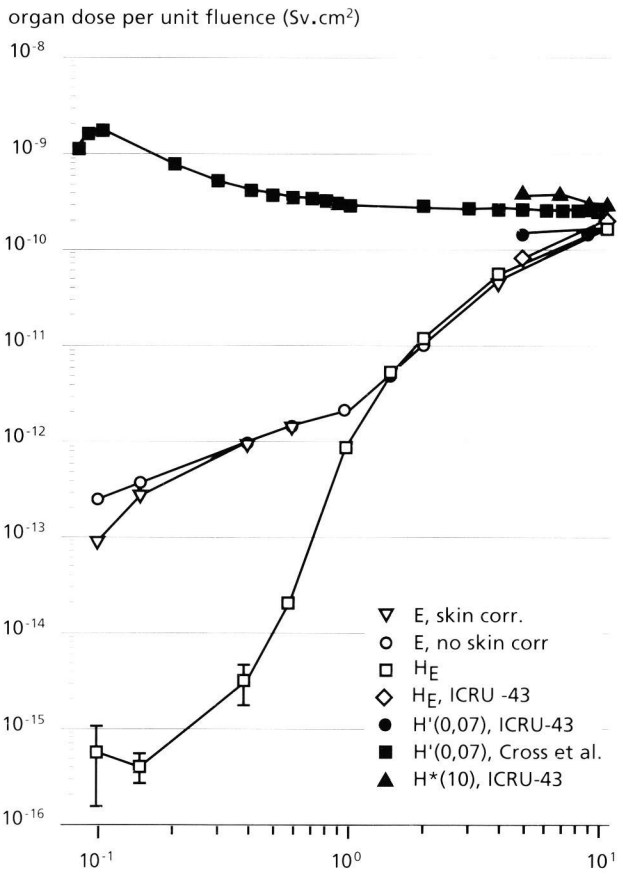

Figure 2. Effective dose, E (with and without correction for radiation sensitivity of the skin) and effective dose equivalent, as a function of electron energy. Statistical uncertainty (1 standard deviation) is indicated by error bars. For higher electron energies, ambient dose equivalent, H'(10) and directional dose equivalent, H'(0.07) in the ICRU sphere are shown. Finally, H'(0.07) in a slab of water, according to Cross et al. (5) is shown.

The directional dose equivalent, H'(0.07) is an operational quantity defined in ICRU Report 33 (4). It is meant to be used to indicate the risk of weakly penetrating radiation. Taking this quantity as a substitute for effective dose in the present case, however, introduces an unnecessarily large safety factor when estimating radiation risk. The calculated effective dose itself already overestimates the radiation risk, for the effect of wearing protective clothing has not been modelled. ❑

A full paper on this subject has appeared under the same titel in Health Physics 70, 498-504, 1995.

1. International Commission on Radiological Protection. Recommendations of the International Commision on Radiological Protection. Oxford: Pergamon Press, ICRP Report 26, 1977.
2. International Commission on Radiological Protection. 1990 Recommendations of the International Commision on Radiological Protection. Oxford: Pergamon Press, ICRP Report 60, 1991.
3. Commision on Radiation Units and Measurements. Determination of dose equivalents from external radiation sources, part 2. Bethesda, Md: ICRU Report 43, 1988.
4. International Commission on Radiation Units and Meausrements. Radiation quantities and units. Bethesda, Md: ICRU Report 33, 1980.
5. WG Cross, PY Wong, NO Freedman. Dose distributions for electrons and beta rays incident normally on water. Radiat Prot Dosim 35, 77-91, 1991.

5. Biological consequences of exposure to radiation

Exposure to ionizing radiations with relatively high doses results in deterministic effects. Acute deterministic effects are for instance reddening of skin and skin burns, late deterministic effects are for instance cataract, loss of organ function such as in kidney and lung, and myelopathy. All these effects will occur when a threshold dose is exceeded. After low as well as high doses stochastic effects may occur for which no threshold doses are assumed. Tumour induction is the most studied stochastic effect. In radiation protection the aim is to prevent deterministic effects and to limit the frequency of stochastic effects to a reasonable extent.

In the following contributions the long-term effects of high-dose total-body irradiation in rhesus monkeys are discussed and a method to determine the proportion of undamaged haemopoietic cells after partial body irradiation as a measure of the fraction of the body not exposed.

The influence of genetical and endocrinological factors on mammary tumour induction in rats is discussed and an answer to the question has been given whether oestrogen supplement as a remedy for (post)menopausal complaints of women taking part in breast cancer screening may lead to enhanced risk of tumour induction. The interaction of radiation and other agents is discussed with respect to acute and late deterministic effects in lung tissue in rats and a literature search has been conducted to determine the minimum dose needed for long lasting pain relief in patients with painful bone metastases. The last contribution in this chapter is an exemple of applied research to encouter the problem of treating metastases using bispecific monoclonal antibodies. The study was performed at the University Hospital in Groningen with the tumour model developed at TNO in Rijswijk.

5.1. Long-term consequences of high-dose total-body irradiation on hepatic and renal function in primates

J.J. Broerse, B. Bakker[1], J. Davelaar[1], M.M.B. Niemer-Tucker[1] and C. Zurcher[2]

High-dose total-body irradiation in combination with intensive chemotherapy followed by bone marrow transplantation has been shown to be of benefit for the treatment of haematological malignancies, some nonmalignant disorders of the haemopoietic system and selected solid tumours. Presently, thousands of patients per year are being treated world-wide with high-dose total-body irradiation (TBI) followed by autologous or allogeneic bone marrow transplantation. The number of patients in long-term follow up after bone marrow transplantation has increased. Delayed effects of this treatment modality therefore become of more importance. The radiation doses involved are at the threshold for acute radiation damage to lung, kidney and liver.

Radiation experiments in primates are of relevance since the response to radiation of monkeys does not seem to be significantly different from that in man. This has been demonstrated for a number of acute effects including those on the haemopoietic and intestinal system and also for some late effects such as tumour induction (1-3). Furthermore, an outbred species such as the Rhesus monkey (Macaca mulatta) is more representative as an animal model to assess the effect of TBI as a single toxic factor than are inbred rodents.

For fractionated irradiations the approximate limits of radiation tolerance dose of different human tissues, including the kidney and liver, are clinically defined. The tolerance dose after fractionated exposure, which is the dose associated with 1-5 per cent complications occurring within 5 years of treatment, is assumed to be 20 Gy for kidney and 30 Gy for liver. There is no universal agreement on the exact tolerance dose of many tissues after single dose TBI including kidney and liver. Rubin et al. (4) mentioned values between 11 and 19 and 15 and 20 Gy, respectively as tolerance doses for kidney and liver after single-dose irradiations. Van Rongen (5) studied radiation-induced alterations in different renal functional and histological parameters in rats after single irradiations with doses in excess of 6 Gy. He observed that deviations from control values start earlier and increase more rapidly with increasing radiation dose. On the basis of the results for fractionated irradiation in man, an isoeffect dose for kidney damage could be derived with the assumption of an α/β ratio of 2 Gy (6, 7). The resulting extrapolated total dose of 40 Gy would imply a tolerance dose of 8 Gy for single-dose irradiation.

In the present study, we investigated the long-term effects of TBI as a common toxic agent in Rhesus monkeys on hepatic and renal function in relation to the time course. Three cohorts of monkeys exposed to TBI with post-irradiation intervals in excess of 15 years, between 10 and 15 year, and less than 10 years, irradiated with doses between 5 and 8.5 Gy were kept under continuous observation. In addition to this experimental group of 42 animals, the control group consisted of 42 non-irradiated monkeys with a comparable age distribution and identical housing conditions. Since radiation was the common toxic agent, the different age groups provided the possibility to investigate the occurrence of deterministic effects after TBI. In the present study emphasis was placed on the assessment of hepatic and renal function and the associated histopathology (8). The values of the liver function parameters, such as alkaline phosphatase and gamma glutamyl transferase in the irradiated group were significantly increased after TBI ($p<0.005$) in the irradiated old-aged cohort (post-irradiation interval >15 years). The impairment of the liver and renal functions did not lead to clinical symptoms and were only associated with mild morphologic changes in the irradiated group of monkeys. These morphological changes include hyperplasia, capsular fibrosis, cholangiofibrosis in the liver and interstitial fibrosis and interstitial inflammation, tubular atrophy and cysts in the kidney.

On the basis of this study alterations in hepatic and renal function parameters after a post-irradiation interval of more than 10 years can be anticipated in the population of bone marrow transplant patients treated with TBI. This could have consequences for the tolerance and toxicity of a broad range of drugs to be administered as additional medication. ❑

1. EJ Ainsworth, GF Leong, EL Alpen. Early radiation mortality and recovery in larger animals and primates. Response of different species to total body irradiation. Edited by: JJ Broerse and TJ Macvittee (Martinus Nijhoff, Boston, p 87-111, 1984.
2. HM Vriesendorp, DW van Bekkum. Susceptibility to total body irradiation. Response of different species to total body irradiation. Edited by: JJ Broerse and TJ Macvittee. Boston: Martinus Nijhoff, pp 43-57, 1984.
3. JJ Broerse, DW van Bekkum, J Zoetelief, C Zurcher. Relative biological effectiveness for neutron carcinogenesis in monkeys and rats. Radiat Res 128, 128-135, 1991.
4. Ph Rubin, LS Constine, DF Nelson. Late effects of cancer treatment: radiation and drug toxicity. In: Practice of Radiation Oncology. Edited by: CA Perez and LW Brady, Philadelphia: JB Lippincott. pp 124-161, 1992.
5. E van Rongen. The influence of fractionation and repair kinetics on radiation tolerance. Studies on rat lung and kidney. PhD thesis, University of Amsterdam, 1989.
6. GW Barendsen. Dose-fractionation, dose rate and isoeffect relationships for normal tissue responses. Int J Radiat Oncol Biol Phys 8, 1981-1999, 1982.
7. HD Thames, JH Hendry. Fractionation in Radiotherapy. London: Taylor & Francis. 1987.

8. MMB Niemer-Tucker, MMJH Sluysmans, B Bakker, et al. Long-term consequences of high-dose total-body irradiation on hepatic and renal function in primates. Int J Radiat Biol 68, 83-96, 1995.

[1]) Department of Clinical Oncology, State University of Leiden, The Netherlands
[2]) Consultant to the Biomedical Primate Research Centre, Rijswijk, The Netherlands

5.2. Biological consequences of partial body irradiation in a rhesus monkey model

J.J. Broerse, P.A.J Bentvelzen, F. Darroudi[1], A.T. Natarajan[1], P.J. Heidt[2], A. van Rotterdam and J. Zoetelief

In case of a radiation accident like in Chernobyl involving high acute doses it is necessary to determine quickly whether the exposure is uniform or not. Such information is helpful to clinicians who have to make decisions on medical management, including transplantation of allogeneic bone marrow or treatment with growth factors.

The conditions of a radiation accident were mimicked by exposure of four rhesus monkeys to either a total body or a partial body X-irradiation with doses of 5 Gy. In case of partial body irradiation the lower parts of the arms were covered by lead gauntlets, resulting in shielding of 5 to 7 per cent of the bone marrow.

Lymphocytes cultures from the irradiated monkeys were set up one, three and seven days after irradiation. Three methods were applied to assess the unirradiated fraction of haemopoietic cells, as well as the persistence of damage and rate of recovery due to regeneration of normal lymphocytes. These three methods were: (a) counting dicentrics in metaphases, (b) counting micronuclei, and (c) estimation of excess of breaks in interphase cells using premature chromosome condensation (PCC). The latter technique, detecting additional chromosomal fragments instead of the normal karyotype of 2n=42 chromosomes, proved to be efficient in detecting the proportion of undamaged cells (Table 1).

The partially irradiated monkeys showed an unirradiated fraction of haemopoietic cells of approximately 5 per cent as expected. ❑

Table 1. Biological monitoring applied to *in vivo* simulated partial body irradiation using the premature chromosome condensation technique

	post-irradiated time (day)	distribution of PCC's 2n=42	43-55	induced PCC's	unirradiated fraction (%)
control		50	0	-	100
total body irr.	1	0	100	6.7	0
partial body irr.	1	5	86	5.9	5.5
total body irr.	3	0	85	6.2	0
partial body irr.	3	6	80	5.4	7.0
total body irr.	7	2	98	5.7	2.0
partial body irr.	7	10	90	4.2	10.0

[1]) Department of Radiation Genetics and Chemical Mutagenesis, State University of Leiden
[2]) Biomedical Primate Research Center, Rijswijk, The Netherlands

5.3. The influence of genetical and endocrinological factors, age and dose-fractionation on mammary tumour induction by ionizing radiation in rats

P.A.J. Bentvelzen and R.W. Bartstra

High doses of ionizing radiation very significantly raise the risk of breast cancer in women, as has been observed in many studies of the effect of medical irradiation (1) and in the follow-up of Japanese atomic bomb survivors (2). Low fractionated dose of X-rays are presently used for the early detection of breast cancer in screening programmes in several countries. It is possible that the radiation induces mammary carcinomas, although the benefit of the early detection of treatable tumours presumably outweighs this detrimental effect (3). Hereditary factors play an important role in human breast cancer (4). It cannot be excluded that carriers of high-penetrance gene mutations, predisposing to breast cancer like BRCA-1, BRCA2 and ATM, are extremely susceptible to the radiation-induction of mammary tumours.

In animal models endocrine manipulation strongly affects the development of mammary neoplasms. A meta-analysis of 54 case-control studies established that for women using oral contraceptives there is a small but definite increase in the risk of having breast cancer while

taking oral conceptives and during ten years thereafter (5).

In the target group for mass screening on breast cancer (age 50-70 years) oestrogenic hormones are often supplemented as remedy for (post)menopausal complaints. Does such oestrogen replacement enhance the risk of breast cancer induction by ionising radiation? Finally, the question rises whether the start of screening using mammography at middle age has an effect on breast cancer risk.

For the study of the factors possibly affecting the risk of breast cancer in relation to mammography, a large-scale investigation has been carried out in the former TNO Radiobiological Institute on the radiation-induction of mammary tumours in three inbred rat strains; SD, BN and WAG. Females of either strain do not develop a mammary tumour spontaneously before the age of two years. Exposure to ionizing radiation (X rays, γ rays or neutrons of different energies) results in the appearance of mammary tumours before two years of age. The SD strain proves to be the most susceptible: a dose of 0.25 Gy of X-rays induces approximately 40 per cent tumours at two years in this strain, but 0 per cent in the two other rat strains (6). The majority of these tumours is non-malignant fibroadenoma. These lesions can be regarded as a precursory stage of malignant carcinomas, however.

The F1 hybrids of SD with either BN or WAG are almost as susceptible to the induction of mammary tumours by X-rays as the SD strain, indicating the dominance of the breast cancer susceptibility gene(s) from the SD. Tumour incidences in a series of backcrosses indicate that the susceptibility of the SD as compared to the BN strain may be controlled by a single gene. Linkage analysis did not yet result in localization of this rat BRCA gene on any of the rat chromosomes. An extensive crossing programme has been carried out between the SD and WAG strains. The female progeny has been irradiated with X-rays (2 Gy) and is being kept under observation for tumour development or other clinical abnormalities. Mammary tumours incidences obtained so far in the various groups after 11/2 year do correspond with the assumption that the difference between these two strains is controlled by a single gene.

The oestrogenic compound oestradiol-17β is known to accelerate both the spontaneous and radiation-induced development of mammary tumours in rats (6). Female WAG rats treated with this compound were subjected to fractionated exposure to Cs-137 gamma rays with fraction sizes of 2.5 mGy, 10 mGy and 40 mGy up to cumulated doses of 1 and 2 Gy. The relative risks (RR) of mammary tumours (after an observation period of 3 years) in comparison to unirradiated controls are presented in Table 1.

At an accumulated dose of 1 Gy the fraction sizes of 2.5 and 10 mGy do not produce a significantly increased RR, while 40 mGy per fraction results in an increased RR comparable to the risk obtained with a single dose of 1 Gy with an RR varying from 6 to 10. At an accumulated dose of 2 Gy the inhibition effect of fractionation on the RR is less striking (RR at a single dose of 2 Gy varies from 5 to 11).

A completely different picture with regard to the effect of fractionation is found in animals not treated with oestradiol-17β (Table 2). The fraction sizes of 2.5 and 10 mGy produce an RR almost as elevated as found for single doses (1 Gy RR varies from 1 to 3; 2 Gy RR varies from 3 to 5). A possible explanation is that single doses of 1 or 2 Gy impairs the endogenous hormone production.

Table 1. Relative risks of mammary tumours in irradiated WAG rats to which oestradiol-17β has been administered

	Relative risk		
total dose (Gy)	2.5 mGy	10 mGy	40 mGy
0	1	1	1
1	1.4 ± 0.5	1.3 ± 0.5	3.3 ± 1.3
2	3.3 ± 1.1	2.2 ± 0.8	4.5 ± 1.8

Table 2. Relative risks of mammary tumours in irradiated WAG rats to which no oestradiol-17β has been administered

	Relative risk	
total dose (Gy)	2.5 mGy	10 mGy
0	1	1
1	3.0 ± 0.8	2.4 ± 0.7
2	2.2 ± 0.6	2.6 ± 0.6

Table 3. Relative risks of mammary tumours in WAG rats to which oestradiol-17β has been administered, and irradiated with single doses at different ages

age at irradiation	Relative risk	
(week)	1 Gy	2 Gy
8	5.9 ± 1.3	9.1 ± 1.7
10	6.6 ± 1.5	10.9 ± 2.0
12	10.4 ± 2.0	5.2 ± 1.0
15	10.4 ± 2.2	9.8 ± 2.0
22	1.6 ± 0.4	4.6 ± 0.9
36	0.6 ± 0.1	1.0 ± 0.2
64	0.5 ± 0.1	0.5 ± 0.1

Table 4. Relative risks of mammary tumours in WAG rats to which no oestradiol-17β has been administered and irradiated with single doses at different ages

age at irradiation	Relative risk	
(week)	1 Gy	2 Gy
8	1.7 ± 0.5	2.8 ± 0.8
12	3.0 ± 0.9	5.1 ± 1.5
16	1.6 ± 0.5	2.9 ± 0.9
22	1.3 ± 0.5	4.2 ± 1.0
36	2.7 ± 0.6	2.8 ± 0.8
64	0.3 ± 0.1	0.7 ± 0.2

When single doses of gamma rays are given at different ages to hormone-treated animals it was observed that in the age range 8 to 15 weeks the RR is strongly elevated but that at later ages (36 and 64 weeks) the RR is significantly lower in comparison with hormone-treated but unirradiated controls (Table 3). In animals, which have not been treated with oestradiol-17β, the single doses do not evoke such an elevated RR. However, at 64 weeks of age the RR's are remarkably low (Table 4). A possible explanation is that in these postmenopausal females single dose of gamma rays result in the sterilization of spontaneously transformed (pre-)neoplastic mammary cells.

In as far as these rat studies are applicable to the human situation, the results suggest that in the age group 50 to 70 years radiation would not lead to an increased risk of breast cancer, whether or not oestrogens are supplemented. The problem of genetic susceptibility in relation to mammography, particularly of premenopausal women, needs further study. ❑

1. United Nations Scientific Committee on the Effects of Atomic Radiation. Sources and effects of ionizing radiation. UNSCEAR 1994. Report to the General Assembly, New York: United Nations, 1994.
2. DA Pierce, Y Shimizu, DL Preston, et al. Studies of atomic bomb survivors. Report 12, part 1. Cancer: 1950-1990. Radiat Res 146, 1-27, 1996.
3. JTM Jansen, J Zoetelief, MBS: a model for risk benefit analysis of mammographic breast cancer screening. Brit J Radiol 68, 141-149, 1995.
4. D Easton, D Ford, J Peto. Inherited susceptibility to breast cancer. Cancer Surveys 18, 95-113, 1993.
5. Collaborative Group on Hormonal Fractors in Breast Cancer. Breast cancer and hormonal contraceptives: collaborative analysis of individual data on 53297 women with breast cancer and 100239 women without breast cancer from 54 epidemiological studies. Lancet 347, 1713-1727, 1996.
6. MJ van Zwieten. The rat as animal model in breast cancer research. A histopathological study of radiation and hormone induced rat mammary tumors. Thesis, University of Utrecht. The Hague: Martinus Nijhoff Publishers, 1984.

5.4. Tolerance of lung tissue to chemotherapeutic agents after prior radiation treatment

H.B. Kal and H.H. Goedoen

The aim of the study, sponsored by the Dutch Cancer Society (project ITRI 90-05), was to determine the tolerance of the WAG/Rij rat lung tissue to several cytostatic agents at 1 or 6 months following local radiation treatment. Drugs were selected that are being used clinically in the treatment of Hodgkin's disease and that result in a response of the lung tissue when applied as single agents.

Non-lethal damage was assessed longitudinally using a functional test (breathing frequency). Acute effects (lethality) within 6 months after treatment was determined. Late effects in long-term survivors at 18 months after treatment will be studied by histology to determine the type of damage and the tissue components involved.

The following experiments were performed:

- Breathing frequencies of all animals in experiment.
- Effectiveness of single agents: radiation, adriamycine, cyclophosphamide, VP 16, BCNU and bleomycine.
- Effectiveness of radiation and the drugs (except bleomycine) with 1 month interval.
- Effectiveness of radiation and the drugs adriamycine and cyclophosphamide with 6 months interval.

The results were as follows:

- A sharp increase in breathing frequency, >100%, approximately 2 months after treatment, and a few weeks later a return to normal values was observed for animals surviving high doses of X-rays and BCNU. A moderate increase in frequency was observed for high doses of adriamycine 1 month after treatment and for cyclophosphamide about 4 months after treatment. No increase in breathing frequency was observed in animals treated with bleomycine and VP16.
- Effectiveness of single agents and of combinations of drugs and X-ray doses of 10 and 11.5 Gy with 1 and 6 month interval, acute toxicity within 26 weeks (Table 1).

From these results the following conclusions can be drawn. The drugs bleomycine and VP16 were not affecting lung function. The other drugs did affect lung function

Table 1. $LD_{50/26w}$ values for radiation and drugs and their combinations for 1 and 6 months interval

	$LD_{50/26w}$ (mg/kg)				
	single dose	10+1*	11.5+1	10+6	11.5+6
X-rays	12.1**				
adriamycine	6.5	6	5	5.8	4.3
cyclophosphamide	100	55	12	65	>70
VP 16	40	40	32		
BCNU	20	20	20***		
bleomycine	>120				

* 10+1: 10 Gy + 1 month interval
** dose (Gy)
*** more acute lethalities within 5 weeks

depending on dose, but return to normal breathing frequencies was observed.

For the combined treatments with 1 month interval only for cyclophosphamide a strong interaction with the radiation doses were observed, indicating that the target cells for radiation and cyclophosphamide are identical. After the dose of 10 Gy no appreciable changes in $LD_{50/26w}$ values for adriamycine, VP16 and BCNU were observed, indicating that repair of subeffective damage in lung tissue is not affected by further drug administration. However, after the dose of 11.5 Gy, clearly not all damage has been repaired and the $LD_{50/26w}$ values for all drugs are lower as compared to those after a dose of 10 Gy.

For the combined treatments with 6 months interval for cyclophosphamide a strong interaction with the radiation doses was observed indicating the presence of permanent damage induced by radiation. This corraborates with the observation that the $LD_{50/26w}$ for adriamycine for 6 months interval is lower.

Histology studies have still to be performed to supplement these functional studies. ❑

5.5. Radiation treatment of painful bone metastases

H.B. Kal

External beam radiotherapy is well known to be effective in the treatment of painful bone metastases in cancer patients. A variety of fractionation schemes is used; commonly doses in the range of 20 to 40 Gy over a period of two to four weeks are applied. In order to reduce the burden to patients there is a continuous interest to administer only one or a few dose fractions in a short overall time for inducing fast pain relief. Some clinical experience suggests an advantage from a few large dose fractions to achieve a rapid response, but this still needs confirmation.

In addition to external beam therapy interest in the use of radiopharmaceuticals is increasing. Long lasting relief of pain has been observed for a number of radiopharmaceuticals among which the frequently used compounds containing P-32 and Sr-89 and recently rhenium-186 (Re-186-hydroxy-ethylidene diphosphonate).

Questions are what dose or activity is needed with external beam therapy or radiopharmaceuticals respectively, for long lasting palliation; whether there is a dose-response relationship for onset and duration of pain relief; and the mechanism by which pain is relieved.

The linear-quadratic (L-Q) concept (1) developed on the basis of experimental radiobiological data, was applied to compare external beam therapy schemes and regimens using radionuclides for the iso-effect pain relief. It provides means for calculating iso-effect total doses for new fractionation schemes and schemes using low dose rate irradiation on the basis of conventional treatment regimens. The influence of fractionation can be described by a formula relating the effectiveness for induction of cellular effects to the dose per fraction d: $E = \alpha d + \beta d^2$. For the calculation of equivalent total doses the concept of extrapolated tolerance dose (ETD) was introduced. ETD can be considered as the tolerance dose for an infinite number of very small fractions. $ETD = D[1 + d(\beta/\alpha)]$ in which D is the total dose.

For low dose rate treatments with a long treatment time: $ETD = D\{1 + (2R/\mu).(\beta/\alpha)\}$ in which R is the dose rate and μ the rate of repair of sublethal damage.

ETD values were calculated for effective pain relief schemes for fractionated or single-dose external beam therapy and for treatments with radionuclides (2), assuming for tumours an α/β ratio of 10 Gy and a μ-value of 0.46 h^{-1} corresponding with the half value for sublethal damage repair of 1.5 h.

Single-dose and fractionated radiotherapy as well as radiopharmaceuticals resulted in partial or complete pain relief in approximately 80 per cent of the patients. Complete responses have been observed in approximately 50 per cent of the patients. For patients responding to treatment, the duration of pain relief is at least 3 to 4 months with reported durations of up to one year or even longer. The duration of pain relief seems to be independent from the dose provided the dose is adequate, i.e. for ETD values in excess of 10 Gy.

Conventional fractionation with small daily fractions is not likely to induce fast pain relief and will cause an unnecessary burden to the patient. A fast relief of pain is not observed for the nuclide Sr-89 due to the low dose rate associated with the long half life of 52 d. Long lasting pain relief commonly starts only 10 to 20 days after beginning of the treatment.

For induction of pain relief within a few days a relatively large total dose in a short overall time or a radiopharmaceutical with a relatively short half life is needed. The use of a dose of 6 Gy (3) or Re-186 with a half life of 90 h is promising.
A single dose of at least 6 Gy (ERD = 9.6 Gy) or a few dose fractions (e.g two fractions of 3.7 Gy, ERD = 10.1 Gy) in a relatively short overall time, is a useful method.

It seems reasonable to look for combined treatments in which a single dose or a few dose fractions are administered by external beam therapy for inducing fast pain relief followed one or two months later with administration of Sr-89 or Re-186. This may improve overall pain control and

delay progression of existing asymptomatic metastases. Results of such a randomized phase III trial are promising (4).

A patient treated with a radiopharmaceutical has to be considered as a potential source for external irradiation and internal contamination of members of the public. P-32 and Sr-89 are β-emitters and a patient treated with these radionuclides can be considered at home only as a source for internal contamination via urine. Normal hygiene will prevent that most of the urine of the patient is being spread. However, assuming that 1 per cent of the urine is spilled and 1 per cent of that will be taken in by an inmate, the effective dose to an inmate will be about 0.01 mSv for a 440 MBq P-32 treated patient and 0.02 mSv for a patient treated with 100 MBq Sr-89 (5). These effective doses are far below the ICRP recommended annual effective dose limit of 1 mSv for members of the public. This indicates that the treatment of patients with bone metastases by administration of radiopharmaceuticals will not provide a serious risk to inmates. ❑

1. GW Barendsen. Dose fractionation, dose rate and iso-effect relationships for normal tissue responses. Int J Radiat Oncol Biol Phys, 8, 1981-1997, 1982.
2. HB Kal. Radiotherapie van botmetastasen. IKR-Bulletin 19, 36-37, 1995.
3. JM Uppelschoten, SL Wanders, JMA de Jong. Single dose radiotherapy (6 Gy): palliation in painful bone metastases. Radiotherapy and Oncology 36, 198-202, 1995.
4. AT Porter, AJB McEwan, JE Powe, et al. Results of randomized phase-III trial to evaluate the efficacy of Sr-89 adjuvant to local field external beam irradiation in the management of endocrine resistant metastatic prostatic cancer. Int J Radiat Oncol Biol Phys, 25, 805-813, 1992.
5. H Beekhuis, JJ Broerse, RAMJ Claessens, et al. Stralingsbelasting van leden van de bevolking als gevolg van medische toepassingen van radiofarmaca voor ontslagcriteria. Rapport nr. 55 of VROM/DGM, The Netherlands,

5.6. Reduction of pulmonary metastases by bispecific-antibody-redirected T-cells

B.J. Kroesen[1], W. Helfrich[1], A. Bakker[1], A.S. Wubbena[1], H. Bakker[1], H.B. Kal, T.H. The[1] and L. de Leij[1]

Treatment of tumours by manipulation of the immune system appears promising with regard to its potential and its specificity. Manipulation of the immune system requires activation of cytotoxic T lymphocytes, for instance by the cytokine IL-2. However, the major obstacle in generating an effective anti-tumour response using T lymphocytes is the unspecificity of the lymphocytes, determined by the T-cell receptor, for tumour antigens on the cell surface of the tumour cells. This specificity can be circumvented using bispecific monoclonal antibodies directed against a triggering receptor on the T lymphocytes and a tumour-associated antigen on the cell surface of the tumour cells.

A rat squamous cell lung carcinoma derived cell line, L37, was used. Transfection of the cell line with a plasmid containing the cDNA for the human pan-carcinoma-associated antigen EGP-2 resulted in a cell line L37.EGP-2 which abundantly expressed EGP-2 on its membrane. After i.v. inoculation of $5x10^6$ L37 or L37.EPG-2 cells via the tail vein of WAG/Rij rats, lung metastases developed.

A bispecific-monoclonal-antibody (BsMAb) BIS-19 was made, recognizing EGP-2 on the transfected tumour cells and the T-cell receptor on T lymphocytes of the rat.

The effectiveness of BsMAb-mediated cellular anti-tumour activity was evaluated in vitro and in vivo in relation to the additional need for T-cell activation in this rat tumour model.

In vitro specific lysis of L37.EGP-2 cells was obtained after treatment with BIS-19 and activated T-lymphocytes in vitro. In vivo T-cell activation could be induced by daily injection of rat rIL-2.

Intravenous treatment of rats bearing L37.EGP-2 metastases with BIS-19 together with rat rIL2 injections resulted in almost complete disappearance of the lung metastases (Fig. 1, column 3). In contrast, animals treated with IL-2 alone or BIS-19 alone showed much less or no tumour

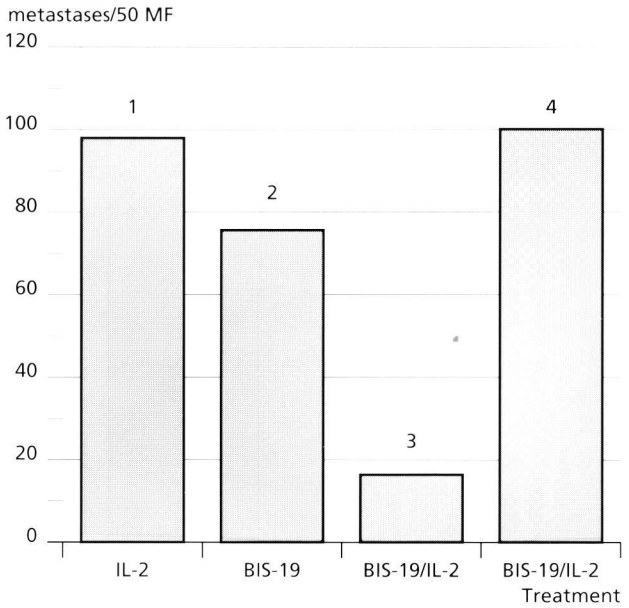

Figure 1. Number of metastases counted in 50 microscopic fields (MF) at 250x magnification expressed as percentage of the control group. Cryosections of the lungs of WAG/Rij rats were obtained 14 days after treatment, 28 days after inoculation of L37.EGP-2 (columns 1-3) or L37 (column 4) tumour cells.

reduction (Fig. 1, columns 1 and 2) as did treatment with BIS-19 together with IL-2 to L37 tumour cells (column 4).

These results show effectiveness of systemic treatment with BsMAb to induce anti-tumour activity in established tumours. Immune activation prior to or during treatment with BsMab, as achieved with IL2, appears to be a prerequisite for successful treatment. ❑

A full paper on this subject has appeared under the same title in International Journal of Cancer 61, 812-818, 1995.

[1]) University Hospital Groningen, The Netherlands

II. Services

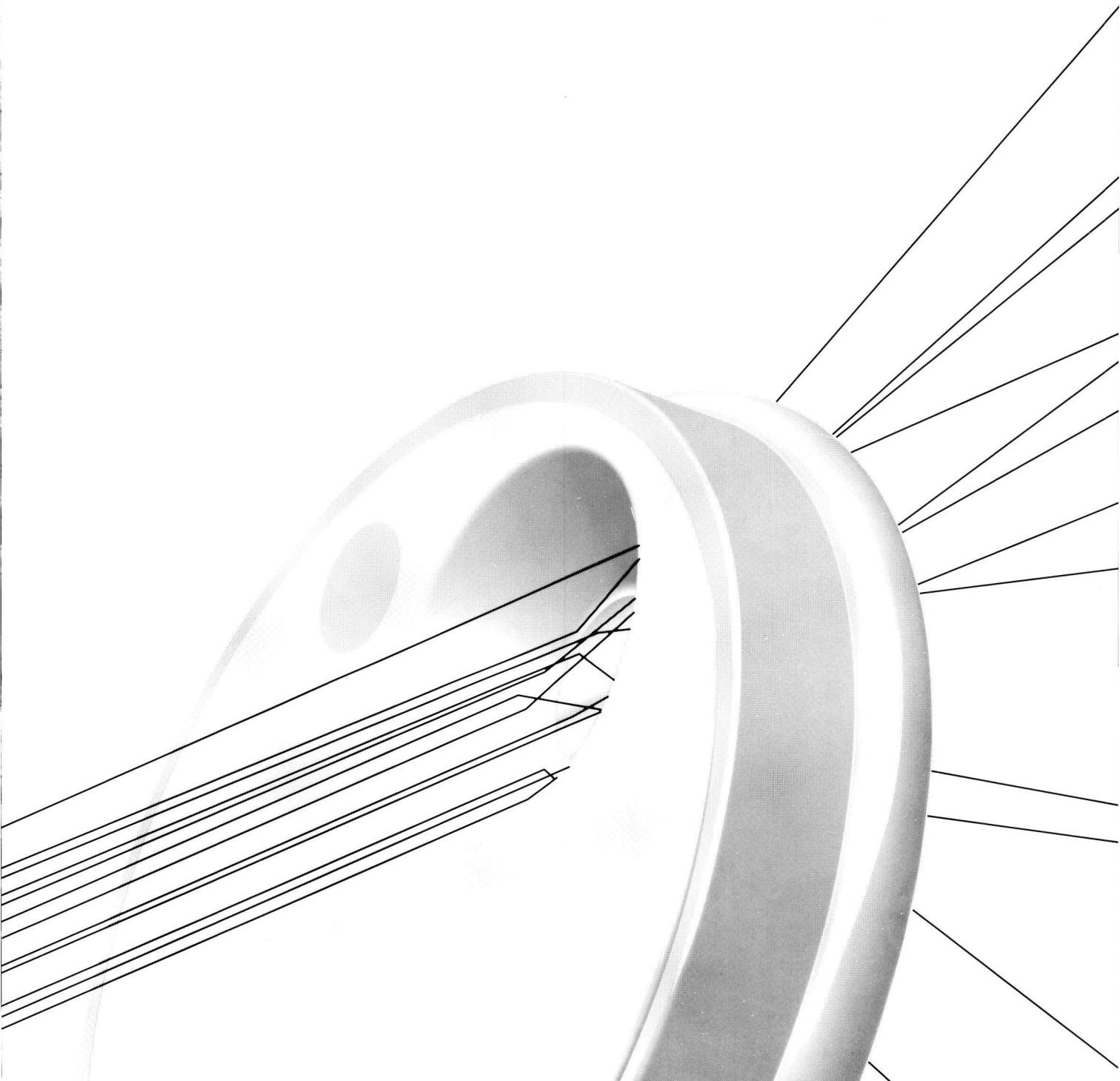

Services

TNO-CSD offers a variety of services among which:

- thermoluminescence dosimetry for individual monitoring and other dosimetry services for special applications.
- a number of analytical services for both environmental and worker conditions. Standard protocols are available for a number of radioactivity analyses. Most of these protocols are tested in international comparisons.
- Quality Assurance (QA) developed for equipment in diagnostic radiology departments. These QA services are intended for those hospitals that do not have the necessary expertise and technical facilities available.
- assistance to investigate the working environment in order to verify that exposure of the radiation worker is kept as low as reasonably achievable.
- a wide range of radiation sources and measuring equipment for calibration and type testing of instruments.
- computer (Monte Carlo) simulations of radiodiagnostic procedures that can be performed to obtain quantitative information on dosimetric quantities in case making measurements is impossible or impractical, e.g. calculation of effective doses, depth-dose curves, influence of filters applied.
- measurements of various patient-related dosimetric quantities, as well as for the assessment of image quality by performing measurements on images of contrast-detail phantoms. This is to ascertain that the radiation exposure to the patient should be kept as low as possible, but still compatible with the image quality required for an adequate diagnosis.

More information about these services are provided in the following contributions.

1. Thermoluminescence dosimetry

J.W.E. van Dijk and H.W. Julius

Individual monitoring

The Individual Monitoring Service of TNO-CSD is an Approved Dosimetry Service, licensed by the Ministry of Social Affairs and Employment. The thermoluminescence dosemeters (TLD's) are issued on a bi-weekly and four-weekly basis. Two types of dosemeters are used, one type is designed to measure both photons (X- and gamma rays) and beta's, the other to detect photons only. The quantities measured are body dose, $H_p(10)$, and skin dose, $H_p(0.07)$. The dosimetry system complies with the 'Technical Recommendations for Monitoring Individuals Occupationally Exposed to External Radiation' (EURATOM document EUR 14852) with respect to energy and angular response and with respect to precision and accuracy (detection limit 0.01 mSv). The dosimetry, the dose record keeping system and the administrative procedures are all included in an extensive Quality Assurance program. TNO monitors approximately 27,000 radiation workers, which is 85 per cent of the national need. The service offered includes return mail, periodical dose reports (English optional), an annual dose report and same day reports for doses higher than 1 mSv.

Special TLDosimetry

The TNO thermoluminescence dosimetry system is a flexible system that allows to offer various TLD based services. Single detectors can be encapsulated in plastic after which they can be swallowed by patients to be treated with ionising radiation. On the other end, detectors with a more robust casing are used on oil production platforms for cost effective measurements of radioactive scaling in the piping. The high reproducibility and low detection limits allow the TNO-TLD's to be used for environmental dosimetry and experimental studies. ❑

2. Radioactivity analyses

P. de Jong and W. van Dijk

TNO Centre for Radiological Protection and Dosimetry provides a number of analytical services, for both environmental and worker oriented research. The many years of experience, together with an adequate quality control system, guarantees highly accurate results that meet international standards. Standard protocols are available for the following services:

- Determination of the natural radioactivity of industrial by-products, (inhomogenous) waste, building materials, gravel, soils, etc (see Fig. 1).
- Determination of internal contamination by whole-body counting.
- Analysis of excreta to estimate the degree of uptake of radionuclides and to determine the effective dose in individuals.
- Wipe and leak tests of encapsulated sources.
- Determination of artificial radionuclides in food stuff and environmental samples.
- Air monitoring in working environments.
- Determination of radon in air, both long-term (integrated) and instantaneous (see Fig. 2).
- Environmental monitoring of radiation fields by thermoluminescence dosimetry or ionization chambers.

Recently a method was developed for the determination of radium (Ra-226) and radon (Rn-222) concentrations in water. In this method the sample of interest is purged by nitrogen gas and the outflowing radon trapped on silica gel at -190 °C. Approximately 16 h after sampling, the silica gel is analyzed by liquid scintillation counting to determine the radon level. The reliability of the method was verified by means of an international intercomparison, organized by the World Health Organization (WHO), the results of which are shown in Table 1. The same method is applied for the determination of the radon exhalation rate of building materials, amongst others employed in studies after the retarding effect of paint systems and the effects of the production process and composition of concrete slabs. During all investigations, the results of the sampling and the counting facility were verified using a laboratory 'standard' phosphogypsum block. Its repeatability was found to be 5 per cent (relative standard deviation) over a period of 8 years.

A method was developed to assess radon progeny concentrations in air, taking into account both the attached

Table 1. Results of an international intercomparison on the determination of Ra-226 concentrations in water

	Ra-226 concentration (Bq/l)	
	Mean	95% confidence interval
All participants (35)	2.07	1.71 - 2.43
WHO results	2.33	2.26 - 2.40
TNO-CSD results	2.26	2.14 - 2.38

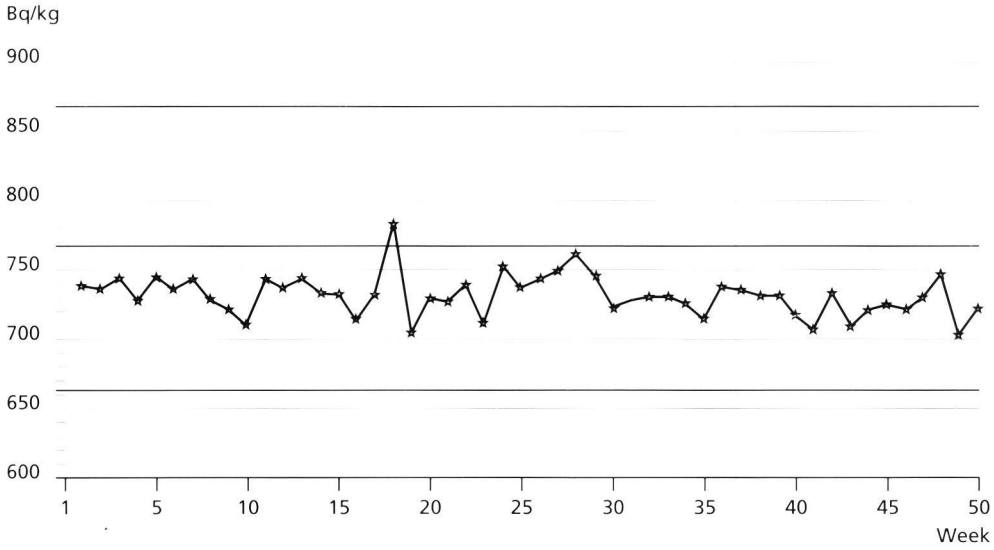

Figure 1a. Example of a control chart of the cesium activity in a reference material: Cs-134.

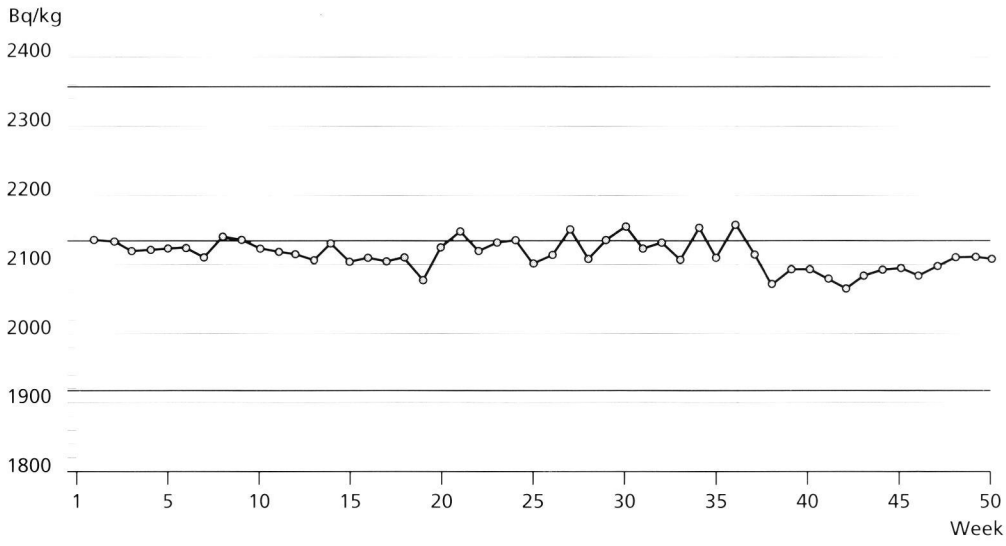

Figure 1b. Ibid, Cs-137.

and the unattached fractions. In the radon inhalation facility a detection limit was obtained of approximately 1 Bq • m^{-3} Rn-EEC for PAEC-values, based on a single measurement. Research is in progress to verify the method under more realistic conditions in a physical model of a dwelling. ❑

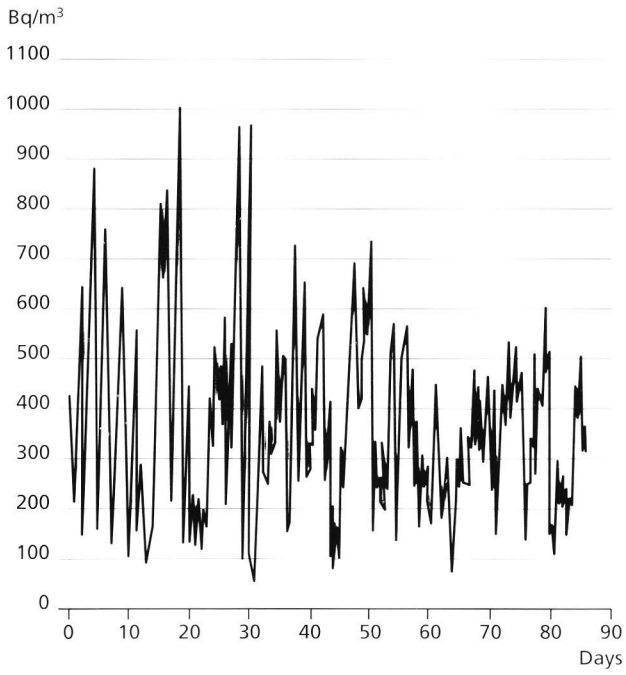

Figure 2. Time course of the radon concentration in a crawl space.

3. Quality assurance in diagnostic radiology

L. van den Berg and J. Moor

Since the publication of the EU Directive Euratom 1984/466 (often referred to as "Radiation Protection of the Patient") and its implementation in the Dutch legislation, attention has increasingly been focused on Quality Assurance (QA) in medical diagnostic radiology. The main aim of QA is to provide good quality diagnostic images, while keeping the dose to the patient as low as reasonably achievable. Achieving and demonstrating good quality requires implementation of a QA programme. A QA programme not only includes systematic testing of diagnostic X-ray equipment and related tools (e.g. viewing boxes and film processors) but also an organizational structure describing the responsibilities of the staff of the radiology department.

Ideally the performance of a diagnostic X-ray unit would be characterized by two key parameters: The effective dose to the patient and the quality of the image produced. However, methods to quantify the image quality are still subject of scientific research, while determination of the dose to the patient is far from straight forward. In practice QA in hospitals can best be assured by testing a set of physical (technical) parameters of the equipment, such as kVp, tube load, beam limitation, filtration, focal spot size and several others.

TNO-CSD, participating in the Working Group "Quality Criteria for diagnostic X-ray Equipment" developed measuring protocols for evaluating the performance characteristics ("status") of X-ray equipment in co-operation with medical professionals and hospital physicists. So far eleven protocols have been prepared (see Table 1). These protocols have been tested in medical practice.

TNO-CSD provides QA services for diagnostic radiology departments in those hospitals that do not have the necessary expertise and technical facilities available. ❑

Table 1. Quality criteria and test protocols have been developed for:

- Tube voltage
- Automatic exposure control systems
- Film processing
- Film/screen combinations
- Dark room conditions
- Half value layer and filtration
- Alignment of light field and X-ray beam
- Anti scatter grids
- Focal spot size
- Viewing boxes
- Geometric indicators

4. Radiation safety at the workplace

L. van den Berg and J. Moor

If persons use or work in the vicinity of sources of ionizing radiation, the working conditions should comply with radiation protection criteria. Individual monitoring, necessary to verify that no worker receives a dose in excess of the specified dose limits, may provide useful information on the radiation safety of the work place. It is, however, often desirable to investigate the working environment to verify that exposure of the worker is kept as low as reasonably achievable (ALARA). In cases where local expertise and/or measuring facilities are not available, TNO-CSD provides assistance. Investigations are made using calibrated instruments and following working procedures approved by the government.

When existing facilities need remodeling or when new constructions meant to accommodate radiation sources are being designed (e.g. X-ray rooms in hospitals), radiation protection aspects, i.e. shielding, require careful consideration. This is another area where TNO-CSD can give advice, having the facilities to assist in making calculations for optimal shielding. ❑

5. Calibration of instruments

L. van den Berg and J. Moor

A wide range of radiation sources and measuring equipment is of paramount importance for scientific research in radiation dosimetry. The facilities available at TNO-CSD are, however, also used to evaluate, type test or calibrate radiation protection instruments for suppliers, hospitals and (nuclear) industry. To report the results certificates are issued. The sources and ionization chambers/electrometers used by CSD are traceable to primary standards, calibration procedures are based on standard protocols.

The following radiation sources are available:

radiation source	(max) energy (keV)	remarks
Co-60	1250	4 sources
Cs-137	662	4 sources
X-rays	10 - 320	filtered beams
Beta rays	225 - 2300	^{147}Pm, ^{204}Tl, ^{90}Sr/^{90}Y

If the customer so desires reference radiations as specified by ISO (International Standards Organisation) are used (Narrow as well as Wide Spectrum Series). ❑

6. Monte Carlo computer codes

F.W. Schultz

Computer (Monte Carlo) simulation is a useful tool to obtain quantitative information on dosimetric quantities in case making measurements is impossible or impractical. Dedicated computer codes are based on mathematical models of radiation physics using quantitative data on interactions between radiation and matter. Users must supply details on the radiation beam and the irradiated object. In a Monte Carlo (MC) simulation events, occuring when radiation particles are transported from a radiation source through matter into the area of interest, are recorded. The fate of a particle is determined by random selections from probability distributions describing the events that are possible (e.g., scatter, creation of secondary particles (also to be transported), and energy deposition). Such distributions depend on the nature of the particle (type, energy) and on properties of the materials it crosses (density, composition). Thus monitoring many source particles (hundreds of thousands to millions) yields statistically reliable mean values (per starting source particle) of the sought dosimetric quantities.

At TNO-CSD the general purpose MC code "MCNP" (Monte Carlo Simulation of N-Particles), version 4.2 is used. The code has been developed at Los Alamos National Laboratory to simulate transport of neutrons, photons and electrons.

Also the widely used code, EGS4 (Electron Gamma Shower 4) developed at Stanford Linear Accelerator Center is available. Both computer codes run on a HP9000 model 777C110 computer.

For calculating organ dose distributions three mathematical anthropomorphic phantoms are available, i.e., the reference adult male and female and a seven years old girl.

Summary of MC simulation applications at TNO-CSD:

A. Radiation Protection of Patients, Radiation Workers and General Public

A1. *Diagnostic Radiology*

- Calculation of conversion factors, which enable making estimates of organ and effective doses from easily obtainable data such as air kerma free in air, entrance skin dose or dose-area-product and irradiation geometry.
- Evaluation of clinical protocols used in hospitals. Effective doses associated with X-ray examinations of thorax, stomach and colon, and with abdominal angiography, mammography, paediatric radiology and CT show a wide variety among hospitals. Intercomparison between hospitals allows optimization of protocols used in diagnostic radiology.

A2. *Radiotherapy*

- Calculation of dose distributions (depth-dose curves, isodose curves), organ doses outside the primary beam (relates to secondary tumour induction), influence of filters applied.

A3. *Personal Dosimetry*

- Evaluation of the practical application of operational quantities as recommended by the ICRU (International Commission on Radiation Units and Measurements), i.e., individual dose equivalent (H_p(d).

A4. *Nuclear Medicine*

- Criteria for the release of radioactive materials.

B. Simulation of Response of Detectors

- Calculation of W values (mean energy necessary to create an ion pair).
- Calculation of Displacement Correction Factors (disturbance caused by placing an ionization chamber in an irradiated object).
- Calculation of Backscatter Factors (change in radiation field due to the presence of an object).
- Calculation of TLD response for dosemeter design and type testing.

C. Miscellaneous

- Calculation of dose distributions in small animals as part of a EULEP (European Late Effects Project Group) study.
- Risk of radioactive iodine contamination during pregnancy.
- Risk of using radiation for permanent epilation.

❑

7. Patient dose and image quality in medical diagnostic radiology

J. Zoetelief, J.Th.M. Jansen and F.W. Schultz

Implementation of the general principles of radiation protection in medical diagnostic radiology implies that clinical procedures for applying X rays or radionuclides are justified and optimized. For diagnostic radiology, optimization means that the radiation exposure of the patient should be kept as low as possible, but still compatible with the image quality necessary for an adequate diagnosis. Optimization implies optimal balance between patient dose and image quality, i.e., balance between radiation risk and adequate medical diagnosis. Demonstration of image quality is becoming a key issue in health care. Presently, in diagnostic radiology, the key question to what extent digital techniques should replace conventional methods, e.g. film/screen radiography.

The dosimetric quantity effective dose (ICRP) is the most suitable quantity for risk assessments(1).

In practice, the assessment of organ dose and effective doses in diagnostic radiology is based upon measurements of relatively simple dosimetric quantities, e.g., entrance surface dose (ESD), X-ray tube output (i.e., air-kerma free-in-air per unit of tube-current exposure-time product - mAs), computed tomography dose index (CTDI) and dose-area-product (DAP). Conversion factors which depend on additional information including radiation quality specified by for instance half value layer and exposure geometry, provide a relation between the basic dosimetric quantities and effective dose.

Practical dose measurements

For the measurement of various dosimetric quantities TNO-CSD can provide adequate means. These include thermoluminescent (TL) dosemeters in various arrangements for ESD measurements on patients as well as various types of ionization chambers which, in combination with appropriate electrometers, can be used for measurement of tube output, CTDI and DAP. The use of TL dosemeters has as the advantage that these can easily be applied by the local staff of a diagnostic radiology department and evaluated at TNO-CSD. Ionization chamber measurements, however, require a TNO employee visiting the diagnostic radiology department.

Assessment of organ dose and effective dose for patients

The same value of a basic dosimetric quantity for different exposure conditions may result in considerable differences in organ and effective doses. It is, therefore, important to apply appropriate factors to convert dosimetric quantities into organ and effective dose. TNO-CSD has available or access to almost all worldwide available data bases of conversion factors. In addition, TNO-CSD has the facilities to calculate conversion factors if adequate information is not available.

Image quality assessment

Dosimetric information without knowledge of the related image quality provides only a basis for risk assessment, i.e., only half the information necessary to demonstrate compliance with good medical practice. Therefore demonstration of adequate image quality is vital. TNO-CSD can provide means for the assessment of image quality by performing measurements on images of contrast-detail phantoms. Although this method provides only semi-quantitative information it still allows clear demonstration of differences in image quality for different situations. The development of a technique for quantifying image quality is an important research area of TNO-CSD. ❑

1. International Commission on Radiological Protection. 1990 Recommendations of the International Commission on Radiological Protection. Oxford: Pergamon Press, ICRP Report 60, 1991.

III. List of publications

III. List of publications

Bentvelzen, P.A.J.
Retroviruses.
In: Infection of vertebrates. vol. 5, Virus infections of rodents and lagomorphs (eds. Horzinek C, Osterhaus ADME). Elsevier, Amsterdam pp. 347-367, 1995.

Bentvelzen, P.A.J.
Antistoffen tegen defecte product p53-gen.
Tijdschrift Kanker 19 (3), 32, 1995.

Bentvelzen, P.A.J.
Een Kaposi sarcoom Herpesvirus.
Tijdschrift Kanker 19 (4), 35, 1995.

Bentvelzen, P.A.J.
Milestone 1995. Van cel naar kanker; van model naar behandeling.
Tijdschrift Kanker 19 (6) 31-32, 1995.

Bentvelzen, P.A.J.
Een alternatieve uitschakeling van tumorsuppressor-genen.
Tijdschrift Kanker 19 (6) 26, 1995.

Bentvelzen, P.A.J.
Het belang van het CDKN2A gen voor de oncologie.
IKR-Bulletin 20 (1) 38, 1996.

Bentvelzen, P.A.J.
Humane kankervirussen.
IKR-Bulletin 20 (1) 66-78, 1996.

Broerse, J.J., Dullemen, S. van.
Stralingsrisico bij medisch handelen.
Patient Care 22(7), 15-28, 1995.

Broerse, J.J. , Bakker, B., Davelaar, J., Leer, J.W.H., Niemer-Tucker, M.M.B., Noordwijk, E.M.
The effects of single dose TBI on hepatic and renal function in non-human primates and patiens. In: Proceedings of the first international conference, Minsk, Belarus: The radiological consequences of the Chernobyl accident. Eds. A. Karaoglou, G. Desmet, G.N. Kelly and H.G. Menzel. European Commission and the Belarus, Russian and Ukranian Ministries on Chernobyl Affairs, Emergency Situations and Health pp 611-617, 1996.

Broerse, J.J., Schultz, F.W.
Dose assessment - possibilities and limitations. ERPET Course, Schloss Reisensburg, 1996.

Broerse, J.J.
Zijn magnetische velden bij hoogspanningskabels nadelig voor de gezondheid?
Vademecum 14, 22, 1996.

Bruggen-Bogaarts, B.A.H.A. van der, Broerse, J.J., Lammers, J.W.J., Waes, P.F.G.M. van, Geleijns, J.
Radiation exposure in standard and high resolution chest CT scans.
Chest 107, 113-115, 1995.

Christensen, P., Julius, H.W., Marshall, T.O.
Technical recommendations for monitoring individuals occupationally exposed to external radiation.
European Commission, Report EUR 14852 EN, ISBN 92-826-7364-2, 1995.

Dijk, J.W.E. van, Bogaerde, M.A. van de, Julius H.W.
The National Dose Registration and Information System: Dose distribution in the Netherlands over the period 1989-1993.
4 Conf. Rad.Prot.Dos. Orlando 1994.

Dijk, J.W.E. van, Julius, H.W.
Dose thresholds and quality assessment by statistical analysis of routine individual monitoring TLD data
Proc. 11 Sol. State Dos. Conf., Boedapest, 1995, to be published.

Geleijns, J., Broerse, J.J., Zweers, D., Zoetelief, J.
General ion recombination for ionization chambers used under irradiation conditions relevant for diagnostic radiology.
Medical Physics 22, 17-22, 1995.

Geleijns, J., Broerse, J.J., Zoetelief, J., Zweers, D., Unnik, J.G. van
Patient dose and image quality for computed tomography in several Dutch hospitals.
Radiat Prot Dosimetry 57, 129-133, 1995.

Jansen, J.T.M., Bentvelzen, P.A.J., Zoetelief, J.
Kankersterfte onder werkers in de nucleaire industrie.
NVS Nieuws 20, 18, 1995.

Jansen, J.T.M., Zoetelief, J.
Computer model for risk-benefit analysis of mammographic breast cancer screening.
Radiat Prot Dosimetry 57, 217-220, 1995.

Jansen, J.T.M., Zoetelief, J.
MBS: a model for risk-benefit analysis of breast cancer screening.
Brit J Radiol 68, 141-149, 1995.

Jansen, J.T.M., Bentvelzen, P.A.J., Zoetelief, J.
Risico op kanker bij werknemers nucleaire industrie. Risicoschattingen voor straling lijken aan de veilige kant.
Tijdschrift Kanker 19 (3), 14-16, 1995.

Jansen, J.T.M., Zoetelief, J.
Risico's en baten bij bevolkingsonderzoek borstkanker.
Tijdschrift Kanker 19, 32-34, 1995.

Jansen, J.T.M., Geleijns, J., Zweers, D., Schultz, F.W., Zoetelief, J.
Calculation of computed tomography dose index to effective dose conversion factors based on measurement of the dose profile along the fan shaped beam.
Brit J Radiol 69, 33-41, 1996.

Julius, H.W.
Some remaining problems in the practical application of the ICRU concepts of operational quantities in individual monitoring
Proc. 11 Sol. State Dos. Conf., Boedapest, 1995, to be published.

Julius, H.W.
Individual monitoring for external radiation, some conceptual and practical aspects
Invited paper IRPA Congress, 1996, Wenen, to be published.

Kal, H.B.
Röntgen, 100 jaar straling doorgelicht.
Inmerc bv, Wormer, 1995.

Kal, H.B.
Radiobiologie in Nederland.
Tijdschrift Kanker 19 (5), 36-38, 1995.

Kal, H.B., Koops, W., Heide-Schoon, G. van der (EDS)
100 Jaar Röntgenstraling, toen, thans, toekomst.
Abstract book Nationaal Congres 100 Jaar Röntgenstraling, 20 oktober 1995, Den Haag, 1995.

Kal, H.B.
Radiotherapie van botmetastasen.
IKR-Bulletin 19 (2, 3), 36-37, 1995.

Kal, H.B., Barendsen, G.W., Kogel, A.J. van der
Honderd jaar radiologie in Nederland. IX. Klinische radiobiologie.
Ned Tijdschr Geneesk 139 (48), 2476-2480, 1995.

Kingma, L.M., Szabó, B.G., Kal, H.B.
Honderd jaar radiologie in Nederland.
Ned Tijdschr Geneesk 139 (46), 2341-2342, 1995.

Niemer-Tucker, M.M.N., Sluysmans, M.M.J.H., Bakker, B., Davelaar, J., Zurcher, C. Broerse, J.J.
Long-term consequences of high-dose total-body irradiation on hepatic and renal function in primates.
Int J Radiat Biol 68, 83-96, 1995.

Kroesen, B.J., Helfrich, W., Bakker, A., Wubbena, A.S., Kal, H.B., The, T.H., Leij, L. de
Reduction of EGP-2 positive pulmonary metastases by bispecific-antibody-redirected T-cells in an immunocompetent rat model.
Int J Cancer 61, 812-818, 1995.

Schmitz, T.H., Waker, A.J., Klianga, P., Zoetelief, J. (EDS)
Design, construction and use of tissue equivalent proportional counters.
Radiat Prot Dosim 61, 297-404, 1995.

Schultz, F.W., Geleijns, J., Zoetelief, J.
Effective doses for different techniques used for PA chest radiography.
Radiat Prot Dosim 57, 371-376, 1995.

Schultz, F.W., Zoetelief, J.
Organ and effective doses in the male phantom ADAM exposed in AP direction to broad unidirectional beams of monoenergetic electrons.
Health Phys 70, 498-504, 1996.

Snijders-Keilholz, A., Keizer, R.W.J. de, Goslings, B.M., Dam, E.W.C.M. van, Jansen, J.T.M., Broerse, J.J.
Probable risk of tumour induction after retro orbital irradiation for Graves' ophtalmopathy.
Radiother Oncol 38, 69-71, 1996.

Taylor, G.C., Jansen, J.T.M., Zoetelief, J., Schuhmacher, H.
Neutron W-values in methane-based tissue-equivalent gas up to 60 MeV.
Radiat Prot Dosim 61, 285-290, 1995.

Vermeij, J., Giessen, P.H. van der, Barendsen, G.W., Kal, H.B.
Honderd Jaar Röntgenstraling in Nederland, Ontwikkelingen in de Radiotherapie, Fysica en Radiobiologie.
Uitgave van de NVRT, NVKF en NVRB, 1995.

Vries, G. de, Zoetelief, J., Jansen, J.T.M.
Calculation of air kerma to average glandular tissue dose conversion factors for mammography.
Radiat Prot Dosim 57, 397-400, 1995.

Zoetelief, J., Beentjes, L.B., Broerse, J.J., Julius, H.W., Busemann-Sokole, E.
Round Table, Appendix 9. Quality assurance and population dose in diagnostic radiology and nuclear medicine imaging: state of the art in the Netherlands.
Radiat Prot Dosim 57, 59-64, 1995.

IV. List of reports

IV. List of reports

Bentvelzen, P.A.J., Rotterdam, A. van, Bartstra, R.W.
Evaluatie van recent gepubliceerde epidemiologische studies over radon en het risico op longkanker.
Report no RD-E/9511-362, 1995.

Dijk, J.W.E. van, Bogaerde, M.A. van de, Julius, H.W.
The National Dose Regisration and Information system: Dose distribution in The Netherlands over the period 1989-1993. (4^{e} Conf. Rad. Prot. Dos. Orlando, 1994).
Report no RD-E/9409-341, 1995.

Dijk, J.W.E. van, Julius, H.W.
Evaluatie stralingsdoses van radiologische werkers in Nederland voor de periode 1989 - 1993
(RD-I/9412-346).

Jong, P. de, Dijk, W. van
Ecolonia: radonmetingen (in opdracht van NOVEM).
Report no RD-E/9406-338, 1995

Jong, P. de, Busscher, F.A.I., Dijk, W. van
Ecolonia: dosistempometingen. (in opdracht van NOVEM).
Report no RD-E/9406-339, 1995.

Jong, P. de, Kal, H.B.
Evaluatie CCRX-meetprogamma radioactieve stoffen.
Report no RD-E/9502 - 345, 1995.

Jong, P. de
Radiologische consequenties verbonden aan het gebruik van reststoffen in bouwmaterialen.
Report no RD-E/9412-344. 1995.

Jong, P. de, Dijk, W. van, Hulst, J.G.A. van, Heijningen, R.J.J. van
The effect of the composition and production process of concrete on the radon-222 exhalation rate.
Report no RD-E/9506-352, 1995.

Jong, P. de, Vries, G. de, Oldengarm, J., Boemen, H.J.Th., Buijs, A.E.
Meetresultaten Ecolonia.
Report no RD-E/9506-353, 1995.

Julius, H.W.
Individuele StralingsControle (RD-E/9509-359).

Julius, H.W.
Kwaliteitsborging in de radiodiagnostiek
(RD-E/9509-360).

Julius, H.W., Broerse, J.J.
Introduction of new operational radiation protection quantities in The Netherlands.
Report no RD-E/9410-343, 1995.